UNIVERSITY OF CALIFORNIA,
IRVINE

Synthesis and Formulation of Acid-responsive Polypeptide Vectors for Gene Therapy Applications

DISSERTATION

submitted in partial satisfaction of the requirements
for the degree of

DOCTOR OF PHILOSOPHY

in Pharmacological Sciences

by

Shirley Yu Wong

Dissertation Committee:
Professor Young Jik Kwon, Chair
Professor Jennifer Prescher
Professor Szu-Wen Wang

2015

DEDICATION

To my parents

for their guidance, love, and support

TABLE OF CONTENTS

LIST OF FIGURES

LIST OF TABLES

ACKNOWLEDGMENTS

I would like to express my deepest appreciation to my advisor, Professor Young Jik Kwon, for his guidance and support throughout my research training. He opened up many opportunities to help me develop professionally. He also taught me to enjoy the process of overcoming challenges.

I would also like to thank my committee members, Professors Jennifer Prescher and Szu-Wen Wang for their constructive comments throughout the training.

I would like to express gratitude towards former and current members of the BioTEL lab for their mentorship, support, and teamwork. I also really enjoyed all the scientific discussions and fun we had together. I made some of my greatest friends here. We stood by each other through thick and thin. Similarly, I would like to thank all of my closest friends who always believed in me. Thank you, Haiyang, for being a huge support towards the end of my graduate career and helping me transition into the next step of my life.

Lastly, I would not be who I am today if it wasn't for my loving family. My mom and dad always taught me to be the best I can be. They were always willing to help me out and cheer me on. My brother and sister were the best siblings anyone could have ever had. They were superb role models and they were always there to lend me a hand. They helped me to see different angles and perspectives in life. I would like to express my deepest appreciation for such as loving family.

CURRICULUM VITAE

Shirley Wong

Education:

2015 University of California, Irvine
Ph.D., Pharmacological Sciences

2010 University of California, Irvine
B.S., Biological Sciences

Field of study:

Acid-responsive polypeptide for gene therapy applications

Publications:

1. Wong, S., Kwon, Y. J. (2011), Synthetically functionalized retroviruses produced from the bioorthogonally engineered cell surface. Bioconjugate Chem., 22: 151-155.

2. Wong S., Shim, M. S., Kwon, Y. J. (2012), siRNA as a conventional drug in the clinic? Challenges and current technologies. Drug Discov. Today: Technologies, 9: 167-173.

3. Wong, S., Shim, M.S., Kwon, Y. J. (2014), Synthetically designed peptide-based biomaterials with stimuli-responsive and membrane-active properties for biomedical applications. J. Mater. Chem. B, 2: 595-615.

4. Wong, S., Kwon, Y. J. (2015), Facile synthesis of high-molecular-weight acid-labile polypeptides using urethane derivatives. J. Polym. Sci. Pol. Chem., 53: 280-286.

ABSTRACT OF THE DISSERTATION

Synthesis and Formulation of Acid-responsive Polypeptide Vectors for Gene Therapy Applications

By

Shirley Yu Wong

Doctor of Philosophy in Pharmacological Sciences

University of California, Irvine, 2015

Professor Young Jik Kwon, Chair

Gene therapy holds great promise for treating diseases that stem from genetic origin. Nevertheless, development of safe and efficient gene delivery vectors is still a major challenge. Multiple hurdles are encountered when nucleic acids are administered into the body; they must avoid nuclease degradation, bypass rapid clearance, limit immune responses, extravasate to desired tissues, get taken up by cells, and traffic to desired intracellular locations. Advances in biotechnology aim to develop nontoxic as well as smart nucleic acid delivery carriers with stimuli-responsive features to overcome these challenges. Peptide-based nanomaterials have become widely used in the field of biotechnology for gene and drug delivery due to their structural versatility and biomimetic properties. Particularly, polypeptide vectors that respond to biological stimuli, such as acidic intracellular environments, have great utility in mediating efficient endosomal escape and drug release. Unfortunately, synthesis strategies for efficient polymerization of acid-labile peptides has been minimal due to conditions that fail to preserve acid-degradable functional groups. In this dissertation, a practical polymerization method was

first developed for the synthesis of high molecular weight acid-labile polypeptides. Stable urethane derivatives of acid-labile amino acid, ketalized serine (kSer), were synthesized and polymerized to high molecular weight under permissive conditions independent of elevated temperature, restrictive solvents, or inert atmosphere. The practicality in the synthesis method allows further advancement of acid-labile polypeptide vectors as novel and functional biomaterials. Consequently, a new formulation strategy utilizing solvent-assisted self-assembly of poly(kSer)-derived peptides with small interfering RNA (siRNA) was developed. The nanoparticles were highly monodisperse and precisely spherical in morphology which has significant clinical implications in definitive biodistribution, cellular internalization, and intracellular trafficking patterns. Cross-linked poly(kSer)/siRNA nanoparticles demonstrated efficient nucleic acid encapsulation, internalization, endosomal escape, and acid-triggered cargo release, which tackles multiple hurdles in siRNA delivery. In summary, this dissertation provides a full comprehensive study from synthesis to formulation of acid-responsive poly(kSer)-derived peptides for gene therapy applications.

Chapter 1: Introduction

Parts of this chapter have been adapted from:

Wong, S., Shim, M.S., Kwon, Y. J. (2014), Synthetically designed peptide-based biomaterials with stimuli-responsive and membrane-active properties for biomedical applications. J. Mater. Chem. B, 2: 595-615.

with permission from The Royal Society of Chemistry.

1.1. Advances in biomaterials

As science progresses, scientists and engineers contribute to new solutions for significant medical problems. No longer is a treatment based solely on conventional pharmaceutical formulations but is now studied down to its molecular science where biotechnology is integrated to encompass biological, physical, and chemical phenomena for curative preparations. These advances are tied closely with the development of new biomaterials. Biomaterials are classified as substances other than food or drugs that are used in therapeutic or diagnostic applications that come in contact with tissue or biological fluids.[1] More than 8,000 separate kinds of medical devices, 2,500 different diagnostic systems, and 40,000 different pharmaceutical products have been prepared using biomaterials, such as contact lenses, kidney dialyzers, implants, cardiac pacemakers, and drug delivery vehicles.[1] Synthetic as well as natural polymers have been commonly used to prepare these biomaterials. With the progressive development utilizing polymeric materials in biological systems, leading researchers have focused on optimizing efficacy as well as safety. Important issues include designing biomaterials to reduce

immunogenicity and promote desirable interactions between them and living cells. Therefore, much attention has shifted towards utilizing biodegradable polymers as biomaterials, including those that can be hydrolytically degraded by the human body (e.g., poly(lactide-*co*-glycolide and polycaprolactone) or enzymatically degraded (e.g., polypeptides and polysaccharides).[2] Among these biodegradable polymers, polypeptides have been identified as one of the most important classes of biomolecules since they are a major component of natural tissues and they offer safety, degradability, and versatility in construction due to a wide assortment of amino acid building blocks.

1.2. Peptide-based platforms for biomedical applications

Peptide-based platforms for biomedical applications have been a subject of intense research due to the versatility of these biomolecules. Unlike proteins which are highly fragile molecules with high cost of production, peptides are composed of synthetic and/or biological building blocks that have protein-mimicking properties.[3–5] Some naturally occurring peptides have various functional activities and can be used in different healthcare areas including drug delivery, tissue engineering, biodiagnostic tools, antibiotics, etc. (**Figure 1.1**).[6–9] More importantly, the assortment of amino acids with distinct functional side chains determines the physicochemical properties of peptides and thus induces supramolecular interactions.[8] These supramolecular interactions include: hydrogen bonding, hydrophobic, aromatic stacking, and electrostatic interactions.[3] The resulting secondary (e.g., α-helix or β-sheet motifs) and tertiary structures (i.e., three dimensional structure) of the peptides determine their unique functionality. Therefore, rationally designed peptides can be tailored to relate structure to function. For instance,

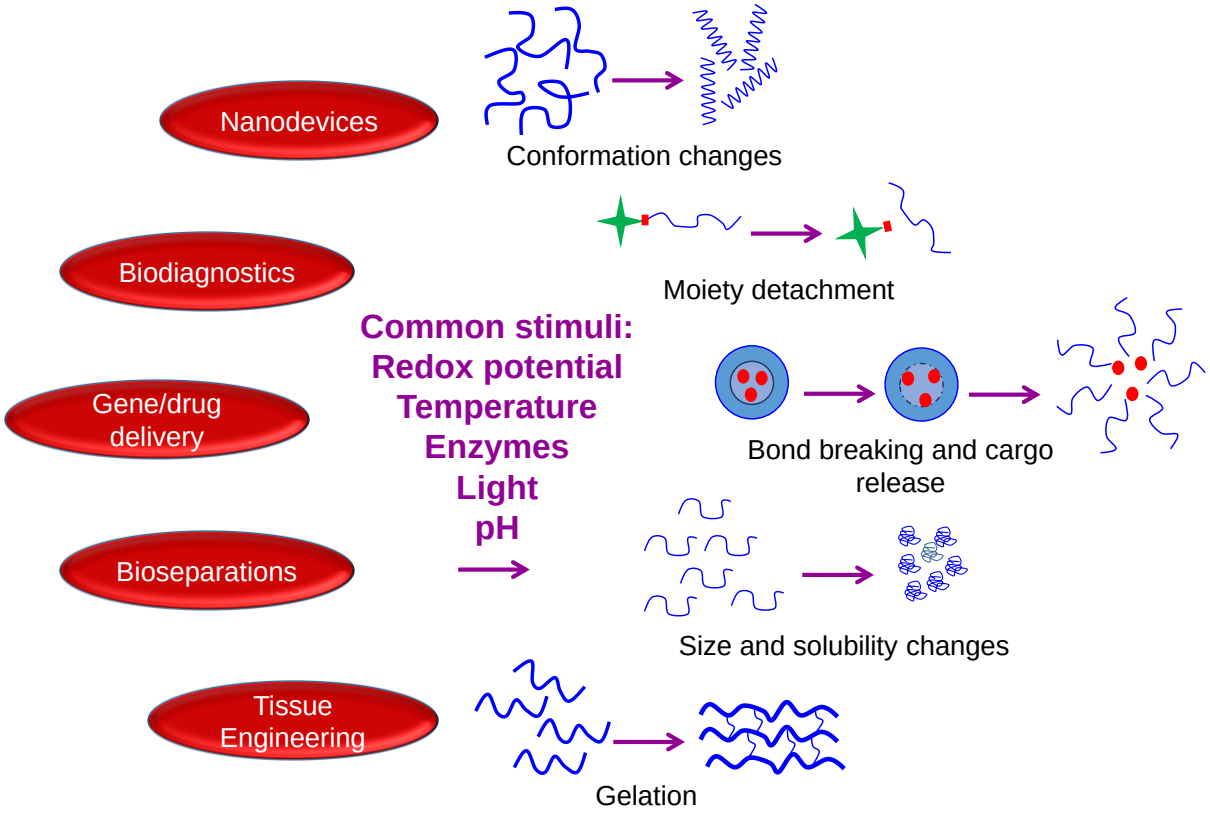

Figure 1.1. General biomedical applications and common stimuli for peptide-based biomaterials.

designed peptides can hierarchically self-assemble into ordered conformations to create intriguing vesicular nanostructures that act as therapeutic encapsulants.[10] Also, controlled conformational changes in secondary and tertiary structures can be attained by incorporating stimuli-responsive switches.[11] The robust flexibility in design, biodegradability, and biocompatibility of peptides make them a suitable class of compounds for biomedical applications.[12]

1.3. Peptide nanocarriers for gene/drug delivery

Nanoparticles (NPs), typically 100 nm range and smaller, exhibit unique physicochemical properties related to their small size and a large surface to mass ratio. Drugs and other therapeutics can be loaded into the NPs by various methods, and the therapeutic index can be improved compared with free drugs due to methods that increase drug solubility, prolong circulation, release drugs at a sustained and controlled fashion, target drugs to desired sites, and even combine multiple therapeutics into one carrier.[13–16] Another major advantage is that NPs can be internalized via mechanisms that bypass simple diffusion, where many hydrophilic and larger molecules experience difficulty in permeating the amphipathic lipid bilayer membrane. For cancer therapy, NPs can exploit the enhanced permeability and retention (EPR) effect, where leaky vasculature and poor lymphatic drainage of tumor tissues allow NPs to selectively accumulate and be retained for enhanced therapeutic efficacy at tumor locations.[17]

Peptide-based vectors have been used to deliver genes and drugs.[18-20] For gene delivery, cationic peptides, which have positively charged groups on their side chain, serve as vectors, since they can electrostatically interact with anionic nucleic acids to encapsulate them. Cell penetrating peptides (CPPs) are a class of cationic or amphipathic peptides that can deliver nucleic acids or small therapeutic molecules through efficient internalization mechanisms and have been widely investigated.[18-19,22] Peptides have also been used for surface conjugation onto NPs to provide additional functionality such as active targeting or fusogenic activity.[22-23] Moreover, peptide amphiphiles have been shown to serve as drug delivery carriers by non-covalently encapsulating drugs into the core of the NP.[20]

Nevertheless, nanocarriers, including peptide-based vectors, still face many challenges in delivering therapeutics to the pathological site. Clearance from the immune system, potential toxicity, poor tissue penetration and cellular uptake, and insufficient cargo protection from enzymatic degradation represent some of the major extracellular hurdles. Once inside the cells, barriers of endosomal escape, cargo unpackaging, and subcellular trafficking are faced.[24] Therefore, developing nanocarriers that can respond to stimuli at different stages of trafficking is promising in order to tackle these hurdles.

1.4. Stimuli-responsive peptides

Among different classes of peptides used for biomedical applications, stimuli-responsive peptides have been relatively well-investigated.[25] Controlling a desired function by tailoring biomaterials that respond to different pathological conditions pre-established by the body has received much enthusiasm. Common stimuli that are used to induce changes include: pH, redox potential, temperature, light, and enzymes.[3,8,25-26] Ionic strength has also been shown to affect peptide-based materials such as in the formation of three-dimensional matrices and fibrillary structures and induction of conformational changes.[25,27–30] Some naturally occurring peptides have also been shown to respond to these stimuli, but much attention has been shifted towards synthetically designed peptides, since even broader control of the structure and function can be attained for different needs. Furthermore, the incorporation of non-natural amino acids or other functional moieties can aid in extending the applications of peptide-based biomaterials.

There are abundant applications that can find use of stimuli-responsive peptides. Stimuli-responsive peptides can undergo conformational changes, promote detachment of functional moieties, release therapeutics, cause changes in size and solubility of vectors, and transition between phases (such as gelation), thus allowing controllable actions in various biomedical fields (**Figure 1.1**).[25-26,31] There has been enormous effort in creating nano-scale therapeutic delivery carriers using peptide-derived materials that have switching mechanisms.

1.5. pH-responsive peptides

Among different stimuli-triggered peptides, those that respond to pH changes have broad applications. Different organs, tissues, subcellular compartments, and pathophysiological conditions have different pH levels and gradients. For instance, the gastrointestinal tract is characterized by a pH gradient; the stomach exhibits pH of 1–3 for digestion, duodenum and ileum of 6.6–7.5 for neutralization, and intestines range from 5.0 to 8.0.[32–35] Cancerous tissues exhibit acidosis as a hallmark trait due to lactic acid accumulation from elevated rates of anaerobic metabolism but reduced rates of oxidative phosphorylation (i.e., a slightly acidic extracellular pH (6.5–6.9) compared with normal tissue (7.0–7.5)).[26-37] Low pH is also seen in implications of serious microbial infections.[33] Moreover, because many NP-based systems rely on endocytosis as a main uptake mechanism, materials that can respond to the acidic environment of endosomes can accelerate the degradation of carriers, release payloads, or control structural changes.[38]

1.6. Poly(ketalized serine) as a pH-responsive peptide gene vector

Acetal, ketal, hydrazone, orthoester, and imines are well-documented acid-labile linkers.[39-40] Although they are widely used in polymeric systems for acid-degradability, the incorporation of the acid-labile linkers into peptide-based systems has been rare. A novel acid-degradable polypeptide where a synthetic amino acid bearing acid-labile ketal linkages that can transform into natural amino acids was used to enhance gene delivery (**Figure 1.2**).[41] This polypeptide consisted of ketalized serine (kSer), which was an analog of lysine (Lys) consisting of cationic amino termini. The polyethylene glycol-conjugated PEG-poly(kSer) was self-assembled with DNA and formed micelles. Upon acid hydrolysis in endosomal pH, PEG- poly(kSer) micelles facilitated the intracellular release of DNA. At the same time, poly(kSer) reverted into poly(serine), a nontoxic natural peptide. The system significantly increased transfection efficiency compared with PEG-poly(Lys) containing non-degradable side chains.

1.7. The scope of the study

1.7.1. Investigation of polymerization strategies for the synthesis of high molecular weight acid-responsive peptides

Generally, greater molecular interactions between the peptide and cargo, such as cationic peptides electrostatically interacting with anionic nucleic acids to form complexes, are achieved using higher molecular weight polymers. Therefore, the development of efficient polymerization chemistries to generate large polypeptides with well-defined homogeneity (low polydispersity index) is important. One way to synthesize peptides reaching beyond 100 residues is by using solution phase chemistry in which monomers are added to the solvent and polymerized with a coupling agent, in contrast to the solid

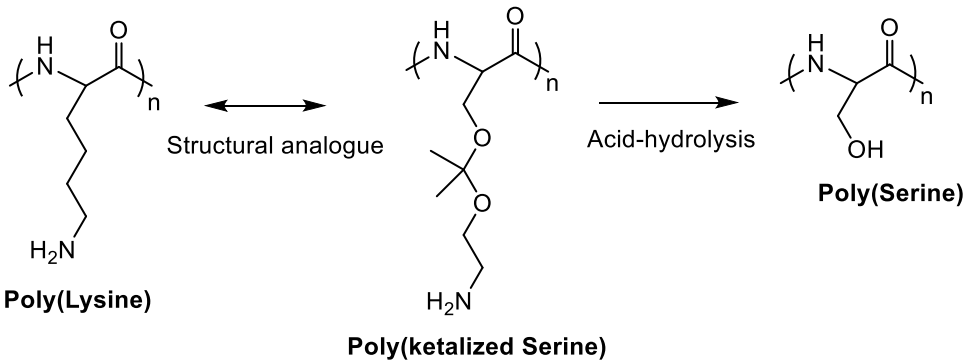

Figure 1.2. Structure of acid-labile poly(ketalized serine).

phase approach where amino acids are added one by one to a solid support for chain growth. However, researchers synthesizing high molecular weight acid-labile peptides have encountered many difficulties since the pre-existing chemistries are generally not compatible to acid-labile moieties or protecting groups.[42]

In this dissertation, different strategies for synthesizing high molecular weight poly(kSer)-derived acid-responsive peptides was first investigated. The strategies employed include carbodiimide coupling chemistry, *N*-carboxyanhydride (NCA) ring-opening polymerization (ROP), and NCA ROP using amino acid urethane derivatives. The success and limitations of each method are documented and evaluated as tools for synthesizing high molecular weight acid-labile peptides.

1.7.2. Investigation of supramolecular assembly of poly(kSer)-derived peptides and their therapeutic applications

Considerable advances have been developed using peptides as building blocks to produce materials that self-assemble into different architectures for diverse biomedical applications, such as in regenerative medicine and drug delivery.[43-45] Self-assembled

peptide systems have been shown to form different shapes such as nanotubes, helical ribbons, fibrous scaffolds, micelles, vesicles, etc. due to supramolecular interactions.[21] Different morphologies can be applied to different applications, such as fibrous networks for regenerative medicine scaffolds or spherical micelles for drug delivery. The molecular self-assembly of the designed peptide systems is governed by weak non-covalent interactions such as hydrogen bonding, electrostatic interactions, hydrophobic interactions, etc. that together collectively produce very stable structures.[27] Controlling the self-assembly process to produce well-defined nanostructures is complex, so in-depth understanding of the phenomena that leads to its construction is key to the design. With the recent growth in nanotechnology, tremendous effort has been devoted to design of materials that self-assemble into well-ordered structures at the nanometer scale.[46] Tunable structures can also be achieved by modifying sequences or adding stimuli-responsive elements, which can tailor specific function to the nanomaterials, such as releasing drug cargos or inducing degradability of peptide materials.

A new frontier in supramolecular peptide-based nanomaterials calls forth combining molecular assembly with stimuli-triggered functionality.[47] Acid-responsive poly(kSer)-derived peptides were shown to self-assemble into intriguing architectures in different conditions. This phenomena was explored and its potential application to biomedicine will be discussed.

1.8. Organization of the dissertation

The motivation behind **Chapter 1** is to illustrate how peptides have emerged as a significant class of biomaterials used in biomedical applications, including gene and drug

delivery. Due to the prevalence of using stimuli-responsive peptides in biotechnological advances, an introduction to poly(kSer) as a model acid-responsive peptide used for gene delivery is given. Improvements towards its original synthesis strategy and applications for gene delivery using supramolecular assemblies was studied to further advance peptide biomaterial science.

Chapter 2 provides details of exploratory work utilizing several conventional polymerization strategies, such as carbodiimide and uronium coupling reagents. This chapter provides molecular mechanisms explaining what causes the termination events leading to unsuccessful polymerization and documents several approaches to bypass them but still falling short of success. Exploratory work on using NCAs synthesized using bisarylcarbonates for polymerization is also documented to show limitations of this approach, including NCA's high sensitivity towards contaminants and moisture. A more versatile technique is proposed and investigated in full detail in the next chapter.

The motivation behind **Chapter 3** is to report a polymerization method that is efficient and tolerable towards synthesizing acid-labile polypeptides. The method utilizes urethane derivatives of amino acids. The polymerization conditions, such as temperature, solvent, atmosphere, and time proved to be extremely mild compared with the originally reported conditions. The reasons behind its efficiency are reported in this chapter.

Chapter 4 demonstrates the utility of the acid-responsive peptides as gene delivery vectors formulated using a novel self-assembly technique that has been rarely reported. Thorough investigation into what causes the self-assembly of NPs and methods to stabilize the structures is documented. After stabilization, their utility as a gene delivery

vector was assessed and promising results carried the study towards experimentation in an in vivo animal model. Full experimental findings are described in this chapter.

Chapter 5 describes the summary of developing poly(kSer)-derived acid-responsive peptide gene delivery vectors from chemical synthesis to final formulation of the therapeutic and leads up to a speculation on the extension of the work.

1.9. References

[1] R. Langer, N. A. Peppas, *AICHE J.*, **2003**, 49, 2990.

[2] L. S. Nair, C. T. Laurencin, *Prog. Polm. Sci.*, **2007**, 32, 762.

[3] D. W. P. M. Lowik, E. H. P. Leunissen, M. van den Heuvel, M. B. Hansen and J. C. M. van Hest, *Chem. Soc. Rev.*, **2010**, 39, 3394.

[4] A. Carlsen and S. Lecommandoux, *Curr. Opin. Colloid Interface Sci.*, **2009**, 14, 329.

[5] F. Checot, A. Brulet, J. Oberdisse, Y. Gnanou, O. Mondain-Monval and S. Lecommandoux, *Langmuir,* **2005**, 21, 4308.

[6] B. Law, R. Weissleder and C.-H. Tung, *Biomacromolecules*, **2006**, 7, 1261.

[7] Y. Chen, X.-H. Pang and C.-M. Dong, *Adv. Funct. Mater.*, **2010**, 20, 579.

[8] J. Huang and A. Heise, *Chem. Soc. Rev.*, **2013**, 42, 7373.

[9] R. E. W. Hancock, *Lancet*, **1997**, 349, 418.

[10] J. Rao, Z. Luo, Z. Ge, H. Liu and S. Liu, *Biomacromolecules*, **2007**, 8, 3871.

[11] H.-C. Huang, P. Koria, S. M. Parker, L. Selby, Z. Megeed and K. Rege, *Langmuir***, 2008**, 24, 14139.

[12] K. Wang, G.-F. Luo, Y. Liu, C. Li, S.-X. Cheng, R.-X. Zhuo and X.-Z. Zhang, *Polym. Chem.*, **2012**, 3, 1084.

[13] L. Zhang, F. X. Gu, J. M. Chan, A. Z. Wang, R. S. Langer and O. C. Farokhzad, *Clin. Pharmacol. Ther.*, **2008**, 83, 761.

[14] M. E. Davis, Z. G. Chen and D. M. Shin, *Nat. Rev. Drug Discov.*, **2008**, 7, 771.

[15] D. Peer, J. M. Karp, S. Hong, O. C. Farokhzad, R. Margalit and R. Langer, *Nat. Nanotechnol.*, **2007**, 2, 751.

[16] J. R. McDaniel, J. Bhattacharyya, K. B Vargo, W. Hassouneh, D. A. Hammer and A. Chilkoti, *Angew. Chem. Int. Ed.*, **2013**, 52, 1683.

[17] J. Su, F. Chen, V. L. Cryns and P. B Messersmith, *J. Am. Chem. Soc*., **2011**, 133, 11850.

[18] R. Pan, W. Xu, R. Yuan, D. Chu, Y. Ding, B. Chen, M. Jafari, Y. Yuan, P. Chen, *Acta Biomaterialia*, **2015**, 211, 74.

[19] W. Xu, M. Jafari, F. Yuan, R. Pan, B. Chen, Y. Ding, T. Shinin, D. Chu, S. Lu, Y. Yuan, P. Chen, *J. Mater. Chem. B*, **2014**, 2, 6010.

[20] X. Xu, Y. Li, H. Li, R. Liu, M. Sheng, B. He, Z. Gu, *Small*, **2014**, 10, 1133.

[21] D. Chu, W. Xu, R. Pan, Y. Ding, W. Sui, P. Chen, *Nanomedicine: NBM*, **2015**, 11, 435.

[22] L. Gamrad, C. Rehbock, J. Krawinkel, B. Tumursukh, A. Heisterkamp, S. Barcikowski, *J. Phys. Chem. C.*, **2014**, 118, 10302.

[23] E. Jin, B. Zhang, X. Sun, Z. Zhou, X. Ma, Q. Sun, J. Tang, Y. Shen, E. V. Kirk, W. J. Murdoch, M. Radosz, *J. Am. Chem. Soc*., **2013**, 135, 933.

[24] T. J. Harris, J. J. Green, P. W Fung, R. Langer, D. G. Anderson and S. N Bhatia, *Biomaterials*, **2010**, 31, 998.

[25] R. J. Mart, R. D. Osborne, M. M. Stevens and R. V. Ulijn, *Soft Matter*, **2006**, 2, 822.

[26] K. Chockalingam, M. Blenner, S. Banta, *Protein Eng. Des. Sel*., **2007**, 20, 155.

[27] M. R. Caplan, E. M. Schwartzfarb, S. Zhang, R. D. Kamm and D. A. Lauffenburger, *Biomaterials*, **2002**, 23, 219.

[28] J. H. Collier and P. B. Messersmith, *Bioconjugate Chem*., **2003**, 14, 748.

[29] J. H. Collier and P. B. Messersmith, *Adv. Mater*., **2004**, 16, 907.

[30] S. Ahn, R. M. Kasi, S.-C. Kim, N. Sharma and Y. Zhou, *Soft Matter*, **2008**, 4, 1151.

[31] J. R. Kramer and T. J. Deming, *J. Am. Chem. Soc*., **2012**, 134, 4112.

[32] M. Magzoub and A. Graslund, Q. *Rev. Biophys*., **2004**, 37, 147-195.

[33] W. Gao, J. M. Chan and O. C. Farokhzad, *Mol. Pharm*., **2010**, 6, 1913.

[34] Y. Ito, Y. S. Park and Y. Imanishi, *Langmuir*, **2000**, 16, 5376.

[35] F. Radovic-Moreno, T. K. Lu, V. A. Puscasu, C. J. Yoon, R. Langer and O. C. Farokhzad, *ACS Nano*, **2012**, 5, 4279.

[36] D. Rotin, B. Robinson and I. F. Tanock, *Cancer Res*., **1986**, 46, 2821.

[37] J. Kim and C. V. Dang, *Cancer Res*., **2006**, 66, 8927.

[38] Z. Liu, M. Zheng, F. Meng and Z. Zhong, *Biomaterials*, **2011**, 32, 9109.

[39] X. Cai, C. Dong, H. Dong, G. Wang, G. M. Pauletti, X. Pan, H. Wen, I. Mel, Y. Li and D. Shi, *Biomacromolecules*, **2012**, 13, 1024.

[40] S. Aryal, C.-M. J. Hu and L. Zhang, *ACS Nano*, **2010**, 1, 251.

[41] M. S. Shim and Y. J. Kwon, *Biomaterials*, **2010**, 31, 3403.

[42] Y. Fujita, K. Koga, H.-K. Kim, X.-S. Wang, A. Sudo, H. Nishida, T. Endo. *J. Polym. Sci., Part A: Polym. Chem.*, **2007**, 45, 5365.

[43] A. Aggeli, I. A. Nyrkova, M. Bell, R. Harding, L. Carrick, T. C. B. McLeish, A. N. Semenov and N. Boden, *Proc. Natl. Acad. Sci. USA*, **2001**, 98, 11857.

[44] M. R. Caplan, P. N. Moore, S. Zhang, R. D. Kamm and D. A. Lauffenburger, *Biomacromolecules*, **2000**, 1, 627.

[45] A. P. Nowak, V. Breedveld, L. Pakstis, B. Ozbas, D. J. Pine, D. Pochan and T. J. Deming, *Nature*, **2002**, 417, 424.

[46] D. N. Reinhoudt and M. Crego-Calama, *Science*, **2002**, 295, 2403.

[47] M. Zelzer and R. V. Ulijn, *Chem. Soc. Rev*., **2010**, 39, 3351.

Chapter 2: Exploratory peptide synthesis using coupling reagents and *N*-carboxyanhydrides

2.1. Introduction

2.1.1. Carbodiimide coupling reagents and uronium salts for peptide synthesis

The synthesis of poly(ketalized serine) (poly[kSer]) has been previously reported using carbodiimide chemistry in solution phase, where kSer monomer formed an active ester through carbodiimides, which allows the nucleophilic amine to readily attack to form a stable amide/peptide bond for polymerization (**Figure 2.1**).[1-2] Carbodiimide-based polycondensation method was chosen instead of utilizing *N*-carboxyanhydride (NCA)-derivatives of α-amino acids for ring-opening polymerization (ROP) due to the high sensitivity of NCA ROP to contaminants, such as water and amines, the highly toxic reagents necessary to make the NCA monomers, as well as acid byrpducts that are generated.[3] Originally, a peptide of moderate length (22 residues) was reported using carbodiimide polycondensation method, but in order to achieve maximal gene transfection, which relies on efficient condensation of DNA from the terminal cationic amines as well as endosomal disrupting effects facilitated by hydrolysis of ketal linkages in mildly acidic conditions, it was rationalized that synthesizing longer peptides was necessary. For example, it was shown that short peptides of poly-lysine (poly[Lys]) could not form stable condensates to protect DNA from degradation.[4] Therefore, different additives as well as coupling reagents were investigated to increase peptide length.

Peptide coupling reagents have been widely investigated and evolved from carbodiimides to uronium salts and others.[2] Carbodiimides alone do not comply as the superior coupling reagent because it provokes racemization and side reactions during the coupling reaction (**Figure 2.1**). Carbodiimide activation starts by a proton transfer followed by the formation of the O-acylisourea, which is a very reactive active ester and can be attacked from the amino component to create an amide bond. However, the O-acylisourea can also undergo rearrangement to form N-acylurea, which will terminate the polymerization since it is not reactive. Therefore, reagents such as 1-hydroxybenzotriazole (HOBt) has been proposed as an additive to carbodiimide coupling to reduce racemization and form more stable active esters than O-acylisourea, in order to preserve the peptide bond formation (path b in **Figure 2.1**).

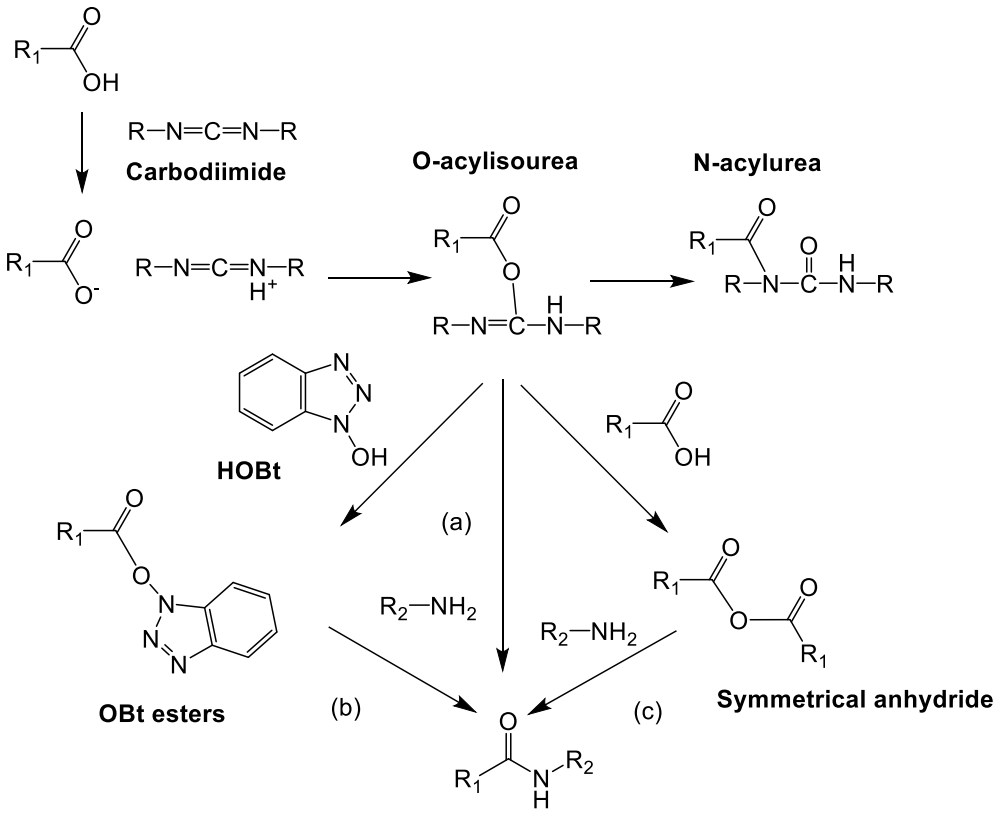

Figure 2.1. Mechanism of peptide bond formation through carbodiimide activation.

Uronium salts have also been introduced as another class of effective coupling reagents. The carboxylate reacts with the uronium salts to form an active ester, which will further react with the amino component to form an amide bond (**Figure 2.2**A). This mechanism differs from that of carbodiimides in which a terminating intermediate (N-acylurea) does not form. Nevertheless, a guanidine derivative can form if the uronium salts react with the amino component, and this can terminate the peptide chain (**Figure 2.2**B).[5]

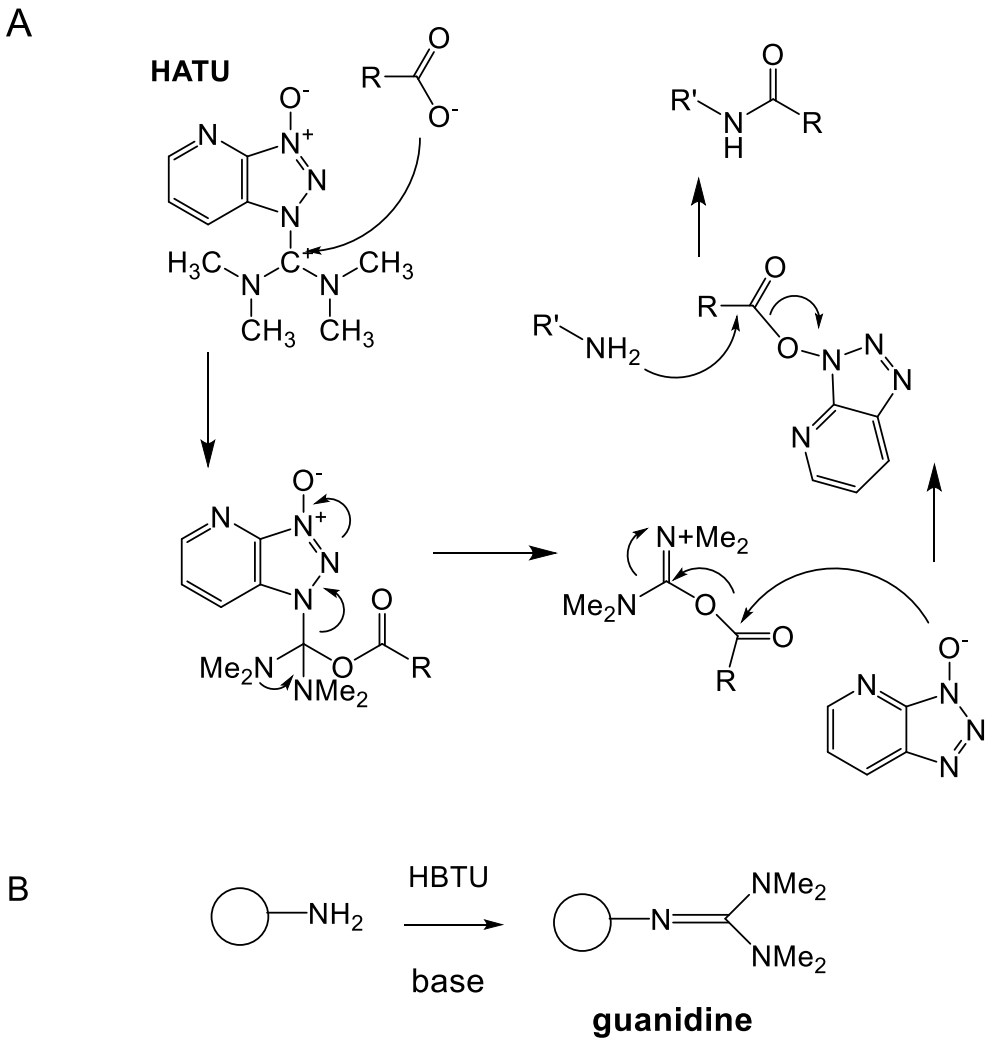

Figure 2.2. A.) Mechanism of peptide coupling using uronium salts. The example is illustrated using HATU. B.) Guanidine formation upon amino end treated with HBTU.

2.1.2. Phosgene-free synthesis of NCAs and NCA ROP

Another solution phase peptide synthesis strategy is NCA ROP (**Figure 2.3**A).[6] NCA ROP is one of the most efficient ways to synthesize high molecular weight peptides, but one of the disadvantages is the use of toxic materials. NCAs have been commonly prepared using phosgene, but the lethal toxicity of phosgene is a drawback for large scale production.[7] Also, the generation of HCl byproduct affects acid-labile groups. Recently, a method that employs phosgene-free synthesis of NCAs using bisarylcarbonates was reported (**Figure 2.3**B).[7] This method utilizes bisarylcarbonates, which when compared to phosgene, is less volatile, more safely handled, and still ensures high efficiency in producing NCAs. Also, bisarylcarbonates release phenols in the reaction, which are less volatile and corrosive than the HCl byproduct produced using phosgene. This approach would also preserve acid-labile functional groups such as the ketal in poly(kSer). This method was explored to synthesize kSer-NCA with trifluoroacteyl groups protecting the

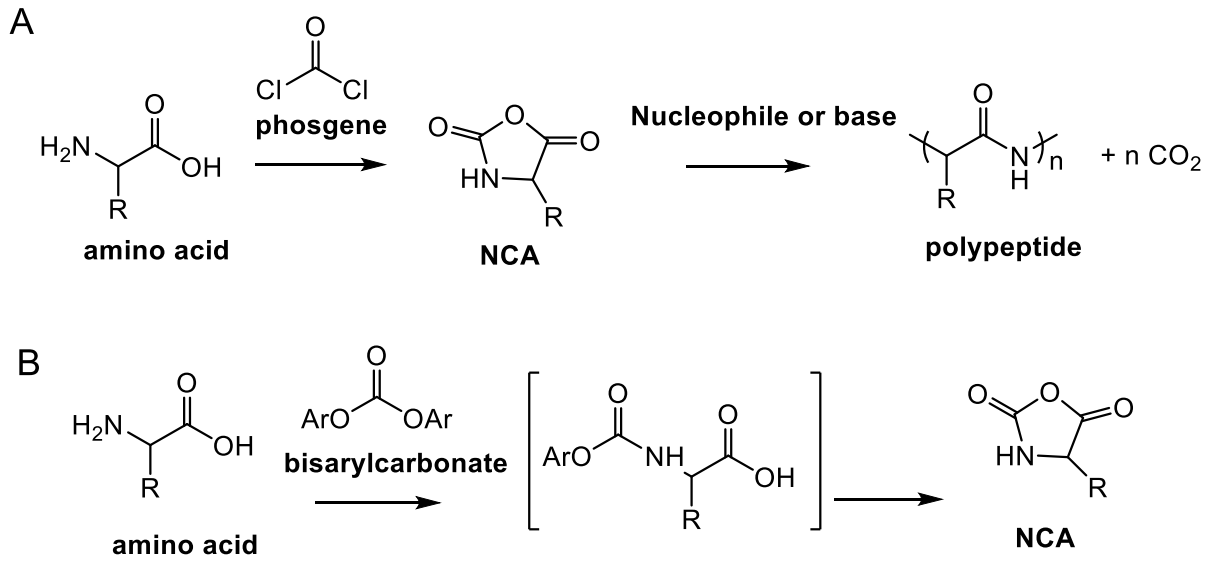

Figure 2.3. A.) A conventional method of synthesizing NCAs using phosgene and its polymerization using NCA ROP. B.) Synthesis of NCAs using bisarylcarbonates.

side chain amine (kSer[TFA]-NCA)to make high molecular weight peptides as well as to control its molecular weight and reduce polydispersity.

Utilizing NCAs has been the an expedient method for synthesizing long polypeptides, but the limitations have been the presence of side reactions that cause chain termination and chain transfer, which will restrict control over molecular weight and give undesirable broad molecular weight distributions.[8] Therefore, the field in NCA ROP for polypeptide synthesis has been extensively investigated to develop methods to control polymerization and achieve well-defined polypeptides, mainly by exploring efficient initiators, conditions for polymerization, and ways to prevent chain termination.[8] Conventional methods in NCA polymerizations have been utilizing primary amines, which are generally good initiators for polymerization due to their nucleophilicity. However, the optimal polymerization conditions for each NCA has not been universally standardized and must be empirically determined individually due to different inherent properties of NCAs and their resulting polymers, such as solubility and reactivity.[8] Also, NCA ROP for non-natural amino acids has not been common.

The most common pathways of NCA polymerizations are through the “amine” and/or the “activated monomer” (AM) mechanisms (**Figure 2.4**). The amine mechanism results from nucleophilic ring-opening chain growth, whereas the AM mechanism occurs through the deprotonation of an NCA, which then acts as a nucleophile for ROP. The polymerization can also switch back and forth between the two mechanisms, and these side reactions lead to different structures predicted by the monomer to initiator (M/I) ratio, limiting control over the polymerization. Termination reactions can also occur under the amine or AM mechanisms, where dead chains develop if the living amine end-groups

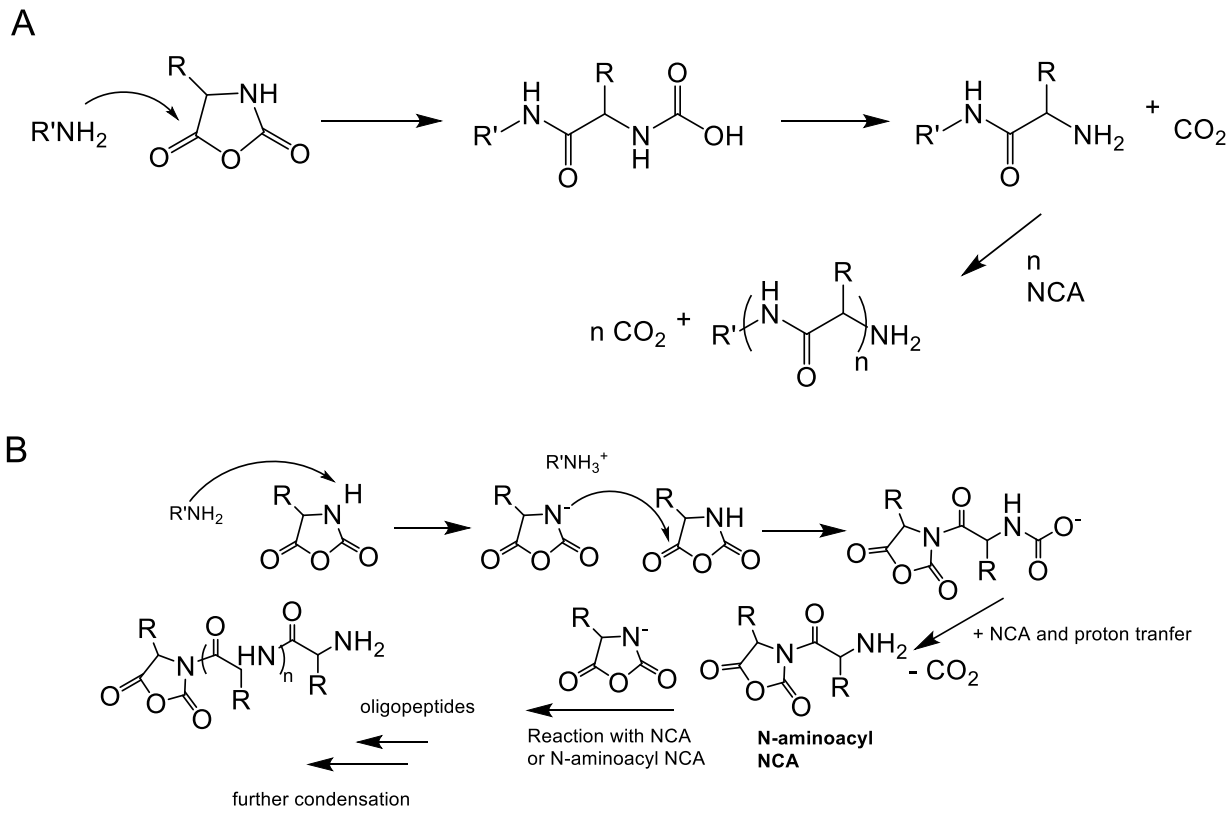

Figure 2.4. The proposed mechanism for NCA polymerization initiated by A.) nucleophilic amines or B.) activated monomers.

react with NCA anions or even dimethylformamide (DMF) solvent and form carboxylate or formyl end-groups (**Figure 2.5**).[8]

With major restrictions over the control of polymerization caused by competing nucleophilic ends and side reactions, this prompted a search for initiators that would bypass the use of amines as initiators. A new approach of controlling NCA polymerization that greatly differed from amine or AM mechanism was observed with

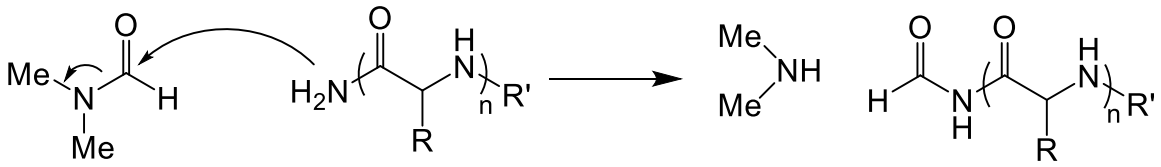

Figure 2.5. A possible chain termination in NCA ROP by reaction with DMF solvent.

hexamethyldisilazane (HMDS) in which the NCA-trimethylsilyl (TMS) intermediate undergoes a rapid ring-opening by the in-situ TMS-amine to form a TMS-carbamate, where then the polypeptide chains propagate through the transfer of the TMS-carbamate to the incoming NCA monomer (**Figure 2.6**).[9]

The following experiments explore poly(kSer) synthesis using different strategies: carbodiimides, uronium salts, and phosgene-free synthesis of NCA and its polymerization. Since different parameters affect polymerization, such as termination events, concentration of reagents, etc., these parameters were explored and

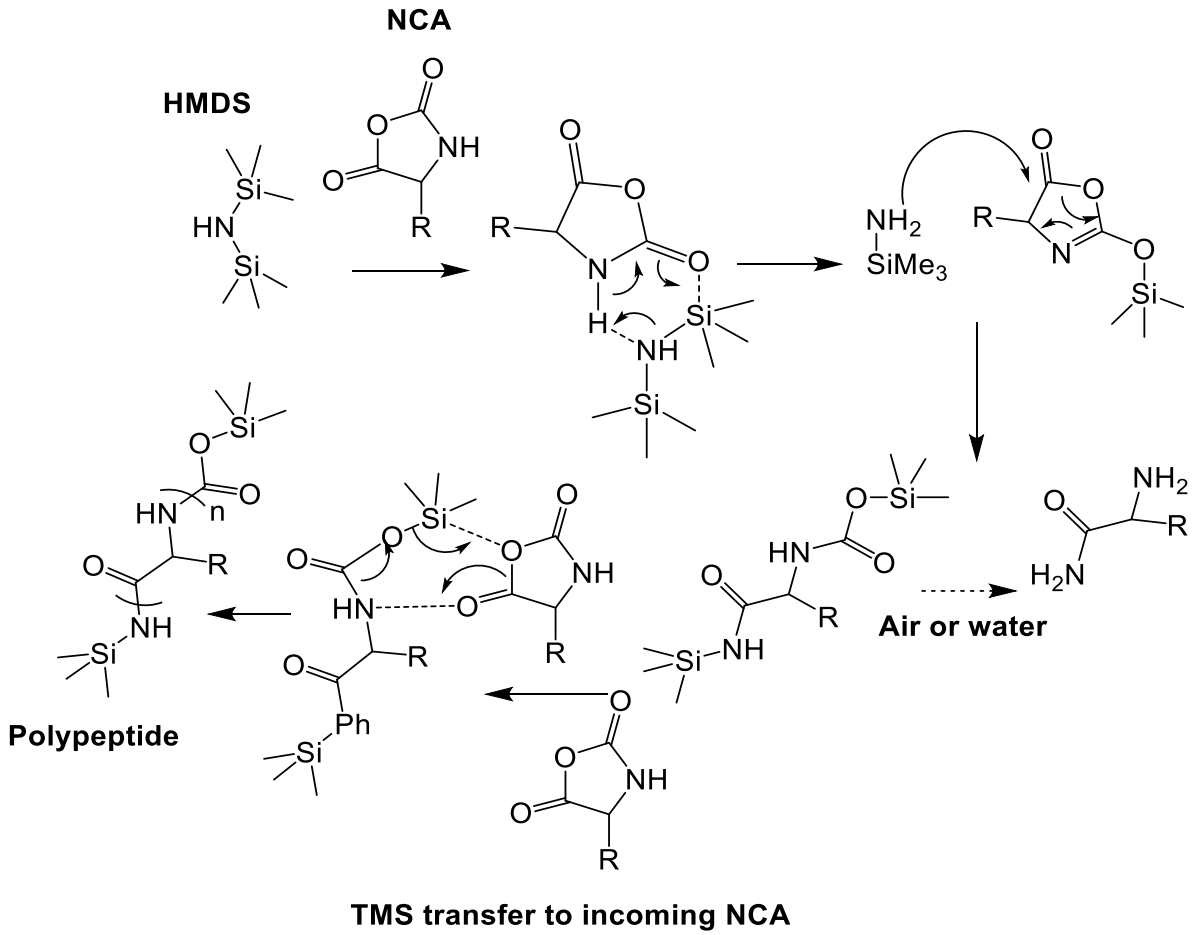

Figure 2.6. Proposed mechanism for NCA ROP polypeptide synthesis using HMDS initiator.

documented. Many exploratory experiments were conducted here, and the results lead to choosing another more facile method, the urethane-derivative mediated NCA ROP, discussed in the next chapter. Nevertheless, first it was pertinent to study the advantages and shortcomings of carbodiimide- and uronium-based coupling as well as direct NCA synthesis and ROP. The first half of experiments in this chapter utilized carbodiimide- and uronium-based reagents, and the second half transitions into NCA ROP-based strategies.

2.2. Experimental

2.2.1. General

All materials were used as received unless otherwise noted. Anhydrous solvents: tetrahydrofuran (THF), acetonitrile (ACN), and methyl ethyl ketone (MEK), and chemicals: fluorescamine, 5Å sieves, and 4-dimethylaminopyridine (DMAP) were purchased from Acros Organics. Anhydrous dimethylformamide (DMF) and hexamethyldisilazane (HMDS) were purchased from Sigma Aldrich. 1-Ethyl-3-(3-dimethylaminopropyl)carbodiimide (EDC), *N,N,N′,N′*-Tetramethyl-*O*-(1*H*-benzotriazol-1-yl)uronium hexafluorophosphate (HBTU), and 1-Hydroxybenzotriazole hydrate (HOBt) were purchased from Advanced ChemTech. Methyoxy PEG Succinimidyl Carbonate 5000 Da (PEG-NHS) was purchased from JenKem Technology. N6-Trifluoroacetyl-L-lysine N-Carboxyanhydride (Lys(TFA)-NCA) was purchased from Toronto research Chemicals Inc. Ethyl acetate and hexanes were purchased from Fisher Scientific and passed through basic alumina column before use for purification of NCAs. All handling of NCA-related materials were handled in 2100 Series Glovebox from Cleatech. ^{1}H NMR spectra were obtained using a Bruker Avance 500 MHz NMR spectrometer. Electrospray

mass spectra were obtained using a Micromass LCT mass spectrometer. Gel permeation chromatography (GPC) spectra were obtained using Agilent 1100 GPC system using 0.1% (v/v) LiBr/DMF solution (1.0 mL/min) as eluent.

2.2.2. Carbodiimide- and uronium-based polymerization strategies

2.2.2.1. Synthesis of *O*-(2-(2-(2,2,2-trifluoroacetamido)ethoxy)propan-2-yl)serine (kSer) and N^6-(2,2,2-trifluoroacetyl)lysine (Lys)

The syntheses of kSer and Lys were performed using previous protocols.[34]

2.2.2.2. Polymerization using various coupling reagents and other conditions

Lys or kSer, structures shown in **Figure 2.7**A, with both N- and C-termini not protected, was polymerized using previously reported protocol having 2.5 equiv EDC and 1 equiv DMAP for every 1 equiv amino acid in DMF at a concentration of 0.1 M for 24 h (**Figure 2.7**B). The molecular weight was determined using gel permeation chromatography (GPC). Uronium salts as the coupling reagent were also tested to compare its efficiency with carbodiimides. 1.5 equiv HBTU was used with 1.5 equiv DIPEA for every 1 equiv amino acid.

Monomer concentration was also increased to 0.2 M to determine if there were any effects on polymerization efficiency when the concentration was doubled. Other exploratory modifications to the procedure included reducing the EDC coupling reagent equiv to 1.5 equiv and 1 equiv DMAP for every 1 equiv amino acid in order to reduce termination events caused by excess coupling reagent.

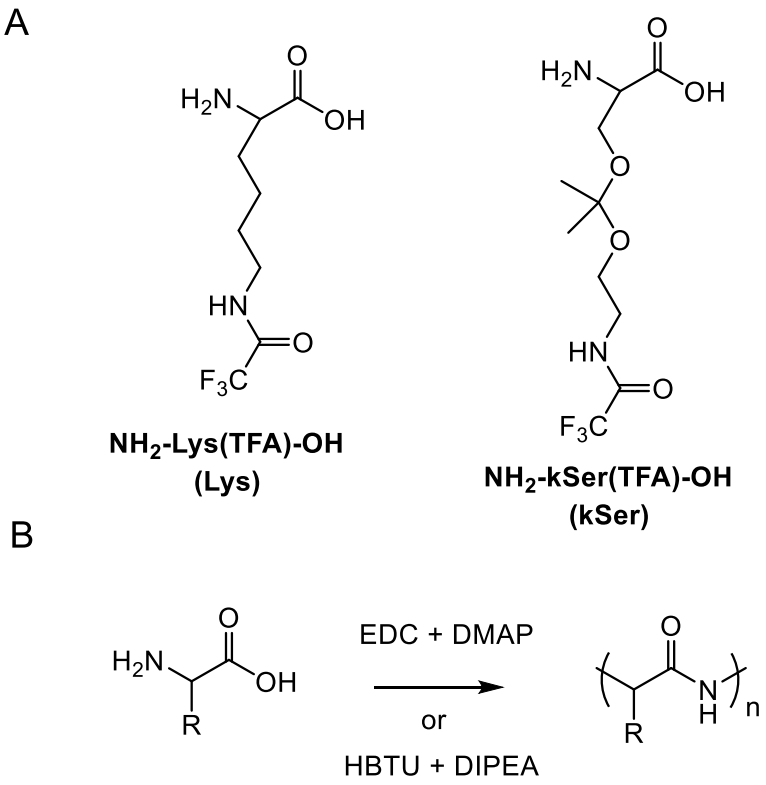

Figure 2.7. A.) Structures of Lys and kSer amino acids. B.) Polymerization of Lys or kSer using EDC or HBTU coupling reagents.

Stepwise monomer addition was performed to test if the polymerization or coupling reagents was still active. To test if the chain terminus was still active after 1 day of polymerization, an additional 20 fold excess of amino acid was added. This was compared with the addition of 20 fold excess amino acids and coupling reagent to see if it was due to the inactivity of coupling reagents that stopped the polymerization.

2.2.2.3. Polymerization using PEG-capping

PEG-NHS (5000 Da) was used to prevent any cyclization that could have been terminating the polymerization since both amino and carboxyl termini were free (**Figure 2.8**). PEG was used since the end goal was to have one of the peptide terminus

PEGylated to increase aqueous solubility of the peptide vector. PEG to amino acids at different molar ratios of 1:5, 1:10, and 1:25 were used to compare the efficiency of increasing molecular weight with one end capped, and the amino acid concentration was kept constant at 0.1 M.

Just as before, to understand if the peptide terminus was still active, 20 equiv of amino acid was added after 24 h of polymerization with and without coupling reagent to also test if the coupling reagent was still active.

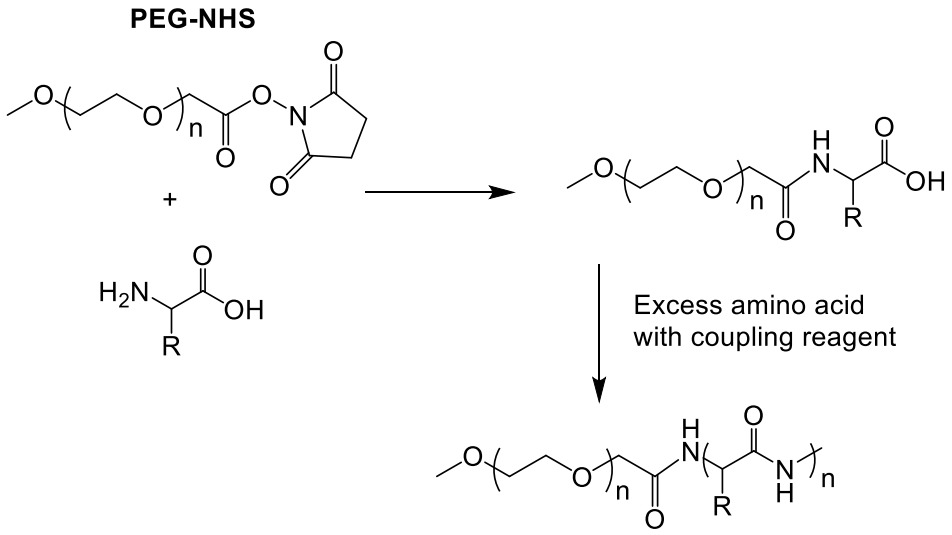

Figure 2.8. Polymerization using PEG end-capping to prevent cyclization.

2.2.2.4. Polymerization using HOBt additive

HOBt was shown as an additive that was efficient at suppressing byproducts that could cause inefficient coupling.[3] Various polymerization conditions and coupling reagents that have been reported elsewhere were tested with HOBt, and the polymerization conditions are summarized in **Table 2.4**. All polymerization reactions included attaching the first amino acid to PEG-NHS and then adding an excess of 20-fold amino acid with coupling reagent and additive.

2.2.3. NCA-based polymerization strategies

2.2.3.1. Synthesis of kSer(TFA)-NCA

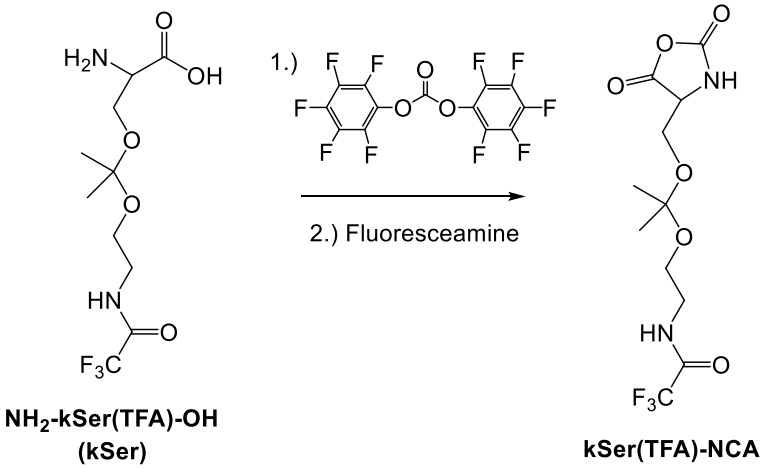

Figure 2.9. Synthesis of kSer(TFA)-NCA.

All procedures related to NCA synthesis or its polymerization were performed in a glovebox infused with dry nitrogen (**Figure 2.9**). 0.51 g of kSer (1 equiv, 1.68 mmol) was dissolved in 16 mL anhydrous THF containing 5Å sieves followed by addition of 0.66 g bis(pentafluorylphenol) carbonate (1 equiv, 1.68 mmol). The reaction was heated to 40 ˚C and stirred for 3h. Following, the product was filtered through glass wool and the solvent removed using high vacuum. The crude product was purified using silica gel column chromatography and eluted using 75% ethyl acetate and 25% hexanes. The product was obtained as a dry light yellow powder (17.2% yield).

^{1}H NMR (DMSO-d_6, 500 MHz): δ 9.47 (t, 1H), 9.02 (s, 1H), 4.66 (t, 1H), 3.67 (m, 2H), 3.57 (m, 2H), 3.44 (m, 2H), 1.27 (s, 6H), yield: 47.6%, ESI-MS $[M+Na]^+$ calcd 351.24, found 351.06.

2.2.3.2. NCA ROP using different monomer/initiator ratios

50 mg of kSer(TFA)-NCA or Lys(TFA)-NCA was dissolved in dry DMF to a concentration of 0.2 M. Subsequently, different amounts of HMDS was added to create monomer to initiator (M/I) ratios of 20, 50, and 100. The polymerization was stirred for 24h before molecular weight analysis using GPC.

Due to unexpected self-polymerization occurring without the use of initiators, amine quenchers (e.g., Fluorescamine) were used to test if free amines were present and initiating the reaction. Fluorescamine was added at different timepoints of the polymerization to assess the kinetics of self-polymerization and to see if this halted the self-polymerization.

2.3. Results and discussion

2.3.1. Carbodiimide- and uronium-based polymerization strategies

2.3.1.1. Effects of various coupling reagents and other conditions

Polymerization was conducted using previously reported protocol.[1] Briefly, non-protected Lys and kSer amino acids (bearing amino and carboxy termini) (1 equiv) was added with EDC (2.5 equiv) and DMAP (1 equiv) in DMF and stirred for 2 days. Surprisingly, using this method, the peptide degree of polymerization (DP) was only roughly 5 although the polydisperisty index (PDI) was low (≤1.21) (**Table 2.1**). Therefore, the uronium coupling reagent, commonly used as a more efficient coupling reagent in solid phase peptide synthesis, HBTU, was also tested, but the DP did not significantly increase to more than 8 (**Table 2.1**). This demonstrates that the termination events occurred.

Table 2.1. Molecular weight of polypeptides synthesized using carbodiimide and uronium coupling reagents

Polymerization conditions	M_n (Da)[a]	M_w (Da)[b]	PDI[c]	DP
1 equiv Lys, 2.5 equiv EDC, 1 equiv DMAP	1,350	1,640	1.21	6
1 equiv kSer, 2.5 equiv EDC, 1 equiv DMAP	1,380	1,650	1.19	5
1 equiv Lys, 1.5 equiv HBTU, 1.5 equiv DIPEA	2,050	2,130	1.04	8

[a,b] Determined by GPC. [c] Calculated by M_w/M_n.

The previously reported protocol used 2.5 equiv of EDC, 1 equiv of DMAP for every 1 equiv of amino acid. An overly excess amount of EDC would form the O-acylisourea to activate the carboxylic acid of the amino acid. However, the competing intramolecular isomerization reaction may occur to form the N-acylurea, which would terminate chain growth. Therefore, a reduction in the amount of EDC to 1.5 equiv was used, and ~8 amino acids were obtained (data not shown). To test if the chain terminus was still active after 1 day of polymerization, an additional 20 fold excess of amino acid was added and resulted in minimal increase of approximately 1 residue, while the addition of 20 fold excess of amino acid in addition to the coupling reagent resulted in the elongation of approximately 1 residue too. This signifies that the chain termination had already occurred within the polymerization time period of 24 h.

Random polymerization is dependent upon many different factors. Among them is the concentration of monomers. Therefore, the effects of monomer concentration on polymerization were tested. The results from GPC analysis showed polymers with molecular weights around ~1,200 to 2,100 Da, indicating that the amino acid residue numbers were ~5-8, shown in **Table 2.2**. The end goal was to reach residue numbers

approximately 20 or higher for efficient complexation with DNA. From the results, the concentration at 0.1 M showed higher molecular weight peptides than at 0.2 for both coupling reagents. Using HBTU was more efficient than using EDC.

2.3.1.2. Effects of PEG-capping on polymerization

Due to both amino group and carboxylic acid group of the amino acid being exposed in the polymerization process, cyclization may have been terminating the chain growth. Because the end goal is to create PEG-peptide block copolymer, PEG was used as a capping agent to prevent cyclization and as the starting point where amino acids would be grown from. Varying molar ratios of PEG to amino acids at 1:5, 1:10, and 1:25 were used to compare the efficiency of increasing peptide length while altogether keeping the amino acid concentration at 0.1 M. The results indicated that the method of using a lower molar ratio of amino acid to PEG was more efficient at growing the peptide chain to greater length (data not shown). The reasoning behind this may be explained by the higher tendency for the amino acids to polymerize with each other than with the PEG-amino acid chain. Therefore, in future studies, PEG was first coupled with 1 amino acid before addition of excess amino acids. This method prevented cyclization on its own end.

PEG-succinimidyl ester (PEG-NHS) of molecular weight 5,000 Da was used as the capping agent to grow the amino acid chain. Polymerization using EDC and DMAP as the coupling reagent, as previously reported, was revisited again while capping the end with PEG-NHS (**Table 2.3**). After 48 hours of polymerization, the number of residues obtained was ~8. Adding 20 equiv more amino acid into the reaction for another 24 hours polymerization resulted in a total of ~9 residues, indicating either a termination had

already occurred or the coupling reagents were no longer active. Adding an excess of 20 equiv amino acid with coupling reagents still produced a total of 9 residues, indicating that the terminus was no longer active.

Table 2.2. Molecular weight of polypeptides using carbodiimmide and uronium coupling reagents at different concentrations

Concentration of amino acid (M)	Coupling reagent	M_n (Da)[a]	M_w (Da)[b]	PDI[c]	DP
0.1	EDC, DMAP	1,340	1,400	1.04	6
0.1	HBTU, DIPEA	2,050	2,130	1.04	8
0.2	EDC, DMAP	1,200	1,340	1.11	5
0.2	HBTU, DIPEA	1,770	1,900	1.07	7

[a,b] Determined by GPC. [c] Calculated by M_w/M_n.

Table 2.3. Molecular weight of polypeptides using carbodiimmide coupling reagents with PEG end capping

Condition	Polymerization conditions	*Coupling reagent	M_n (Da)[a]	M_w (Da)[b]	PDI[c]	DP
--	PEG-NHS	--	4,000	4,260	1.06	--
A	PEG-NHS was activated with 1 equiv aa, followed by 20 fold aa	1.5 equiv EDC, 1 equiv DMAP	5,370	5,900	1.10	8
--	Addition of 20 equiv aa to condition A	None	5,490	6,040	1.10	9
--	Addition of 20 equiv aa to condition A	1.5 equiv EDC, 1 equiv DMAP	5,510	6,040	1.09	9

[a,b] Determined by GPC. [c] Calculated by M_w/M_n. Amino acid is abbreviated as aa

2.3.1.3. Polymerization using HOBt additive

HOBt was shown as an additive that was efficient at suppressing byproducts.[3] Therefore, different polymerization conditions and coupling reagents were used in conjunction with HOBt, and the results are summarized in **Table 2.4**. All polymerization reactions included attaching the first amino acid to PEG-NHS and then adding an excess of 20-fold amino acid. The results in **Table 2.4** showed that using HBTU, HOBt, and DIPEA was able to consistently achieve greater than 10 residues. However, the DP was still not as high as desired.

Table 2.4. Molecular weight of polypeptides using carbodiimmide and uronium coupling reagents with HOBt additive

Polymerization conditions	M_n (Da)[a]	M_w (Da)[b]	PDI[c]	DP
3 equiv EDC and 2.2 equiv HOBt	7,070	7,660	1.08	10
1 equiv HBTU, 1 equiv HOBt, 2 equiv DIPEA	6,880	7,560	1.09	11
Adding 50 fold excess instead of 20 using the above EDC and HOBt reagents	6,750	7,110	1.05	11
Adding 50 fold excess instead of 20 using the above HBTU, HOBt, DIPEA coupling reagents	6,680	7,560	1.13	10
1 equiv HCTU, 1 equiv HOBt, 2 equiv DIPEA	5,740	6,200	1.08	6
1.5 equiv EDC, 3 equiv HOBt	6,240	3,920	1.10	9

[a,b] Determined by GPC. [c] Calculated by M_w/M_n.

2.3.2. NCA ROP-based polymerization strategies

2.3.2.1. Synthesis of kSer(TFA)-NCA

Bis(pentafluorophenyl)carbonate was tested for the preparation of kSer(TFA)-NCAs. Solvents having different polarity, including THF, MEK, DMF, and ACN, were also tested since the reaction rate significantly depended on the polarity. Reacting bis(pentaflurophenyl)carbonate (1 equiv) with kSer (1 equiv) in THF at 40˚C for 3 h resulted in the desired NCA.

2.3.2.2. NCA ROP using different monomer/initiator ratios

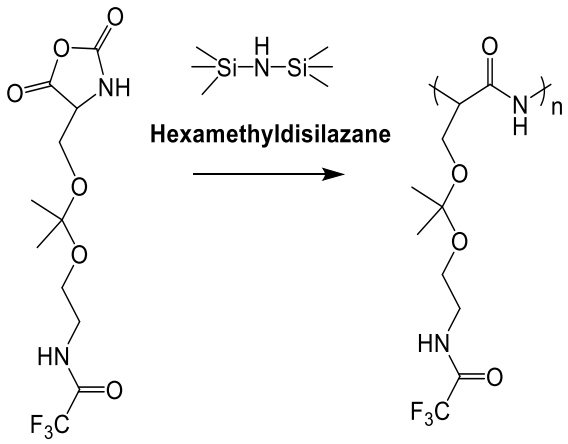

Figure 2.10. Hexamethyldisilazane-initiated NCA ROP.

Lys(TFA)-NCA and kSer(TFA)-NCA were polymerized at different M/I ratios (e.g., 20, 50, and 100) using HMDS as the initiator (**Figure 2.10**). Surprisingly, the DP did not match the feed ratio except for kSer at M/I 20 and Lys at M/I 50 (**Table 2.5**). The trend of increasing molecular weight with increasing M/I ratio and DP being close to the expected M/I output (e.g. DP of 100 for M/I of 100) was not observed. Therefore, the reason for uncontrolled polymerization was explored. A control utilizing only NCAs without initiator was also tested, and surprisingly, polymerization occurred. The DP for Lys and kSer

indicates that out of 143 Lys(TFA)-NCAs molecules, one acted as an initiator, while the same occurred with one out of 20 kSer(TFA)-NCAs molecules.

In order to control the polymerization, it was necessary to explore what was causing the self-polymerization. Therefore, if it undergoes the amine mechanism, introducing amine inhibitors like fluorescamine would inhibit polymerization. Indeed, when fluorescamine was added at different timepoints to the Lys sample, polymerization was quenched (**Table 2.6**). This also indicates that the self-polymerization was not spontaneous and slow to complete since it was after 13 h that the peptide had 44 residues out of 56 when quenching was not performed. It was hypothesized that half-life of NCA and HMDS and its sensitivity to moisture played an important role in producing unwanted amines by reverting back to amino acids (with amino and carboxyl termini) after hydrolysis of NCAs and causing the uncontrolled polymerization.

Table 2.5. Molecular weight of polypeptides using NCA ROP with different M/I ratios

Amino acid	M/I ratio	M_n (Da)[a]	M_w (Da)[b]	PDI[c]	DP
kSer	No initiator	5,470	7,430	1.35	19
kSer	20	5,170	6,700	1.29	18
kSer	50	3,570	5,220	1.46	13
kSer	100	3,250	4,450	1.36	12
Lys	No initiator	31,810	37,220	1.17	142
Lys	20	9,380	11,840	1.26	42
Lys	50	12,000	15,590	1.29	53
Lys	100	14,460	18,600	1.28	64

[a,b] Determined by GPC. [c] Calculated by M_w/M_n.

Table 2.6. Molecular weight of poly(Lys) at different time points after quenching amines

Time of quenching	M_n (Da)[a]	M_w (Da)[b]	PDI[c]	DP
None	12,660	15,470	1.22	56
30 min	--	--	--	--
3.5 h	2,630	3,050	1.16	12
6 h	7,760	9,350	1.20	35
13 h	9,980	12,550	1.25	44

[a,b] Determined by GPC. [c] Calculated by M_w/M_n.

2.3.3. Significance of findings

The exploratory experiments utilizing carbodiimides, uronium coupling reagents, and NCAs did not efficiently polymerize poly(kSer) to very high DPs of greater than 20 as desired. Polymerization conducted using carbodiimides can cause terminations due to formation of O-acylisourea rearrangement to N-acylurea. Likewise, polymerization using uronium salts can also undergo terminations when a guanidine derivative forms. PEG-capping was hypothesized to rule out any cyclization events occurring, but still did not yield high molecular weight peptides due to the inefficiency of the coupling reagents in solution phase. Adding HOBt as an additive did moderately increase the DP but not to the desired length. Therefore, NCA ROP method was tested. NCA ROP has been reported to be very efficient. However, acid-labile NCAs cannot be synthesized using conventional approaches using phosgene. A different route using bisarylcarbonates was able to retrieve kSer(TFA)-NCAs. Nevertheless, there were problems associated with controlling the DP. This is hypothesized to be correlated with its moisture sensitivity since self-polymerization events were observed, indicating initiation from contaminants.

Because these problems were encountered which prevents polymerizing to high molecular weights, another method was tested, which will be discussed in Chapter 3.

2.4. References

[1] M. S. Shim and Y. J. Kwon, *Biomaterials*, **2010**, 31, 3404.

[2] O. Marder and F. Albericio, *Chimica Oggi*., **2003**, 1.

[3] A. Okamura, T. Hirai, M. Tanihara and T. Yamaoka, *Polymer*, **2002**, 43, 3549.

[4] M. E. Martin and K. G. Rice, *AAPS. J*., **2007**, 9, 18.

[5] L. V. Dubey and I. Y. Dubey, *Ukrainica Bioorganica Acta*., **2005**, 1, 13.

[6] Y. Fujita, K. Koga, H.-K. Kim, X.-S. Wang, A. Sudo, H. Nishida and T. Endo, *J. Polym. Sci. A1***, 2007**, 45, 5365.

[7] S. H. Wibowo, A. Sulistio, E. H. H. Wong, A. Blencowe and G. G. Qioa, *Chem. Comm*., **2014**, 50,4971.

[8] J. Cheng and T. J. Deming, *Top. Curr. Chem*., **2011**, 1.

[9] H. Lu and J. Cheng, *J. Am. Chem. Soc*., **2007**, 129, 14114.

Chapter 3: Facile synthesis of high molecular weight acid-labile polypeptide using amino acid urethane derivatives

This chapter has been reproduced and slightly modified from:
Wong, S., Kwon, Y. J. (2015), Facile synthesis of high-molecular-weight acid-labile polypeptides using urethane derivatives. J. Polym. Sci. Pol. Chem., 53: 280-286.
with permission from Wiley Periodicals, Inc.

3.1. Introduction

Polypeptides are biodegradable, biocompatible polymers consisting of amino acid building blocks which make them easily engineered for various biomimetic activities.[1] Their molecular versatility and biocompatibility makes them suitable for many biomedical applications, such as drug and gene delivery, tissue engineering, sensors and biodiagnostics, and antibiotics.[2–5] Recently, materials that transform in response to biological stimuli have been increasingly investigated for biomedical applications.[6–8] For instance, various materials have been developed to target cancer, where mildly acidic extracellular pH is a hallmark trait of the disease.[6] In addition, intracellular delivery of biomacromolecular therapeutics such as proteins and nucleic acids from the acidic endosome/lysosome is a key design feature in nanomedicine.[9,10] Acid-labile linkers such as acetal, hydrazone, orthoester, and imine moieties, have been employed onto drug carriers in order to achieve accelerated degradation of polymeric carriers and rapid

payload release when induced by the acidic conditions in cancerous tissues or in the endosomal/lysosomal compartment.[11–15]

Tailoring acid-responsive features onto a natural polypeptide backbone has not been popularly investigated due to limited peptide chemistry that allows efficient polymerization of acid-labile amino acid monomers. Recently we synthesized an acid-responsive cationic polypeptide, poly(ketalized serine) (poly[kSer]), that reverts itself into natural and neutral poly(Ser) under acidic stimuli for gene delivery applications.[8] Although the peptide was moderately short (22 amino acid residues), its PEGylated version, PEG-poly(kSer), was able to efficiently release nucleic acid cargo upon acid-hydrolysis of ketal linkages in the endosome upon transformation into poly(Ser), displaying minimal cellular toxicity.

Generally, greater molecular interactions with nucleic acids (e.g., complexation) can be achieved by high molecular weight polymers, requiring the development of an efficient polymerization strategy to obtain large polypeptides with well-defined structural homogeneity and desired functionality (e.g., acid-hydrolysis for cargo release).[16] To date, much research has been conducted in both solid and solution phase peptide chemistry to maximize polymerization efficiencies.[16–18] The solid phase approach is generally used to synthesize small polypeptides containing few dozens amino acids with specific sequences due to truncations that may result from inefficient coupling or deprotection steps as the molecular weight increases.[18,19] On the contrary, solution phase peptide synthesis is capable of synthesizing high molecular weight polypeptides, many reaching beyond 100 residues. Nevertheless, overwhelming difficulties arise when synthesizing high molecular weight acid-labile polypeptides using either solid or solution phase

approach, since most often the currently available peptide chemistries work against keeping the acid-labile moieties intact.[20] Moreover, utilizing acid is very common during solid phase peptide synthesis for deprotection or cleaving off from the resin, making this method impractical for synthesis of acid-labile polypeptides. The most reliable and straightforward approach for creating homo and di-block polypeptides is using *N*-carboxyanhydride (NCA) ring-opening polymerization (ROP).[16]

NCA ROP method also has its limitations when synthesizing polypeptides with acid-labile functionality (**Table 3.1**). Most commonly, NCAs are prepared by treating amino acids with phosgene or phosgene derivatives (triphosgene) that release a highly corrosive hydrochloric acid (HCl) gas that affects acid-labile groups.[20,21] Phosgene-free synthesis using bisarylcabonates have also been attempted to prepare NCAs, where they release phenols rather than HCl.[20] However, usage of NCAs still requires very careful handling such as ensuring water- and amine-free conditions.[22] Unwanted oligomerization often occurs during the preparation of NCAs using bisarylcarbonates, and depending on the properties of the NCA it may be difficult to purify it by recrystallization.[20] Flash chromatography under inert atmosphere (e.g., nitrogen) is an alternative method for NCA purification, but it is time- and labor-intensive and hardly desirable.[23]

Recently, urethane derivatives of amino acids have been reported as an alternative to using NCA monomers to synthesize high molecular weight polypeptides.[21,24–26] Urethane derivatives are stable enough for prolonged purification and storage with minimal caution to moisture or heat sensitivity, overcoming major limitations of producing and utilizing NCAs at a practical scale.[25,27] Since urethane derivatives of amino acids still proceed as NCA intermediates through intramolecular cyclization, the polymerization is

Table 3.1. Pros and cons towards polymerization methods utilizing NCA ROP to synthesize high molecular weight acid-labile polypeptide

Description of monomers	Pros	Cons
NCAs prepared via phosgene	▪ Efficient formation of NCA	▪ Acid from monomer synthesis is not compatible with acid-labile groups ▪ Usage of highly toxic materials ▪ High moisture sensitivity
NCAs prepared via bisarylcarbonates	▪ Phosgene-free ▪ Release of non-corrosive phenol rather than HCl gas	▪ Oligomerization ▪ Difficult purification ▪ High moisture sensitivity
NCAs formed via urethane derivatives	▪ Stable, isolatable ▪ Moisture-insensitive urethane derivative monomers	▪ High moisture sensitivity of NCA intermediates ▪ Requires restrictive conditions for NCA formation (elevated temperatures, highly polar solvents)

still very effective. However, using extremely polar solvents like anhydrous dimethylsulfoxide (DMSO), anhydrous dimethylformamide (DMF), and anhydrous dimethylacetamide (DMAc) under anhydrous conditions at elevated temperatures for intramolecular NCA formation may still be a remaining drawback for this method of polymerization, particularly for acid-labile ones.[27] While investigating the synthesis of poly(kSer) utilizing urethane derivatives, we discovered rapid polymerization under mild, unrestrictive, and practical polymerization conditions, such as at room temperature and in various solvents even with exposure to the atmosphere. Various parameters that affect polymerization were investigated and optimized. The highly facile synthesis strategy

working under a broad spectrum of easily achievable conditions can be exploitable for polymerization of various amino acids that tend to be sensitive toward moisture and elevated temperatures or have poor solubility in certain solvents.

3.2. Experimental

3.2.1. General

All chemicals purchased from various vendors were used as received without further purification. Anhydrous acetonitrile (ACN), anhydrous tetrahydrofuran (THF), anhydrous ethyl acetate (EtOAc), dichloromethane (DCM), tetrabutylammonium hydroxide, diphenyl carbonate, 5 Å molecular sieves, triethylamine (TEA), and pyridinium p-toluenesulfonate (PPTS) were purchased from Acros Organics. Anhydrous DMF and DMSO were purchased from Sigma Aldrich. Anhydrous DMAc was purchased from Alfa Aesar. O-*tert*-Butyl-L-serine was purchased from Chem-Impex International, Inc. Trifluoroacetic acid (TFA), HCl, and anhydrous magnesium sulfate were purchased from Fisher Scientific. ^{1}H NMR spectra were obtained using a Bruker Avance 500 MHz NMR spectrometer. Electrospray mass spectra were obtained by using a Micromass LCT mass spectrometer. For the determination of molecular weight of polypeptide, AB SCIEX MALDI TOF-TOF 5800 instrument was used. All polymerized polypeptides were subjected to deprotection of trifluoroacetyl group in 1 M NaOH overnight to obtain final peptide before molecular weight measurement. The samples were prepared using 2,5-dihydroxybenzoic acid as matrix material. The samples were irradiated with 349 nm of diode-pumped solid state Nd:YAG laser and detected on linear high mass positive mode. For the molecular weight analysis, both M_n and M_w and polydispersity index (PDI) (M_w/M_n)

was calculated using Data Explorer software. First, the molecular weight distribution was gated followed by its peak detection. Then, applying the Polymer Analysis Toolbox function, the gated range was calculated for M_n, M_w, and PDI. The degree of polymerization (DP) was estimated based on the molecular weight of the individual amino acid residue. Synergy H1 Hybrid Multi-Mode Microplate Reader was used for spectroscopic analysis.

3.2.2. Synthesis and characterization

3.2.2.1. Synthesis of 3-Hydroxy-2-(phenoxycarbonylamino)propionic acid (Compound 1)

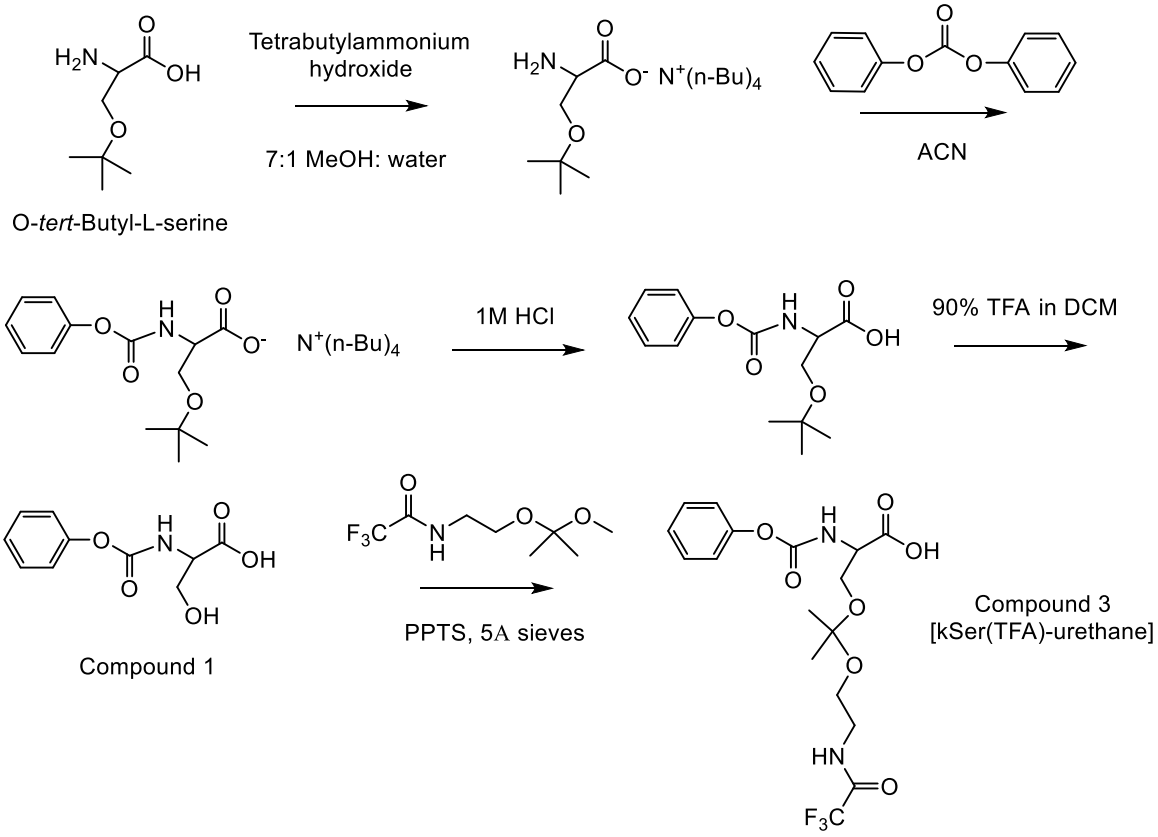

Figure 3.1. Synthesis of kSer(TFA)-urethane derivative monomer.

To a solution of O-*tert*-Butyl-L-serine (5 g, 31 mmol, 1 equiv) in 87 mL ACN and 12 mL water, tetrabutylammonium hydroxide (8.04 g, 31 mmol, 1 equiv) was added (40% in MeOH) (**Figure 3.1**). After stirring for 1 h at room temperature, the solvent was evaporated under high vacuum. The resulting residue was re-suspended in 62 mL ACN and 7 mL water and added dropwise to a solution of diphenyl carbonate (6.63 g, 31 mmol, 1 equiv) in 62 mL ACN and stirred for 12 h, followed by adding 33 mL of 1 N HCl. The mixture was transferred into a separation funnel containing 75 mL ethyl acetate and 75 mL water, and the aqueous layer was extracted three times with 75 mL ethyl acetate. The organic fractions were combined and dried over magnesium sulfate. The evaporated suspension was then dissolved in 1 mL DCM, and 9 mL trifluoroacetic acid was added to deprotect the *tert*-butyl group for 3 h at room temperature. The product was purified by silica gel column chromatography using 3:1 ethyl acetate:hexane as eluent. The product was obtained as white solid (42.9% yield).

^{1}H NMR (500 MHz, DMSO-d_6, δ): 3.75 (m, 2H), 4.134 (m, 1H), 4.87 (s, 1H), 7.11–7.13 (d, 2H), 7.22 (t, 1H), 7.40 (t, 2H), 7.85–7.87 (d, 1H), 12.78 (s, 1H) (Supporting Information in Appendix A **Figure A3.1**). (ESI, m/z): $[M + Na]^+$ calcd for $C_{10}H_{11}NO_5$, 248.20; found, 248.03.

3.2.2.2. Synthesis of 2,2,2-Trifluoro-1-[2-(1-methoxy-1-methylethoxy)-ethylamino]-1-ethanone (Compound 2)

Compound 2 in **Figure 3.1** was synthesized according to the procedures as previously reported.[8]

3.2.2.3. Synthesis of 3-{1-Methyl-1-[2-(2,2,2-trifluoroacetylamino)-ethoxy]ethoxy}-2-(phenoxycarbonylamino)propionic acid (Compound 3; kSer(TFA)-urethane)

Compound 1 (1.30 g, 5.77 mmol, 1 equiv) was dissolved in 10 mL THF followed by the addition of PPTS (0.43 g, 1.73 mmol, 0.3 equiv) (Scheme 1). After stirring for 5 min, 5 Å molecular sieves were added to the reaction mixture. After another 5 min stirring, Compound 2 (1.98 g, 8.65 mmol, 1.5 equiv) was added dropwise and stirred for 24 h. After sieves were filtered, the product was purified using silica gel column chromatography using 1:3 methanol: ethyl acetate as eluent with addition of 0.3% (v/v) TEA in the eluent solvent. The product was obtained as light yellow oil (38.0% yield).

^{1}H NMR (500 MHz, DMSO-d_6, δ): 1.28 (s, 6H), 3.28 (m, 1H), 3.47 (m, 2H), 3.61 (m, 1H), 3.68-3.72 (m, 2H), 3.98 (m, 1H), 7.10-7.11 (d, 2H), 7.21 (t, 1H), 7.31 (d, 1H), 7.39 (t, 2H), 9.92 (s, 1H). (ESI, m/z): $[M + Na]^+$ calcd for $C_{17}H_{21}F_3N_2O_7$, 445.35; found, 445.09.

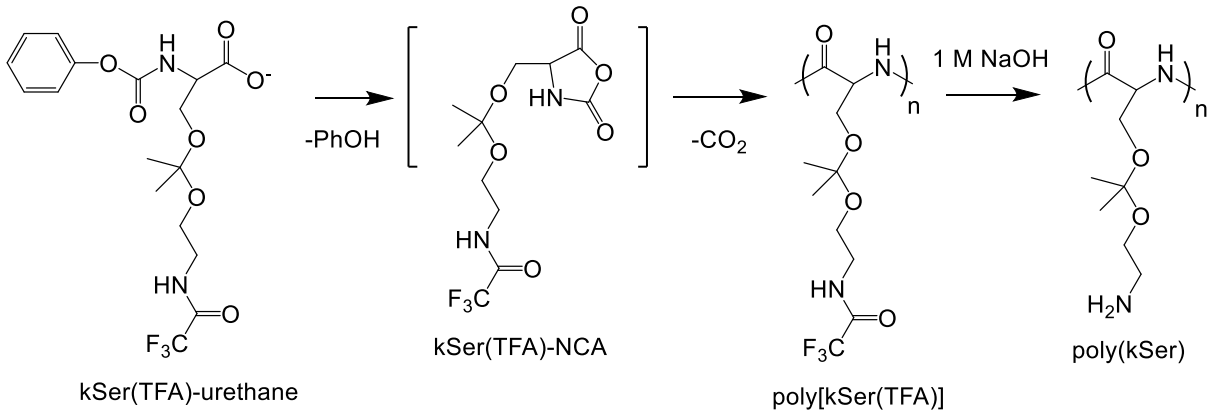

Figure 3.2. Synthesis of poly(kSer) via polymerization of kSer(TFA)-urethane, followed by TFA-deprotection.

3.2.3. Effects of various conditions on polymerization

kSer(TFA)-urethane was polymerized to form poly[kSer(TFA)] under various conditions, and the resulting polypeptides were deprotected for TFA group in order to obtain poly(kSer) (**Figure 3.2**).

3.2.3.1. Temperature and solvent

kSer(TFA)-urethane (23 mg, 55.2 mmol) was added to an oven-dried 4 mL shell vial and placed under high vacuum (2 x10^{-3} mBar) for 5 min. Next, 0.2 mL ACN was added to the reaction vial and the reaction was stirred for 12 h at 4 °C, 25 °C, and 60 °C. Additional solvents, including those of moderate polarity (EtOAc and THF) and high polarity (DMAc, DMF, DMSO), were also used instead of ACN.

3.2.3.2. Atmosphere

To a reaction of kSer(TFA)-urethane (23 mg, 55.2 mmol) in 0.2 mL ACN, the atmosphere was either left alone to air in a closed system, filled continuously with N_2 after three cycles of purge and refill, or subjected to a vacuumed closed system. ACN was added and stirred for 12 h at 25 °C. ACN was used for the remaining studies due to its efficient polymerization and ease of handling (e.g., fast evaporation for subsequent steps).

3.2.3.3. Kinetics

At different polymerization time points, 100 µL samples were obtained, and solvent was removed through high vacuum prior to adding 1 M NaOH for deprotection overnight and analyzed for molecular weight.

3.2.3.4. Concentration

kSer(TFA)-urethane (12, 23, 46, or 92 mg) was placed under high vacuum for 5 min before 0.2 mL ACN was added to the reaction vial. The resulting concentrations for polymerization were 0.138, 0.276, 0.55, and 1.1 M, respectively. The reaction was stirred for 12 h at 25 °C followed by molecular weight measurement as described earlier.

3.2.3.5. Conversion (polymerization efficiency) estimation

The percent conversion was assessed by spectroscopic analysis measuring the remaining kSer(TFA)-monomer after 12 h polymerization, which has maximum absorbance at 350 nm. The percent conversion was calculated using a standard curve of kSer(TFA)-urethane monomer.

3.3. Results and discussion

3.3.1. Synthesis of acid-cleavable kSer(TFA)-urethane monomer

Urethane derivative of TFA-protected ketalized serine, kSer(TFA)-urethane, was synthesized as shown in Scheme 1. kSer(TFA)-urethane monomer was purified by silica gel column chromatography. Due to the possibility of hydrolyzing ketal linkages in the slightly acidic silica gel column, a small amount of TEA (0.3% v/v) was added in the elution solvent. The obtained kSer(TFA)-urethane was found to be in a deprotonated carboxylate form and associated with protonated TEA, as confirmed by ^{1}H NMR detecting the presence of protonated TEA at 1.14 ppm (t, 9H) and 2.96 ppm (q, 6H) (**Figure. 3.3**). These remaining peaks after subjecting to high vacuum for several hours indicates strong molecular association of kSer(TFA)-urethane with TEA, presumably as salt of anion and

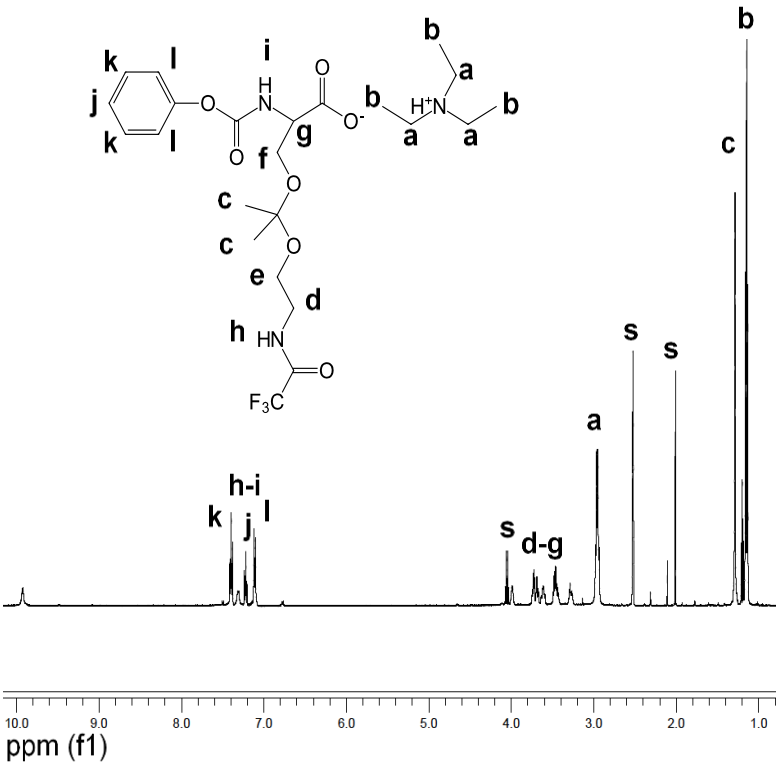

Figure 3.3. ^{1}H NMR of kSer(TFA)-urethane.

cation. In earlier literature, addition of increasing amounts of base externally from 2 to 10 mol % increased the kinetics of NCA ROP polymerization.[27] In the study reported here, the base (e.g., TEA) was required in column chromatography for the purification of kSer(TFA)-urethane, thus removing the need for adding base later during polymerization. Additional evidence from electrospray MS shows the mass of kSer(TFA)-urethane associated with base at 524.21. The presence of kSer(TFA)-urethane in its carboxylate form implicates faster polymerization due to its higher reactivity than its protonated carboxylic acid counterpart.

3.3.2. Temperature effects on kSer(TFA)-urethane polymerization

As previously reported for the investigation on urethane-type derivatives of amino acids, selective heating in polar solvents leads to intramolecular cyclization to form NCA intermediates for polymerization.[27] These conditions were necessary to supply sufficient thermal energy in conjunction with polar aprotic solvents to favor the carboxylic acid to react with the urethane carbonyl. It was also reported that merely heating to 60 °C in medium polar solvents such as THF and EtOAc only resulted in the formation of NCAs without further polymerization.[27] Therefore, this temperature and solvent dependency of kSer(TFA)-urethane polymerization was first investigated, since urethane amino acids in their carboxylate form may now be more nucleophilic and prone to intramolecularly cyclize without additional influence. Indeed, when kSer(TFA)-urethane was polymerized at various temperatures ranging from 4 °C to 60 °C, polymerization occurred at all temperatures and gave polymers with high molecular weights (>25 kDa) and DP of 135–145 with narrow PDI of less than 1.14 (**Table 3.2**).

Table 3.2. Effects of temperature on polymerization of kSer(TFA)-urethane

Temperature (˚C)	M_n (Da)[a]	M_w (Da)[b]	PDI[c]	DP	Conversion (%)[d]
4	26,800	29,400	1.09	142	44
25	27,400	30,900	1.13	145	36
60	25,400	27,800	1.09	135	--

[a,b] Determined by MALDI-TOF after TFA de-protection. [c] Calculated by M_w/M_n.
[d] Determined by UV-Vis Absorbance.

When examining conversion through spectroscopic analysis of remaining monomers (max absorbance at 350 nm), the polymerization at 4 °C had slightly greater

conversion than at room temperature (44% compared with 36%). Therefore, it is speculated that since the carboxylated monomers are highly reactive, lowering the temperature preserves the stability of kSer(TFA)-urethane or prolongs the NCA intermediate, such that it can be incorporated into the polypeptide chain.

Previous studies on NCA ROP have reported that lowering the reaction temperature decreased the end group termination and side-reactions,[28,29] which could have also resulted in slightly higher conversion. At elevated temperatures of 60 °C, a slight yellow color change that interferes with spectroscopic analysis was also noticed and ^{1}H NMR spectra indicated a partial (25% loss) hydrolysis of ketal groups compared with polymerization conducted at lower temperatures (Supporting Information in Appendix A **Figure A3.2**). Although the overall conversion is moderate, this method still allows polymerization at lower temperatures to achieve high molecular weight peptides with a narrow molecular weight distribution while preserving acid-degradable moieties intact.

3.3.3. Solvent effects on kSer(TFA)-urethane polymerization

When examining the polymerization of kSer(TFA)-urethane in various solvents with different polarities, high molecular weight polymers were obtained in all solvents tested (**Table 3.3**). A previous study reported efficient polymerization of amino acid urethane derivative only in highly polar aprotic solvents like DMSO, DMF, and DMAc because it favored the nucleophilic attack of the carboxyl group on the urethane carbonyl.[27] On the contrary, the carboxylate form of kSer(TFA)-urethane is a stronger nucleophile and results in its cyclization regardless of solvent polarity. However, when examining its conversion, solvents with high polarity still yielded greater conversion. This

may be due to better solubility of kSer(TFA)-urethane and polypeptide in more polar solvents. This method for amino acid polymerization is advantageous because it is applicable in a diverse array of solvents that best meets the solubility of the monomer.

Table 3.3. Effects of solvent on polymerization of kSer(TFA)-urethane

Solvent	M_n (Da)[a]	M_w (Da)[b]	PDI[c]	DP	Conversion (%)[d]
THF	27,200	29,800	1.09	144	17
EtOAc	18,600	20,000	1.07	99	14
ACN	27,400	30,900	1.13	145	36
DMF	26,200	29,600	1.13	139	40
DMAc	28,800	32,400	1.12	153	40
DMSO	35,800	41,700	1.17	190	42

[a,b] Determined by MALDI-TOF after TFA de-protection. [c] Calculated by M_w/M_n.
[d] Determined by UV-Vis Absorbance.

3.3.4. Atmosphere effects on kSer(TFA)-urethane polymerization

Since NCAs are highly moisture-sensitive, and anhydrous and inert atmosphere are required for efficient NCA ROP, the relationship between polymerization atmospheres required for kSer(TFA)-urethane polymerization and polymerization efficiency was also investigated. Polymerization conducted in three different systems was examined: in a closed system with air, under continuous N_2 after being purged, and in vacuum conditions. Earlier studies have reported improvements to controlling NCA ROP polymerization when subjected to vacuum, by successfully removing the CO_2 byproduct in order to drive the polymerization forward and produce fewer chain end terminations.[30,31] The kinetics of

kSer(TFA) polymerization in these three conditions were simultaneously examined. Surprisingly, under all conditions tested, poly(kser) of high molecular weights were obtained (**Table 3.4**). The rate of polymerization was very rapid for all cases, completing within 15 min (Supporting Information in Appendix A **Table A3.1**). The reason why polymerization was able to occur under all atmospheres tested may be due to its rapid completion driven by its higher reactivity. A previous report on NCA ROP demonstrated that significantly accelerated polymerization rates can minimize the side reactions/terminations that moisture may introduce.[30] A speedy polymerization method that results in narrow polydispersity of less than 1.2 yet obtaining high-molecular-weight peptides is desirable in synthesizing acid-labile polypeptides.

Table 3.4. Effects of atmosphere on polymerization of kSer(TFA)-urethane

Solvent	M_n (Da)[a]	M_w (Da)[b]	PDI[c]	DP	Conversion (%)[d]
Air	36,300	41,900	1.15	192	42
Nitrogen	41,200	44,400	1.17	219	31
Vacuum	37,500	42,400	1.13	199	38

[a,b] Determined by MALDI-TOF after TFA de-protection. [c] Calculated by M_w/M_n.
[d] Determined by UV-Vis Absorbance.

3.3.5. Concentration effects on kSer(TFA)-urethane polymerization

Finally, the effect of concentration on kSer(TFA) polymerization was studied (**Table 3.5**). At all concentrations tested, peptides of molecular weights greater than 17 kDa were obtained. As concentration increases from 0.138 to 0.55 M, molecular weight also increases. However, at 1.1 M, where concentration reaches saturation (indicated by

partial precipitation; data not shown), the molecular weight drops. Therefore, kSer(TFA)-urethane efficiently polymerized only when fully dissolved in solvents. At a low concentration (e.g., 0.138 M), polymerization of kSer(TFA)-urethane was slower than higher concentrations, resulting in a low molecular weight (e.g., ~18 kDa) with a low PDI (e.g., 1.11). On the contrary, polymerization at a high concentration (e.g., 0.55 M) synthesized poly(kSer) with a high molecular weight (e.g., ~37 kDa) with a slightly increased PDI (e.g., 1.14). Generally, among the tested conditions, 0.276 M seemed to be the optimized concentration for polymerization of kSer(TFA) to obtain poly(kSer) with a high DP of 145, a relatively low PDI of 1.13, and a higher conversion rate of 36%.

Table 3.5. Effects of concentration on polymerization of kSer(TFA)-urethane

Concentration (M)	M_n (Da)[a]	M_w (Da)[b]	PDI[c]	DP	Conversion (%)[d]
0.138	17,900	19,800	1.11	95	32
0.276	27,400	30,900	1.13	145	36
0.55	36,600	41,600	1.14	194	26
1.1	22,500	25,800	1.15	119	29

[a,b] Determined by MALDI-TOF after TFA de-protection. [c] Calculated by M_w/M_n.
[d] Determined by UV-Vis Absorbance.

3.3.6. Significance and implications of kSer(TFA)-urethane polymerization

The polymerization method described here utilizing carboxylated urethane derivatives of kSer(TFA) demonstrated successful synthesis of high molecular weight acid-labile polypeptides in mild conditions. The temperature for polymerization at room temperature and below proved to be advantageous, causing neither degradation of acid-

labile groups nor premature termination of the polymerization that tends to severely limit polypeptide molecular weight. The solvent used for polymerization does not need to be restricted to highly polar aprotic solvents but selected as the one that best meets the solubility of the monomer. Additionally, rapid completion of the polymerization does not necessitate the strict use of inert atmospheres. The implications of the polymerization strategy investigated in this study provide stable, easily handled synthesis of high-molecular weight acid-labile polypeptides using amino acid urethane derivatives that are capable of undergoing facile polymerization in highly permissive conditions (**Figure 3.4**). Incubation of poly(kSer) in 1 M HCl for 4 h at room temperature resulted in a approximately 50% decrease in molecular weight, indicating acid-responsive cleavage of ketal linkages (Supporting Information in Appendix A **Table A3.2**).

3.4. Conclusions

Use of acid-responsive polypeptides in biomedical applications has been hampered by limited synthesis methods. A new method that utilizes urethane derivatives of amino acids was developed in order to overcome challenges in the synthesis of high molecular-weight acid-labile peptides that conventional methods fail to accomplish. Acid-cleavable kSer(TFA)-urethane monomers synthesized in a carboxylate form showed the ability to undergo rapid polymerization under atmospheric conditions with negligible sensitivity to moisture. The temperature did not need to be elevated nor was the polymerization selective to highly polar solvents. Polymerization under air, N_2, or vacuum all proceeded in a rapid manner, completing in minutes. The high molecular weight poly(kSer) (DPs >100) with narrow PDIs was obtained with a moderate conversion.

Precisely controlled molecular weight and elucidated initiation mechanisms of kSer(TFA)-NCA polymerization (e.g., normal amine vs. activated monomer pathways) have yet to be explored in subsequent studies. This study demonstrates promises of a practical synthesis strategy for preparing acid-labile polypeptides by circumventing highly selective and restrictive conditions required by the conventional polypeptide synthesis methods.

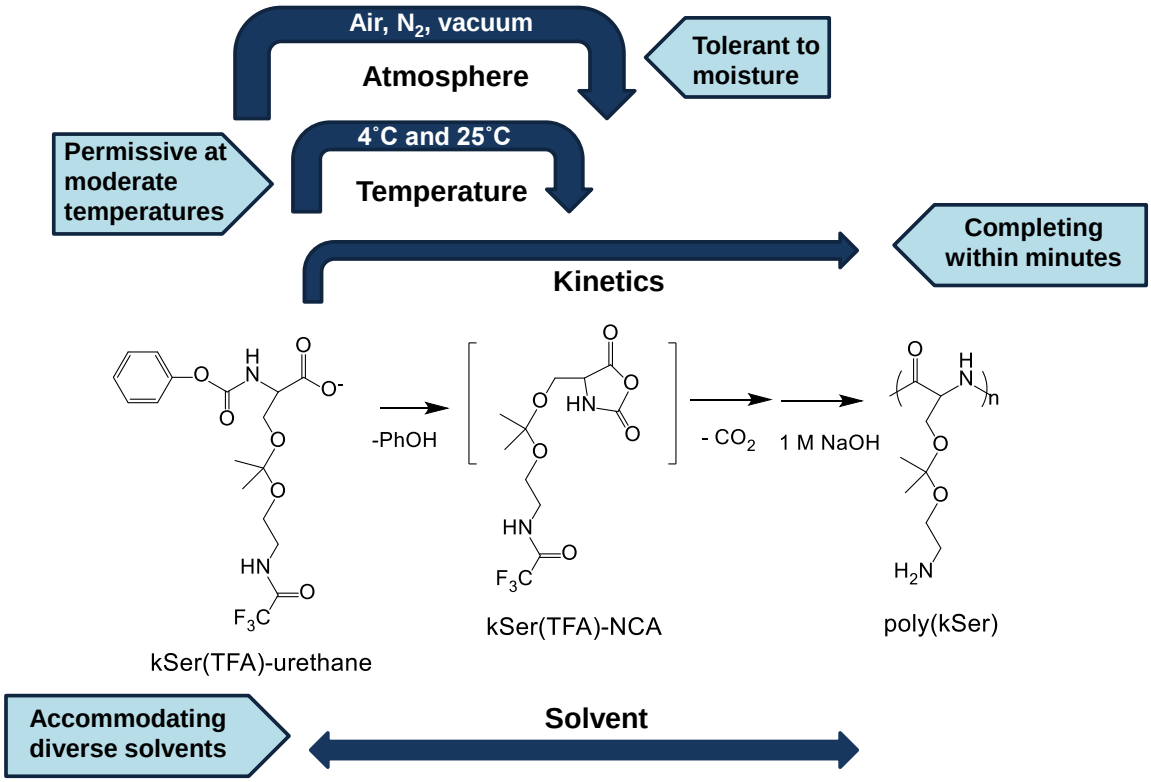

Figure 3.4. Summary of polymerization parameters via carboxylated urethane derivatives of acid-labile kSer(TFA)-urethane monomer.

3.5. References

[1] H. Enomoto, B. Nottelet, S. A. Halifa, C. Enjalbal, M. Dupre, J. Tailhades, J. Coudane, G. Subra, J. Martinez, M. Amblard, *Chem. Comm*., **2013**, 49, 409.

[2] H. J. Lee, Y. Bae, *Biomacromolecules*, **2011**, 12, 2686.

[3] N. P. Gabrielson, H. Lu, L. Yin, D. Li, F. Wang, J. Cheng, *Angew. Chem. Int. Ed*., **2012**, 51, 1143.

[4] E. P. Holowka, D. J. Pochan, T. J. Deming, *J. Am. Chen. Soc*., **2005**, 127, 12423.

[5] P. C. F. Oyston, M. A. Fox, S. J. Richards, G. C. Clark, *J. Med. Microbiol*., **2009**, 58, 977.

[6] L. Yao, J. Daniels, A. Moshnikova, S. Kuznetsov, A. Ahmed, D. M. Engelman, Y. K. Reshetnyak, O. A. Andreev, *Proc. Natl. Acad. Sci. USA*, **2013**, 110, 465.

[7] X. Cai, C. Dong, H. Dong, G. Wang, G. M. Paulettie, X. Pan, H. Wen, I. Mehl, Y. Li, D. Shi, *Biomacromolecules*, **2012**, 13, 1024.

[8] M. S. Shim, Y. J. Kwon, *Biomaterials*, **2010**, 31, 3404.

[9] S. Binauld, M. H. Stenzel, *Chem. Commun*., **2013**, 49, 2082.

[10] H. C. Kang, Y. H. Bae, *Adv. Funct. Mater*., **2007**, 17, 1263.

[11] V. Knorr, V. Russ, L. Allmendinger, M. Oris, E. Wagner, *Bioconjugate Chem*., **2008**, 19, 1625.

[12] Y. Nie, M. Gunther, Z. W. Gu, E. Wagner, *Biomaterials*, **2011**, 32, 858.

[13] F. Y. Dai, W. G. Liu, *Biomaterials*, **2011**, 32, 628.

[14] R. P. Tang, W. H. Ji, D. Panus, R. N. Palumbo, C. Wang, *J. Controlled Release*, **2011**, 151, 18.

[15] Y. H. Kim, J. H. Park, M. Lee, Y. H. Kim, T. G. Park, S. W. Kim, *J. Controlled Release*, **2005**, 103, 209.

[16] N. Hadjichristidis, H. Iatrou, M. Pitsikalis, G. Sakellariou, *Chem. Rev*., **2009**, 109, 5528.

[17] S. Y. Han, Y. A. Kim, *Tetrahedron*, **2004**, 60, 2447.

[18] O. Lagrille, G. Danger, L. Boiteau, J.-C. Rossi, J. Taillades, *Amino Acids*, **2009**, 36, 341.

[19] F. Albericio, *Curr. Opin. Chem. Biol*., **2004**, 8, 211.

[20] Y. Fujita, K. Koga, H.-K. Kim, X.-S. Wang, A. Sudo, H. Nishida, T. Endo, *J. Polym. Sci., Part A: Polym. Chem*., **2007**, 45, 5365.

[21] K. Koga, A. Sudo, H. Sishida, T. Endo, *J. Polym. Sci., Part A: Polym. Chem.,* **2009**, 47, 3839.

[22] A. Okamura, T. Hirai. M. Tanihara, T. Yamaoka, *Polymer*, **2002**, 43, 3540.

[23] J. R. Kramer, T. J. Deming, *Biomacromolecules*, **2010**, 11, 3668.

[24] Y. Kamei, A. Nagai, A. Sudo, H. Sishida, K. Kikukawa, T. Endo, *J. Polym. Sci., Part A: Polym. Chem*., **2008**, 46, 2649.

[25] Y. Kamei, A. Sudo, H. Nishida, K. Kikukawa, T. Endo, *J. Polym. Sci., Part A: Polym. Chem*., **2008**, 46, 2525.

[26] S. Yamada, K. Koga, T. Endo, *J. Polym. Sci., Part A: Polym. Chem*., **2012**, 50, 2527.

[27] Y. Kamei, A. Sudo, T. Endo, *Macromolecules*, **2008**, 41, 7913.

[28] G. J. M. Habraken, M. Peeters, C. H. J. T. Dietz, C. E. Koning, A. Heise, *Polym. Chem*., **2010**, 1, 514.

[29] G. J. M. Habraken, K. H. R. M. Wilsens, C. E. Koning, A Heise, *Polym. Chem*., **2011**, 2, 1322.

[30] J. Zou, J. Fan, X. He, S. Zhang, H. Wang, K. L. Wooley, *Macromolecules*, **2013**. 46, 4223.

[31] D. L. Pickel, N. Politakos, A. Avgeropoulos, J. M. Messman, *Macromolecules*, **2009**. 42, 7781.

Chapter 4: Solvent-assisted assembly for monodisperse acid-responsive peptide nanoparticles for siRNA delivery

4.1. Introduction

Designing nanoparticles for small interfering RNA (siRNA) delivery has gained interest due to their clinical potency of controlling protein activation post-transcriptionally from genes that cause pathological disorders.[1] Consequently, RNA interference (RNAi) can be used to treat a number of diseases, including cancer, HIV infection, Parkinson's disease, and age-related macular degeneration.[2-4] Despite the promise, successful clinical RNAi therapy still faces many challenges, particularly in formulating carriers that are multifaceted to tackle hurdles in its delivery, starting from efficient siRNA encapsulation, to its cellular uptake, and endosomal escape.[5] Other major concerns include the safety profile of the carriers.[6]

Monodisperse nanoparticles confer properties that aid in gene and drug delivery. Particles with high uniformity have definitive biodistribution, cellular internalization, and intracellular trafficking patterns that are interdependent of their size, shape, and surface chemistry.[7] However, conventional nanoparticles used to deliver therapeutics, such as liposomes and polymeric systems lack uniformity in size, composition, and surface chemistry. Subsequently, this heterogeneity leads to suboptimal performance which hampers in vivo efficacy.[8] Therefore, a method that imparts controllability for well-defined homogeneous particles is pertinent.

The effectiveness of siRNA delivery is also largely dependent on the physicochemical properties of the engineered nanocarrier, such as size, shape, and charge. Interactions between nanoparticle and biological interfaces greatly influence cellular uptake, expression of gene, and toxicity levels.[9-10] For instance, charge can play a critical role on uptake and toxicity. Although positively charged nanocarriers electrostatically interact with cell membranes and favor surface adhesion, they may cause cell membrane damage, hemolysis, platelet aggregation, and elicit immune responses.[11-12] Strategies to avoid these adverse effects is fundamental.

Additional considerations for clinically translatable RNAi therapeutics is its scalability into the commercial realm. For these preparations, technological designs that are advanced and functional yet simplistic in preparation is very attractive. Recently, considerable advances have been made using peptides as building blocks to produce materials that self-assemble into appropriate architectures for nanomedicine because they can self-organize into nanoparticles with desirable physicochemical properties suitable for gene and drug delivery.[13-16]

Molecular self-assembly to construct peptide-based nanoscale materials is attractive due to its simplicity in self arrangement into well-defined ordered architectures.[17] Inclusive non-covalent forces such as electrostatic, hydrophobic, van der Waals, and hydrogen bonds drive the formation into steady state positions that balance attractions and repulsions.[18] Particularly, cationic peptides can be exploited as promising siRNA delivery carriers due to their ability to electrostatically interact with nucleic acids while offering high biocompatibility, low toxicity, biodegradability, and versatile molecular arrangements.[17] But higher N/P ratios may be needed to encapsulate siRNA due to these

short oligonucleotide segments of approximately 21 base pairs which form rigid structures; this increases the likelihood for toxicity and should be avoided. In order to take advantage of peptide's unique molecular self-assembly to encapsulate cargo, the physicochemical interactions between biomaterials and siRNA therapeutics must carefully designed.[19]

In this chapter, we employed a novel formulation strategy that utilizes solvent-driven forces with acid-responsive poly(ketalized serine) [poly(kser)] peptide to molecularly self-assemble peptide and siRNA into monodisperse encapsulated nanospheres (**Figure 4.1**). These nanoparticles were successfully cross-linked in solvent and re-suspended in water with preserved morphology. These nanoparticles exhibited favorable physicochemical properties, such as low anionic charge, small size of ~150 nm in diameter, and spherical dimensions, and were able to demonstrate therapeutic application enabling efficient uptake, kinetically favorable acid-triggered endosomal escape for nontoxic RNAi therapy. Because this type of solvent-driven assembly has rarely been observed in literature, extensive focus on materials characterization was first implemented to understand the phenomena before illustrating therapeutic applications.

4.2. Experimental

4.2.1. General

All chemicals purchased from various vendors were used as received without further purification. Anhydrous acetonitrile, anhydrous tetrahydrofuran (THF), anhydrous ethyl acetate (EtOAc) were purchased from Acros Organics (Thermo Fisher). Anhydrous dimethylformamide (DMF), dimethylsulfoxide (DMSO), branched polyethylenimine (PEI,

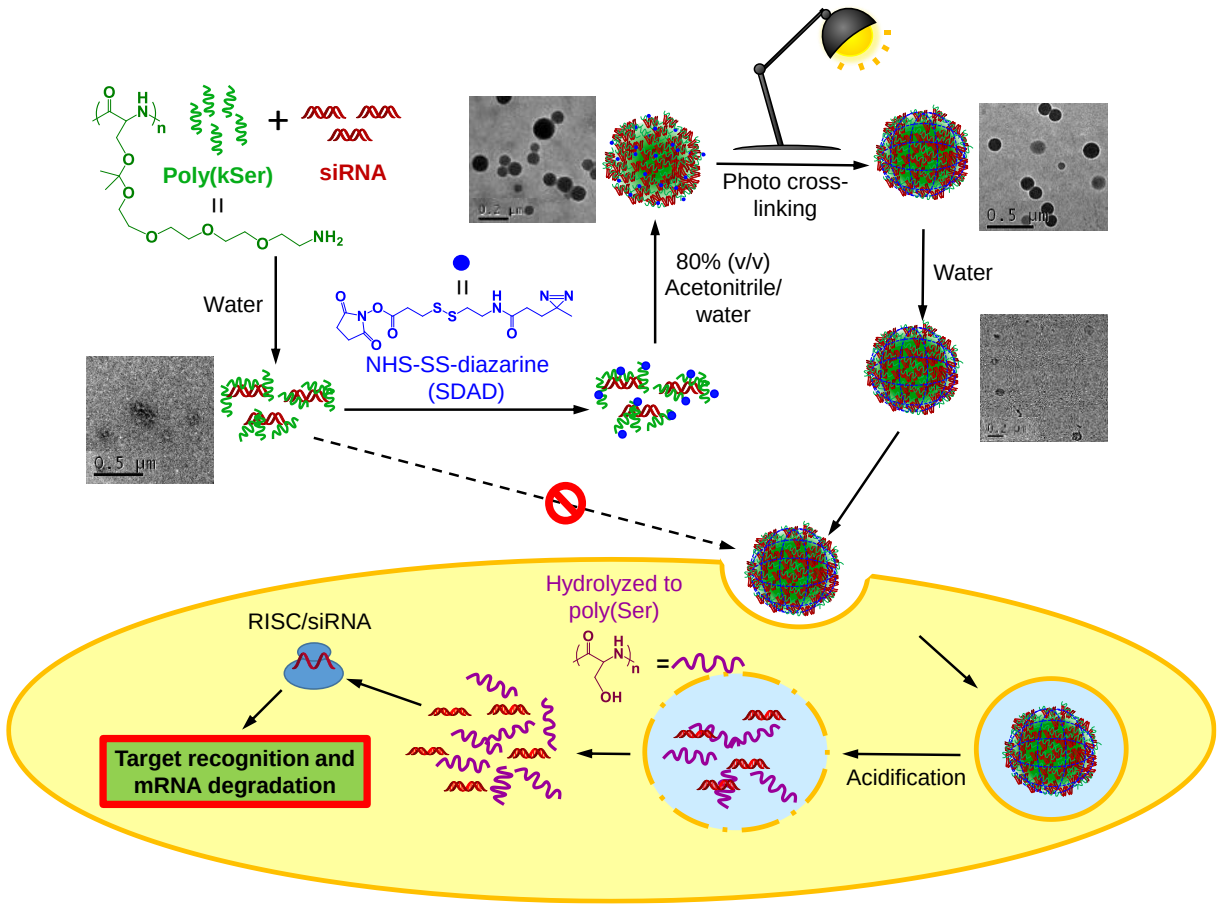

Figure 4.1. Schematic illustration of formulating cross-linked poly(kSer)/siRNA nanoparticles using solvent-assisted self-assembly and respective TEM images of each step. First, poly(kSer)/siRNA is prepared in water at N/P ratio of 20 and functionalized with diazarine. Next, acetonitrile is added to a final 80% (v/v) acetonitrile/water concentration, photo cross-linked, and finally re-dispersed in water. The bottom illustrates the schematic of cellular uptake, acid-triggered hydrolysis to poly(Ser), endosomal escape, disassembly, and intracellular trafficking for RNAi.

25 kDa) and 3-(4,5-dimethyl-2-thiazolyl)-2,5-diphenyltetrazolium bromide (MTT) were supplied from Sigma Aldrich. Anhydrous dimethylacetamide (DMAc) was purchased from Alfa Aesar. Ethidium bromide was purchased from Fisher Scientific. 2-(2-(2-(2-Aminoethoxy)ethoxy)ethoxy)ethan-1-ol was purchased from Santa Cruz Biotechnology. Silencer anti-GFP siRNA (sense strand 5′-CAAGCUGACCCUGAAGUUCdTdT-3′ and antisense strand 5′-GAACUUCAGGGUCAGCUUGdTdT-3′) and scrambled siRNA

(sense strand 5′-AGUACUGCUUACGAUACGGdTdT-3′ and antisense strand 5′-CCGUAUCGUAAGCAGUACUdTdT-3′) and Cy3-labeled control siRNA were purchased from Ambion. Amicon Ultra Centrifugal filters (MWCO 3 and 30 kDa) were supplied from Millipore. Human cervical cancer (HeLa) cells, mouse lymphoma (EL4) cells, ovalbumin (OVA)-expressing mouse lymphoma (E.G7-OVA) cells were bought from ATCC and transduced with eGFP-encoding retrovirus and sorted for cells with high eGFP expression using a cell sorter.

4.2.2. Cell culture

GFP-expressing HeLa and EL4 cells (HeLa-eGFP and EL4-GFP) were cultured in Dulbecco's Modified Eagle Medium (MediaTech) supplemented with 10% fetal bovine serum (FBS) (Hyclone) and 1% antibiotics (MediaTech). Ovalbumin (OVA)- and eGFP-expressing mouse lymphoma E.G7-OVA cells (E.G7-OVA-eGFP) were cultured in RPMI-1640 medium (MediaTech) supplemented with 10% FBS, 50 μM of 2-mercaptoethanol (Invitrogen), 2 mM of L-glutamine (MediaTech), 400 mg L−1 of G418 (MediaTech), 2.5 g L−1 of glucose (MediaTech), 10 mM of HEPES (Media-Tech), and 1 mM of sodium pyruvate (MediaTech). All cells were cultured at 37 °C with 5% CO_2.

4.2.3. Chemical synthesis

For all chemical synthesis, ^{1}H NMR spectra were obtained using a Bruker Avance 500 MHz NMR spectrometer (Bruker Biospin Corporation). Electrospray mass spectra of intermediates were obtained using a Micromass LCT mass spectrometer (Micromass Ltd.).

4.2.3.1. Synthesis of 3-Hydroxy-2-(phenoxycarbonylamino)propionic acid (Compound 1)

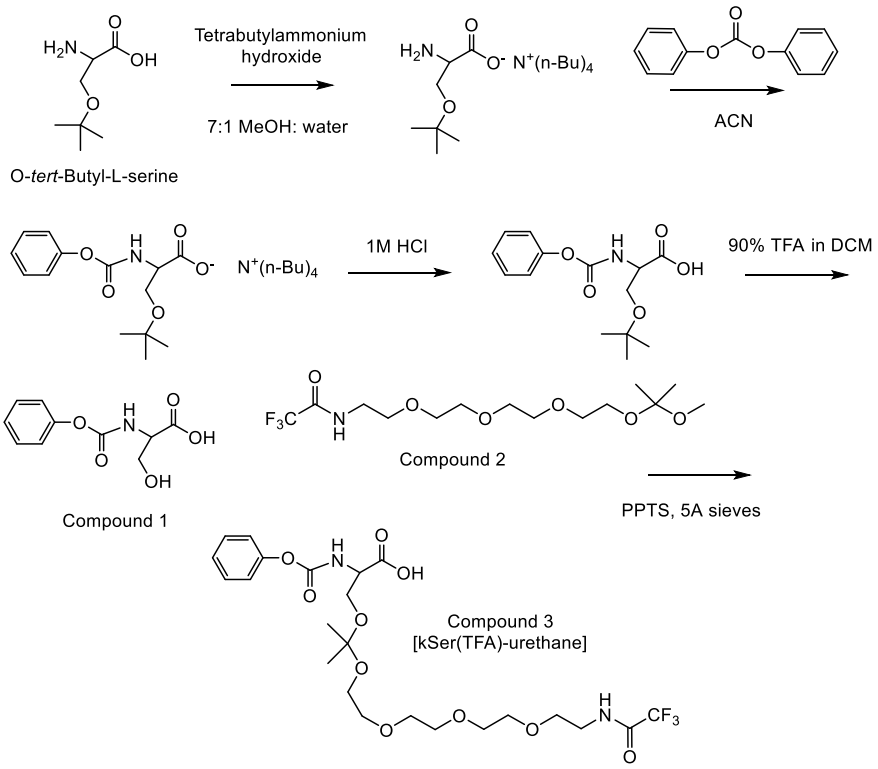

Figure 4.2. Synthesis of kSer(TFA)-urethane monomer.

Compound 1 in **Figure 4.2** was synthesized according to the procedures as previously reported.[20]

4.2.3.2. Synthesis of 2,2,2-trifluoro-N-(2-(2-(2-(2-hydroxyethoxy)ethoxy) ethoxy)ethyl)acetamide (Compound 2')

Compound 2' in **Figure 4.3** was synthesized according to these procedures: 2 g (10.3 mmol,1 equiv) of 2-(2-(2-(2-aminoethoxy)ethoxy)ethoxy)ethan-1-ol was added to 10 mL MeOH. 1.57 g (15.5 mmol, 1.5 equiv) trimethylamine was then added. Finally, 1.76 g (12.4 mmol, 1.2 equiv) ethyl 2,2,2-trifluoroacetate was added dropwisely and stirred

overnight. The product was recovered by removing methanol and extracting the crude product three times using ethyl acetate in water with a 4:1 ratio. Magnesium sulfate was used to remove residual water in the organic phase, and then the solvent was removed to recover the final product. The product was recovered as a clear oil (87.2% yield).

^{1}H NMR (500 MHz, DMSO-d_6, δ): 3.36 (q, 2H), 3.43 (t, 2H), 3.52 (m, 12H), 4.58 (t, 1H), 9.49 (s, 1H); (ESI) *m/z*: $[M + Na]^+$ calcd for $C_{10}H_{18}F_3NO_5$, 312.3; found, 312.2.

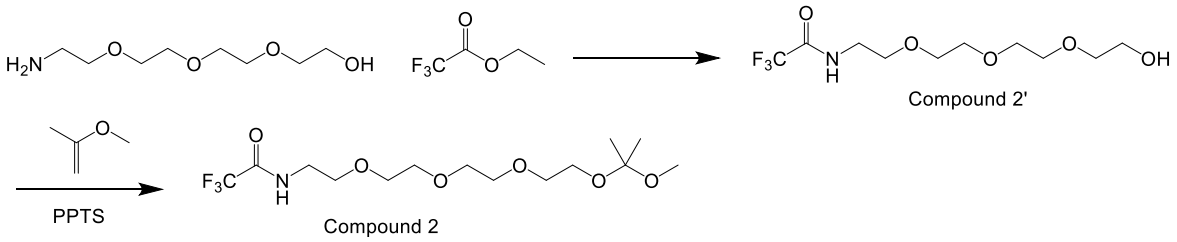

Figure 4.3. Synthesis of *N*-(3,3-dimethyl-2,4,7,10,13-pentaoxapentadecan-15-yl)-2,2,2-trifluoroacetamide (Compound 2).

4.2.3.3. Synthesis of *N*-(3,3-dimethyl-2,4,7,10,13-pentaoxapentadecan-15-yl)-2,2,2-trifluoroacetamide (Compound 2)

2.87 g (9.9 mmol, 1 equiv) Compound 2' was dissolved in 18 mL dry THF. 0.25 g (0.99 mmol, 0.1 equiv) pyridinium p-toluenesulfonate (PPTS) was then added and stirred for 10 min. 5Å molecular sieves was added to fill a quarter of the solvent and stirred for another 10 min. Lastly, 2.85 mL 2-methoxypropene (29.7 mmol, 3 equiv) was added and stirred for 3 hours on ice. 2 mL trimethylamine was added to quench the reaction. The molecular sieves was filtered, and the solvent was removed before purification of final

product using silica gel column chromatography. The final product was recovered as a clear oil (62.0% yield).

^{1}H NMR (500 MHz, DMSO-d_6, δ): 1.26 (s, 6H), 3.10 (s, 3H), 3.36 (q, 2H), 3.43 (t, 2H), 3.53 (m, 12H), 9.47 (s, 1H); (ESI) *m/z*: [*M* + Na]$^+$ calcd for $C_{14}H_{26}F_3NO_6$, 384.4; found, 384.3.

4.2.3.4. Synthesis of 1,1,1-trifluoro-16,16-dimethyl-2-oxo-19-((phenoxycarbonyl) amino)-6,9,12,15,17-pentaoxa-3-azaicosan-20-oic acid [kSer(TFA)-urethane (Compound 3)]

Compound 1 (0.5 g, 2.2 mmol, 1 equiv) was dissolved in 5 mL dry THF followed by the addition of PPTS (0.17 g, 0.66 mmol, 0.3 equiv). After stirring for 10 min, 5 Å molecular sieves were added to the reaction mixture. After another 5 min stirring, Compound 2 (0.96 g, 2.6 mmol, 1.2 equiv) was added dropwise and stirred for 24 h. After sieves were filtered, the product was purified using silica gel column chromatography using 1:3 methanol: ethyl acetate as eluent with addition of 0.3% TEA in the eluent solvent. The product was obtained as light yellow oil (31.0% yield).

^{1}H NMR (500 MHz, DMSO-d_6, δ): 1.29 (s, 6H), 3.18 (s, 2H), 3.34 (m, 2H), 3.52 (m, 12H), 3.67 (m, 2H), 4.07 (m, 1H), 7.12 (m,3H), 7.22 (t, 1H), 7.39 (t, 2H), 7.54 (m, 1H), 9.53 (s, 1H); (ESI) *m/z*: [*M* + Na]$^+$ calcd for $C_{23}H_{33}F_3N_2O_{10}$, 577.5; found, 577.3.

4.2.3.5. Synthesis and characterization of acid-transforming polypeptide

Acid-responsive polypeptides were synthesized using previously reported procedures (**Figure 4.4**).[20] Briefly, the monomers were added to an oven-dried glass vial and the air was removed via high vacuum for 10 min. Subsequently, anhydrous acetonitrile was added to a final concentration of 0.28 M. The reaction was stirred at room temperature for overnight. For molecular weight determination of polypeptide, AB Sciex MALDI TOF/TOF 5800 (Foster City, CA) instrument was used. All polymerized polypeptides were first deprotected of trifluoroacetyl group in 1 M NaOH overnight to obtain final peptide before molecular weight measurement. 2,5-dihydroxybenzoic acid was used as the matrix material for molecular weight analysis. The samples were irradiated with 349 nm diode-pumped solid state Nd:YAG laser and detected on linear high mass positive mode. M_w, M_n, polydispersity index (PDI) (M_w/M_n) was determined using Data Explorer software where the Polymer Analysis Toolbox function was used on the gated range of the molecular weight peaks. The degree of polymerization (PD) was determined approximated based on the molecular weight of the individual amino acid residue.

4.2.4. Formation of poly(kSer)/siRNA complexes in acetonitrile/water mixture

Different N/P ratios of peptide to siRNA was prepared by adding 1 µg siRNA in 10 µL DI water dropwisely to a total volume of 23 µL peptide dissolved in DI water and vortexed briefly before incubating for 15 min at room temperature. Then 128 µL acetonitrile was added directly to the peptide/siRNA mixture to achieve 80% (v/v) acetonitrile/water and incubated for another 10 min. A 2 µL aliquot of the peptide/siRNA complexes in 80% (v/v) acetonitrile/water was deposited onto a carbon-coated copper

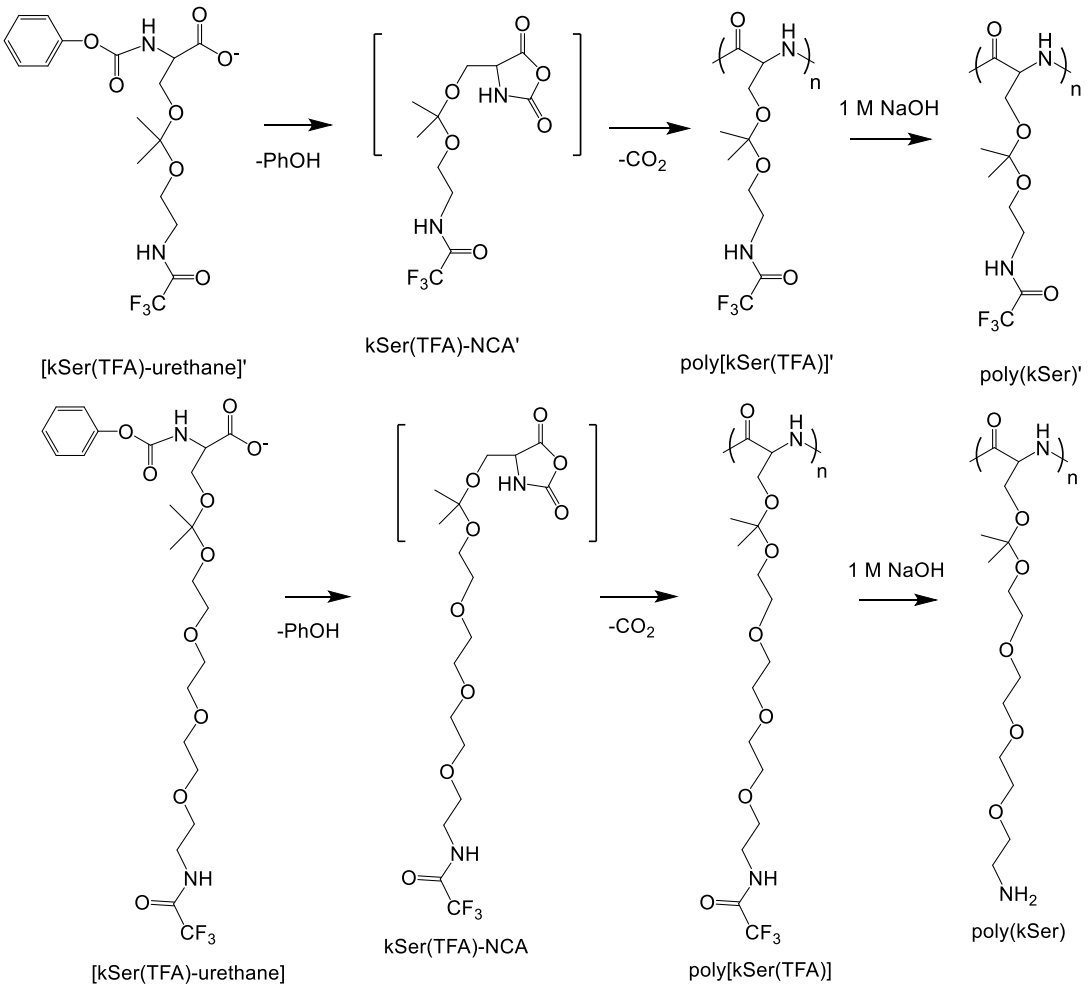

Figure 4.4. Polymerization of two different analogues of acid-responsive peptide using urethane derivatives of amino acids. Top: poly(kSer)', bottom: poly(kSer).

TEM (Ted Pella) and allowed to dry in air completely followed by additional drying in a vacuumed chamber for 20 min. 1% uranyl acetate staining was applied onto the grid and allowed to air dry for 24 h before viewing under transmission electron microscope at 200 kV (Phillips electronic Instruments).

4.2.5. Stabilization of poly(kSer)/siRNA particles in acetonitrile/water mixture

Poly(kSer)/siRNA complexes were prepared in DI water at N/P ratio of 20, where 1 µg siRNA in 10 µL DI water was added dropwisely to peptide in a total volume of 23 µL

and incubated for 15 min. After, different mole % of amines (e.g.,10 or 50) on peptide was reacted with succinimidyl 2-[(4,4´-azipentanamido)ethyl]-1,3´-dithioproprionate (NHS-SS-Diazirine or SDAD) (Thermo Scientific) dissolved in DMSO for 2 h at 4°C. Excess unconjugated SDAD was removed using centrifugal filtration with molecular weight cutoff of 30 kDa spinning at 13200 RPM for 5 min and washing twice with DI water. The concentrated diazarine-functionalized peptide/siRNA complexes were recovered and 128 µL acetonitrile was added to achieve 80% (v/v) acetonitrile/water and incubated at room temperature for 10 min. Then, 365 nm wavelength UV light was irradiated directly onto the sample for 30 min to initiate cross-linking with the unreacted amines or any nucleophiles on the surface. Then, acetonitrile was removed via high vacuum, and the stabilized particles were re-dispersed in 500 µL water. A 2 µL aliquot of the peptide/siRNA complexes in 80% (v/v) acetonitrile/water was deposited onto a carbon-coated copper TEM, and allowed to dry in air completely followed by additional drying in a vacuumed chamber for 20 min. 1% uranyl acetate staining was applied onto the grid and allowed to air dry for 24 h before viewing under transmission electron microscope at 200 kV. For samples dispersed in water, 8 µL of the sample was deposited onto the surface of the grid for 10 min before removing and staining with 1% uranyl acetate and left to air dry overnight.

4.2.6. DNA condensation, size, and surface charge of cross-linked poly(kSer)/siRNA particles

The DNA condensation efficiency was determined using the ethidium bromide (EtBr) exclusion assay. Briefly, cross-linked poly(kSer)/siRNA particles were prepared

using the methods outlined in the experimental section, but with siRNA (1 µg) mixed with 0.25 µg EtBr before stabilization. Controls include non-cross-linked poly(kSer)/siRNA and 25 kDa bPEI/siRNA at N/P 10. Fluorescence intensity of unshielded siRNA was measured using a fluorescence plate reader (BioTek Synergy H1) at excitation and emission wavelength of 320 nm and 600 nm, respectively. The fluorescence was normalized to that of free DNA.

The average diameter and zeta-potential of cross-linked poly(kSer)/siRNA particles were measured using dynamic light scattering on Zetasizer Nano-Zs (Malvern, Instruments Ltd.).

4.2.7. Acid hydrolysis of cross-linked poly(kSer)/siRNA and kinetics of siRNA release

Cross-linked and non-cross-linked poly(kSer)/siRNA complexes were subjected to agarose gel electrophoresis after incubation in acidic conditions to test for acid-responsive release of siRNA. Cross-linked poly(kSer)/siRNA were formulated as described in the methods section. Non-cross-linked peptide/siRNA were prepared by mixing 1 µg siRNA in 10 µL DI water dropwisely to a total volume of 23 µL of peptide dissolved in DI water, vortexed, and incubated at room temperature for 15 min. 100 mM pH 5.0 acetate buffer was added to the peptide/siRNA complexes at 1:1 volume and incubated at 37°C for 4 h. After 4 h hydrolysis, the volume was concentrated using centrifugal filtration at 3000 Da molecular weight cut off and spinning at 13200 RPM for 5 min. The retained sample was collected and ran on a 1% agarose gel to observe siRNA release before and after acid-hydrolysis. siRNA was also quantified before and after acid hydrolysis using RNA Quantification kit (Quant-iT RNA Assay Kit, Life Technologies).

The kinetics of acid release was also investigated. Cross-linked poly(kSer)/siRNA particles carrying 1 µg siRNA were prepared with the same procedures mentioned above. 1:1 volume of 100 mM acetate buffer at pH 5.0 or 1X PBS at pH 7.4 was added and incubated at 37°C. At various time points of 0, 0.5, 1, 2, 4, 8, 12, and 24 h, siRNA release was investigated using 1% agarose gel electrophoresis. Released siRNA was also quantified using RNA quantification kit.

4.2.8. Gene silencing and cytotoxicity of cross-linked poly(kSer)/siRNA

HeLa-eGFP cells were plated in DMEM containing 10% FBS at a density of 50,000 cells/well in a 24-well plate 24 h prior to transfection. The cross-linked poly(kser)/siRNA particles were first prepared for a dose-dependent gene silencing study using anti-eGFP siRNA and siRNA with a scrambled sequence (Scr siRNA). The final volume of the cross-linked polykSer)/siRNA particles was concentrated down to 35 µL using centrifugal filters with molecular weight cutoff of 30 kDa. The particles were supplemented with 1X PBS prior to adding directly to cells in 0.3 mL serum-free media for 4 h. The different doses of siRNA delivered in 0.3 mL serum-free media were 0.27 µM, 0.54 µM, 1.1 µM, or 2.2 µM corresponding to 1, 2, 4, or 8 µg siRNA/well respectively. After the 4 h incubation, the medium was replaced with fresh DMEM containing 10% FBS, and the cells were further incubated for 3 days before assessing eGFP silencing using Guava EasyCyte Plus flow cytometer (Guava Technologies, Inc.). 25 kDa bPEI at N/P ratio of 10 carrying 1 µg siRNA was used as the control. Specific gene silencing was assessed by normalizing against cells treated with its respective dose of scr-siRNA. EL4-GFP cells were also used to assess gene silencing and were plated at 50,000 cells/well on the day of transfection following similar transfection protocols.

Cytotoxicity of cross-linked poly(kSer)/siRNA particles at various doses (0.27 µM, 0.54 µM, 1.1 µM, or 2.2 µM) was quantified using the conventional MTT assay. Cross-linked poly(kSer)/siRNA particles were prepared using 0.2 µg siRNA for the lowest siRNA amount to 10,000 HeLa-eGFP cells/well plated in a 96-well plate 24 h prior to transfection. The cross-linked poly(kSer)/siRNA particles in water was supplemented with 1X PBS before adding directly to cells in 60 µL serum-free media for 4 h. After the 4 h incubation, the medium was replaced with 200 µL fresh DMEM media containing 10% FBS for another 24 h before conducting MTT assay. 0.5 mg/mL MTT in PBS was added to cells in a final volume of 100 µL complete media for 2 h. Subsequently, the medium was removed and 200 µL DMSO was added to dissolve the formazan crystals. The relative viability of the cells was assessed by measuring UV absorbance at 561 nm.

4.2.9. Cellular uptake of cross-linked poly(kSer)/siRNA

The cellular uptake of poly(kSer)/siRNA was investigated using confocal laser scanning microscopy. Cy3-labled siRNA at 1 µg or 4 µg was used for preparation of cross-linked poly(kSer) using the method described above. 30,000 HeLa-eGFP cells were plated on a Falcon 8-well culture slide 24 h prior to transfection. Cells were transfected with same procedures outlined above. After 4 h incubation, the media was removed and the nuclei of cells were stained with NucBlue Live Cell Stain (Molecular Probes, Life Technologies) for 5 min, washed twice with PBS, fixed with 4% p-formaldehyde for 10 min, and further washed twice with PBS, all done under dark conditions. Cells were analyzed using Olympus IX2 inverted microscope equipped with a Fluoview 1000 confocal laser scanning microscopy setup (FV10-ASW, Olympus America). The cells

were scanned in three dimensions using z-stacking, and an image traversing the middle of the cellular height was used for analysis.

4.2.10. In vivo eGFP silencing

8 week old female C57BL/6 mice were purchased from Charles River Laboratories with the approval of the Institutional Animal Care and Use Committee (IACUC) at University of California, Irvine. Mice were kept under anesthesia using isoflurane inhalation during the procedures to minimize pain and discomfort. Tumors were first established using subcutaneous injection of 1x 10^6 ovalbumin (OVA)-expressing mouse lymphoma E.G7-OVA cells at the flank and monitored for 1 week before administrating nanoparticles through tail vein. Nanoparticles were prepared using 20 µg siRNA with the same procedures as outlined before. After three days post injection, tumors were harvested and IVIS Lumina (Caliper Life Sciences) was used to measure epi-fluorescence.

4.3. Results and discussion

4.3.1. Synthesis of acid-transforming polypeptide

To begin, two versions of the acid-responsive peptide, one bearing an extended short oligo(ethylene oxide) chain for improved water solubility [poly(kSer)], whereas the other one lacked it (and denoted as poly(kSer)'), was first synthesized using previously reported polymerization method that utilized urethane derivatives of acid-labile amino acid monomers (**Figure 4.2 to Figure 4.4**).[20] Molecular weight analysis using MALDI-TOF revealed high molecular weight peptides of approximately 127 residues for poly(kSer)'

and 84 residues for poly(kSer) with low PDIs of 1.15 and 1.18, respectively (**Table 4.1**). The longer side chain of kSer may have added slight sterics in the polymerization process which lead to shorter peptide chains in comparison to the side chain on kSer'. Nevertheless, both peptides are of high molecular weights and expected to provide increased robustness for encapsulating therapeutics.

Table 4.1. Molecular weight analysis of acid-labile polypeptides

Sample	MW_n (Da)[a]	MW_w (Da)[b]	PDI[c]	DP
Poly(kSer)'	23,900	27,500	1.15	127
Poly(kSer)	26,100	30,700	1.18	84

[a,b] Determined by MALDI-TOF after TFA de-protection. [c] Calculated by M_w/M_n.

4.3.2. Relationship between molecular structure and self-assembly

Transmission electron microscopy (TEM) was taken at various steps throughout the synthesis and unexpectedly revealed that the crude product of poly(kSer[TFA]) and poly(kSer[TFA])' in acetonitrile formed spherical self-assembled structures (**Figure 4.5A-i and 4.5A-ii**). Poly[kSer(TFA)]' formed larger, heterogeneous, nearly perfect spheres whereas poly[kSer(TFA)] having more water soluble side chains exhibited smaller homogeneous architectures. To better understand if solvent forces were largely at play in fabricating these assemblies, both products were transferred into water. Both peptides saw a reduction in the amount of self-assembled particles: Poly[kSer(TFA)' still formed a few spheres but now in smaller sizes, whereas with the additional oligo(ethylene oxide) chain on poly[kSer(TFA)] full solubility was reached and no particles were present

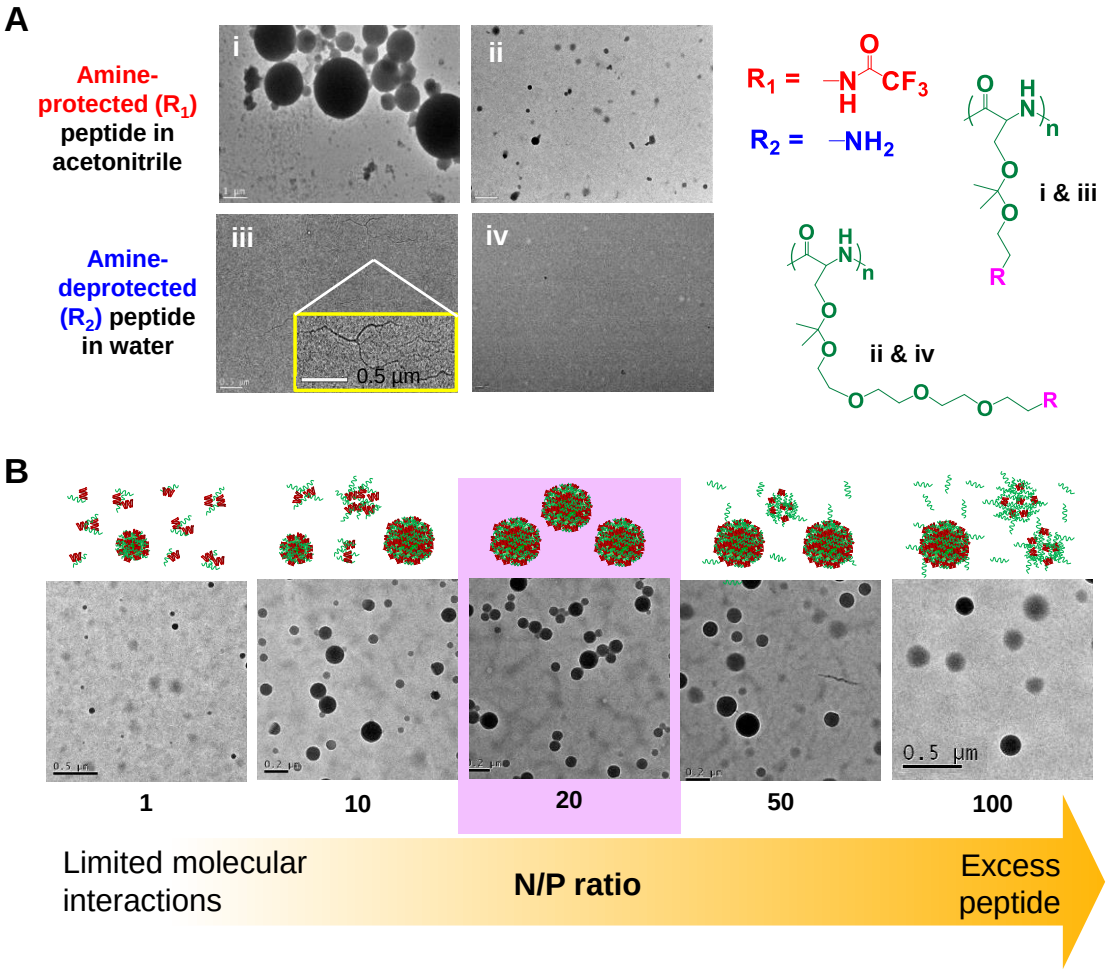

Figure 4.5. A.) TEM images of acid-responsive peptides in acetonitrile when amino end is protected with trifluoroacetyl (TFA) group (i and ii) and deprotected of TFA group in water (iii and iv). B.) Schematic illustration and TEM images of poly(kSer)/siRNA in 80% (v/v) acetonitrile/water at different N/P ratios.

(**Figure 4.6**). This demonstrates that solvent was largely responsible in driving the molecular assembly.

Because the nature of self-assembly is highly dependent on the solvent, with acetonitrile producing near-perfect spheres, different solvents were tested in the polymerization to understand how polarity of solvent effected the process (**Figure 4.7**). Poly[(kSer)]' was chosen for this since it featured larger and more prominent self-

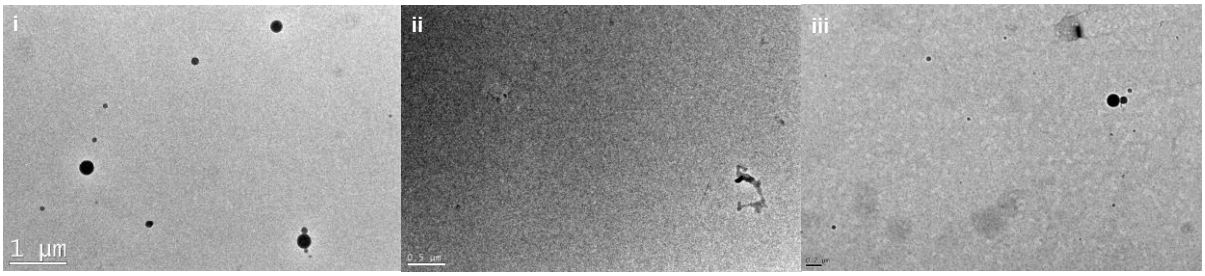

Figure 4.6. TEM images of i.) poly(ker[TFA])' and ii.) poly(kSer[TFA]) in water. iii.) TEM image of poly(kSer) in acetonitrile.

assembly than its counterpart. None of the additional solvents used (dimethylformamide [DMF], tetrahydrofuran [THF], dimethylacetamide [DMAc], dimethylsulfoxide [DMSO], or ethyl acetate [EtoAc]) showed as pronounced effects on self-assembly as it did in acetonitrile. Since acetonitrile is a polar aprotic solvent, it was anticipated that other polar aprotic solvents like DMF, DMSO, or DMAc would also induce the effect, but only minor aggregation and association was observed. Less polar solvents like THF resulted in some larger scattered particles but overall nothing very prominent. Acetonitrile was chosen to be used for further experimentation.

Next, to gain further insight into peptide structure and its assembly, trifluoroacetyl (TFA) group was de-protected to expose the amino terminus and tested in acetonitrile or water, where it would exist as a charged molecule. When the TFA group was removed, poly(kSer)' did not show very good solubility in water, as shown by the formation of threadlike structures (**Figure 4.5A-iii**). This low solubility results from the hydrophobic ketal branches and aliphatic chains on a high molecular weight peptide. Its analogue, poly(kSer), however, consisting of multiple ethylene oxide groups, was completely soluble (**Figure 4.5A-iv**). Now, as poly(kSer), with its amino terminus exposed, was placed back into acetonitrile, limited assemblies formed (**Figure 4.6-iii**), indicating the assembly is

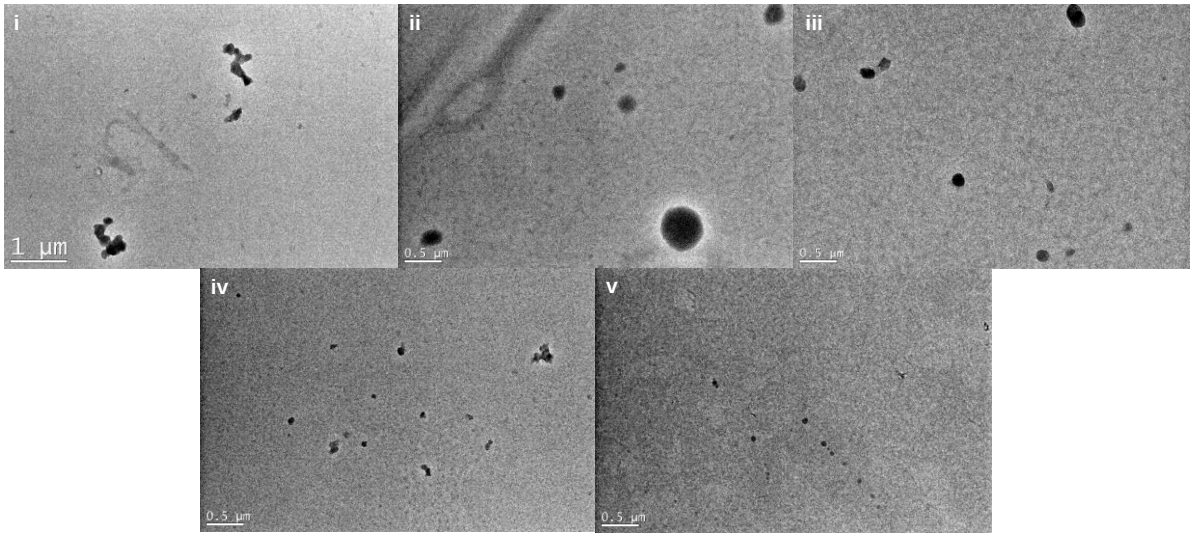

Figure 4.7. TEM images of poly(kSer[TFA])' polymerized in different solvents. i.) DMF, ii.) THF, iii.) DMAc, iv.) DMSO, v.) EtoAc.

highly dependent on the amino terminus being protected by the TFA group rendering it uncharged and less polar.

4.3.3. Formation of poly(kSer)/siRNA complexes in acetonitrile/water mixture

Because of poly(kSer)'s superb water solubility and self-assembling properties in acetonitrile when amino terminus is protected, we next wanted to utilize these features to see if encapsulation of therapeutic siRNA was possible. We chose to work with poly(kSer) due to its high solubility in water. When the cationic terminus of poly(kSer) interacts with siRNA, even at lower N/P ratios, the cationic charge can be paired with an anionic phosphate group to neutralize charge. As siRNA is also not totally soluble in acetonitrile, a complex of poly(kSer)/siRNA in acetonitrile is hypothesized to entropically favor its exclusion from the solvent, driving a network of associations together. Therefore, we prepared poly(kSer) with siRNA to see if encapsulation it in acetonitrile was possible. Poly(kSer) and siRNA were mixed together at various N/P ratios in minimal amounts of

water to first form electrostatic interactions. It should be noted that poly(kSer) was found to not complex siRNA very effectively in water, most likely due to sterics from bulky ketal linkages and high electronegativity from the oxygens in the ethylene oxide chain (data not shown). However, when poly(kSer)/siRNA complexes were added with acetonitrile to make 80% (v/v) acetonitrile/water mixture, well-defined, almost perfectly spherical nano-sized particles were formulated (**Figure 4.5B**). When increasing the N/P ratio from 1 to 20, the number of particles increased. The sizes of the particles also increased from approximately 50 nm to 150 nm. Starting from N/P ratio of 50 to 100, the formation of a mixture of obscurely faint and dense particles was observed. It is speculated that at N/P ratios 50 to 100, excess peptide was present causing the formation of faint particles, which may be consisting of partial interaction with siRNA or peptide itself. Therefore, N/P ratio of 20 was chosen for further studies.

4.3.4. Stabilization of poly(kSer)/siRNA particles in acetonitrile/water mixture

In order for the solvent-driven self-assembled poly(kSer)/siRNA particles to have therapeutic application, the particles must fully encapsulate siRNA when solvent is removed and particles are re-dispersed in water. However, using only the solvent-driven assembly process, the transfer of particles back into water completely disrupted the interaction between poly(kSer) and siRNA (data not shown), demonstrating acetonitrile as the main component orchestrating the assembly, just as before when using peptides alone. Therefore, in order to stabilize poly(kSer)/siRNA in acetonitrile, photo-initiated cross-linking technique was implemented. Briefly, succinimidyl 2-[(4,4´-azipentanamido)ethyl]-1,3´-dithioproprionate (NHS-SS-Diazirine or SDAD) was used to photo cross-link the amines on the surface as well as other nucleophiles available on the

surface of poly(kSer)/siRNA complex in acetonitrile. It was shown that diazarine-functionalized poly(kSer/siRNA) was still able to self-assemble into spherical and well-defined structures when mixed with 80% (v/v) acetonitrile/water (**Figure 4.1**). 10 or 50 mole % of amines on the peptide was used for diazarine-functionalization using NHS chemistry (**Table 4.2**). However, only conjugation with 50 mole % of amines resulted in stabilized particles of approximately 150 nm in diameter with low polydispersity index of 0.225 after removal of solvent and re-dispersing into water (**Figure 4.1**). Using 10 mole % of amines resulted in incomplete cross-linking having large particle sizes greater than 300 nm and PDI greater than 0.5, indicating incomplete stabilization. The zeta potential of cross-linked poly(kSer)/siRNA was slightly negative (-1.2 mV), signifying that a majority of the amines on the surface was used for cross-linking. This may also suggest that the particles consist of some siRNA on its surface, and may be potentially cross-linked together with the peptide, as SDAD cross-linking involves any amines or nucleophiles present to participate in the cross-linking chemistry. The particles exhibit a low anionic charge and may avoid bioadverse interactions with serum proteins demonstrating suitability for in vivo applications.

4.3.5. Efficient siRNA condensation and rapid acid-triggered siRNA release

Non-cross-linked poly(kSer) was not able to condense siRNA at N/P ratio 20, as shown in conventional ethidium bromide (EtBr) exclusion assay and gel electrophoresis (**Figure 4.8A and B**). However, after being stabilized, cross-linked poly(kSer) showed a reduction in fluorescence shielding from EtBr exclusion assay as well as retention of siRNA from gel electrophoresis. Still, cross-linked poly(kSer)/siRNA exhibited higher EtBr fluorescence than 25 kDa branched PEI (25 kDa bPEI), providing evidence that siRNA

may be partially localized on its surface as the negative zeta potential indicates. RNA quantification showed that non-cross-linked versions had approximately 66.2% free siRNA whereas stabilizing and cross-linking the particles reduced it to only 1.15% (**Figure 4.8B**). Additionally, acid-responsive properties of poly(kSer) was demonstrated by incubating the particles at pH 5.0 acetate buffer for 4 h and assessing siRNA release. **Figure 4.8B** shows that a majority, approximately 57% of the siRNA that was encapsulated in the cross-linked particles, can be released after acid hydrolysis, suggesting high efficiency in siRNA release.

Table 4.2. Characterization of cross-linked poly(kSer)/siRNA

Mole % of amines used for cross-linking	Size (nm)	Zeta potential (mV)	PDI
10	392.3	-17.6	0.555
50	150.2	-1.20	0.225

Further, the kinetics of siRNA release from the carrier is a major factor defining the effectiveness of RNAi therapy, so the kinetics of siRNA release from the acid-responsive peptide was compared at different pHs (5.0 and 7.4) at 37°C to mimic intracellular conditions (**Figure 4.8C**). The gel electrophoresis images and RNA quantification both identify treatment in acidic conditions having faster as well as more siRNA being released than at neutral conditions. From start to about 1 h, minimal siRNA was detected in acid, but at 2 h, a substantial amount of hydrolysis caused a drastic sharp increase in siRNA release. At 4 h, a majority of siRNA was released and a plateau was already reached. On the other hand, when treated with pH 7.4 PBS buffer, minimal siRNA was detected up to 2 h. At 4 h, 6.83% free siRNA was detected and steadily increased to 32.9% at 24 h. The

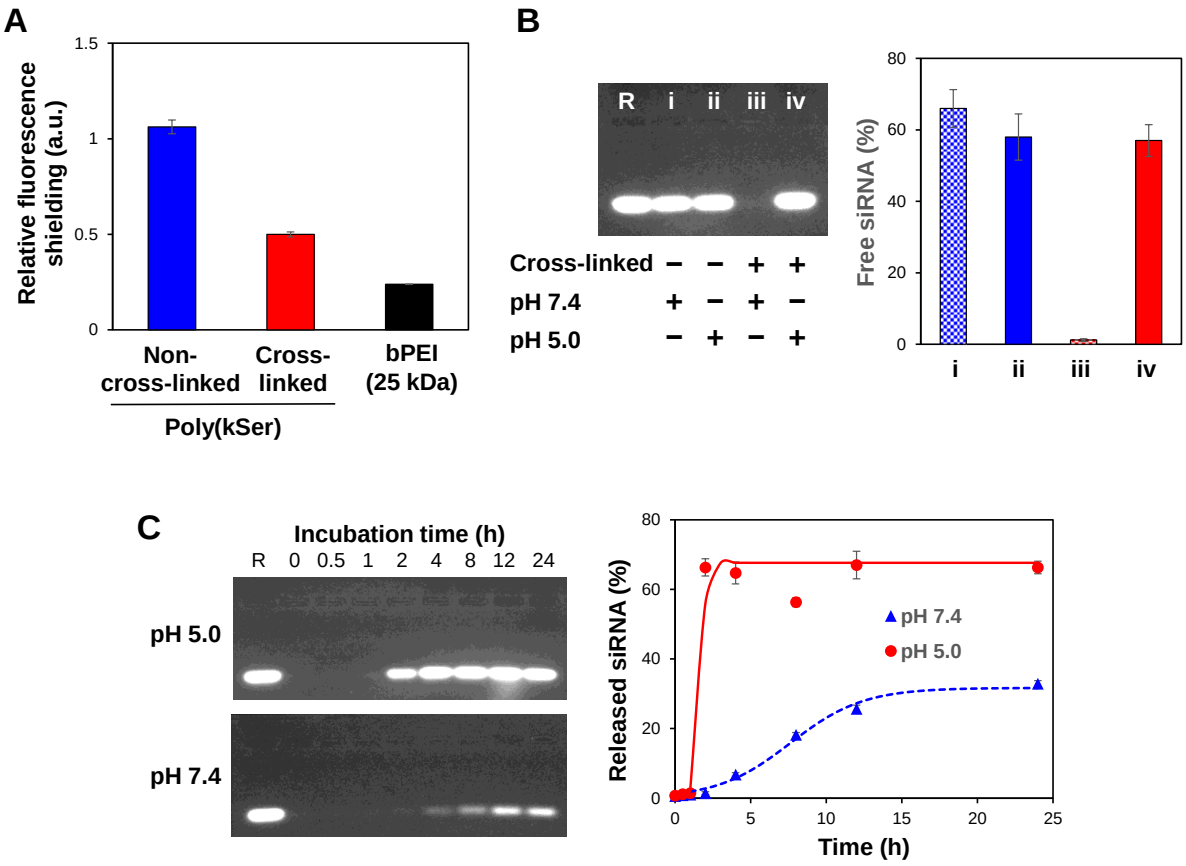

Figure 4.8. A.) Ethidium bromide exclusion assay showing fluorescence shielding of non-cross-linked and cross-linked poly(kSer)/siRNA particles. B.) Agarose gel electrophoresis and RNA quantification of non-cross-linked and cross-linked poly(kSer)/siRNA at neutral (pH 7.4) and acidic (pH 5.0) conditions. C.) Agarose gel electrophoresis and RNA quantification showing kinetics of siRNA release in acidic (pH 5.0, top) and neutral (pH 7.4, bottom) conditions at 37°C. R in agarose gel electrophoresis represents 1 µg free siRNA as the control.

rate of siRNA release was steady at pH 7.4 demonstrating stability of the particles, whereas release was abrupt when treated with acid, exemplifying fast release under acidic cues such as the endosome.

4.3.6. Low cytotoxicity and gene silencing potential of cross-linked poly(kSer)/siRNA

Next, a dose-dependent study was performed to assess cytotoxicity of cross-linked poly(kSer)/siRNA particles (**Figure 4.9A**). Tolerable toxicity levels, such as greater than 80%, was obtained for doses of 0.27, 0.54, and 1.1 µM siRNA, which corresponds to 1, 2, and 4 µg siRNA per well, respectively. At 2.2 µM or 8 µg siRNA per well, cell viability decreased to around 63%. The particles showed low toxicity up to a high dosage of 4 µg siRNA per well. This fares much better than the high toxicity, approximately only 63% viability, exhibited from 25 kDa bPEI/siRNA particles when administering only 1 µg siRNA. Low cytotoxicity demonstrates high versatility in the usage of cross-linked poly(kSer)/siRNA particles. The low anionic surface charge and acid-hydrolysis forming a natural, neutral, and biodegradable poly(serine) peptide are features contributing to low toxicity.

Subsequently, the dose-dependent gene silencing study was conducted on HeLa-eGFP cells. Moderate gene silencing of approximately 32% at a dose of 4 µg siRNA/well was demonstrated (**Figure 4.9B-D**). At lower siRNA doses, such as 1 or 2 µg siRNA/well, gene silencing was negligible and further studies were later conducted to understand the rationale behind this. The highest gene knockdown obtained by cross-linked poly(kSer)/siRNA at 4 µg siRNA/well compares similarly with 25 kDa bPEI at N/P ratio of 10. On the contrary to high molecular weight PEI vectors, poly(kSer)/siRNA displays low cytotoxicity. EL4-GFP suspension cells were also tested for gene silencing. Cross-linked poly(kSer)/siRNA displayed approximately 31% silencing and compares similarly with 25 kDa bPEI, which showed 30% gene knockdown (data not shown**)**. Although delivering higher dosages were required, the efficacy matched closely to the gold standard 25 kDa bPEI.

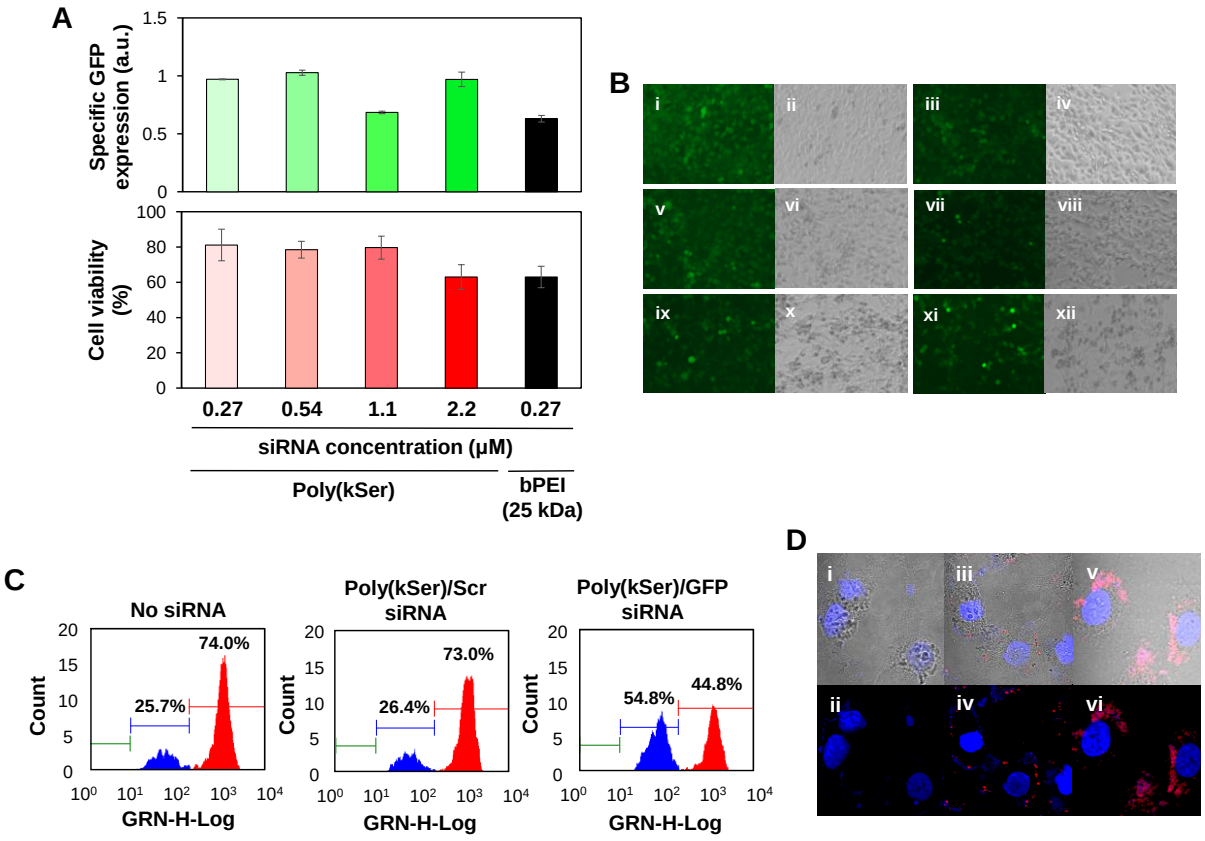

Figure 4.9. A.) Dose-dependent specific gene silencing and cell viability of cross-linked poly(kSer)/siRNA using flow cytometry and MTT assay, respectively. B.) Fluorescence and bright field microscopy images of i-ii.) HeLa-eGFP cells, iii-iv.) cross-linked polyk(Ser) delivering 1 μg siRNA, v-vi.) 2 μg siRNA, vii-viii.) 4 μg siRNA, ix-x.) 8 μg siRNA, xi-xii.) 25 kDa bPEI delivering 1 μg siRNA. C.) Flow cytometry histograms demonstrating eGFP gene silencing. D.) Confocal laser scanning microscopy of i-ii.) HeLa-eGFP cells, iii-iv.) cells treated with 25 kDa bPEI delivering 1 μg Cy3-labeled siRNA, v-vi.) cells treated with cross-linked poly(kSer) delivering 4 μg Cy3-labeled siRNA at 4 h.

4.3.7. Cellular uptake of cross-linked poly(kSer)/siRNA

To understand why a moderately high dosage of siRNA was needed to show gene silencing effects, confocal laser scanning microscopy was used to visualize cellular uptake, using Cy3-labled siRNA. Confocal microscopy images revealed that while 25 kDa bPEI/siRNA vectors had very localized punctate red dots at 4 h, 1 μg- and 4 μg-treated cells using cross-linked poly(kSer) showed siRNA dispersed in the cytoplasm (**Figure**

4.10). Delivering 4 µg siRNA showed a higher density of siRNA in the cytoplasm than 1 µg. Overall, this demonstrates that cross-linked poly(kSer)/siRNA particles were able to get taken up by the cells despite the slight anionic surface charge. One reason for this may be due to the amphiphilic nature of poly(kSer), having hydrophobic ketal linkages and hydrophilic oligo(ethylene oxide) tails. Amphiphilic molecules have been shown to aid in cellular uptake.[21] siRNA being dispersed in the cytoplasm using cross-linked poly(kSer) demonstrates its enhanced rapid endosomal escape properties compared with 25 kDa bPEI. Hydrolysis of ketal branches increased osmotic pressure and prompted rupture of the endosome. Excluding uptake and endosomal escape as factors preventing efficient RNAi, this most likely suggests that some siRNA may still be interacting with the hydrolyzed peptide through non-covalent forces or possibly still cross-linked after being released from the endosome, thus necessitating higher dosages.

4.3.8. In vivo eGFP silencing

Due to the particles having sufficient siRNA complexation efficiency, cellular uptake, fast siRNA release, endosomal escape properties, moderate silencing, and low toxicity, the particles were treated in vivo to assess therapeutic effects. All animal experiments were approved by the Institutional Animal Care and Use Committee (IACUC) at University of California, Irvine. C57BL/6 mice were subcutaneously injected with E.G7-OVA-eGFP cells on their flank to establish a tumor. After tumors were established, the mice were injected with cross-linked poly(kSer)/anti-eGFP siRNA and other controls (saline, free siRNA, 25 kDa bPEI/anti-eGFP siRNA, and cross-linked poly(kSer)/scrambled (Scr) siRNA) via tail vein and left alone for 3 days untiltumors were

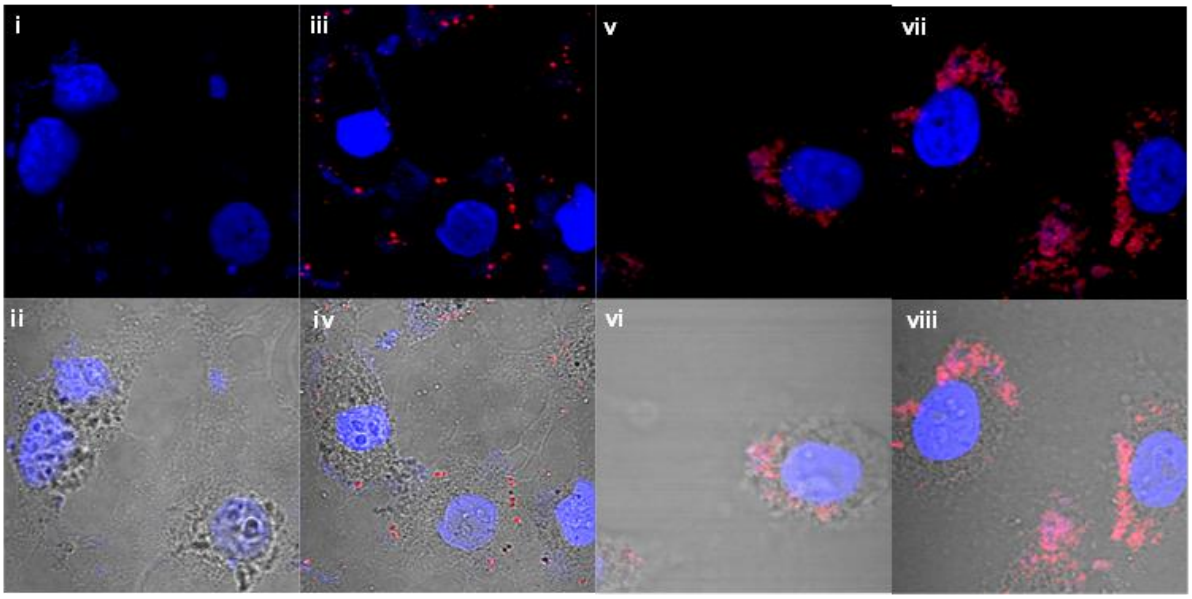

Figure 4.10. Confocal laser scanning microscopy showing cellular uptake of Cy3-labeled siRNA in cells treated with i-ii.) HeLa-eGFP cells, iii-iv.) 25 kDa bPEI/siRNA at 1 µg, v-vi.) cross-linked poly(kSer)/siRNA at 1 µg, vii-viii.) cross-linked poly(kSer)/siRNA at 4 µg.

harvested and the epi-fluorescence (measured by the radiant efficiency) was determined on all tumors. Mice treated with saline (PBS) and free siRNA showed tumors at its baseline fluorescent levels, whereas mice treated with 25 kDa bPEI/siRNA or cross-linked poly(kSer)/Scr siRNA showed an unexpected increase in fluorescence levels in both mice. Mice treated with cross-linked poly(kSer) delivering anti-eGFP displayed an average decrease in fluorescence, demonstrating potential in vivo gene knockdown (**Figure 4.11**).

4.4. Conclusion

In this study, we demonstrated a new formulation strategy constructing effective siRNA carriers from acid-responsive poly(kSer) and siRNA self-assembled and cross-

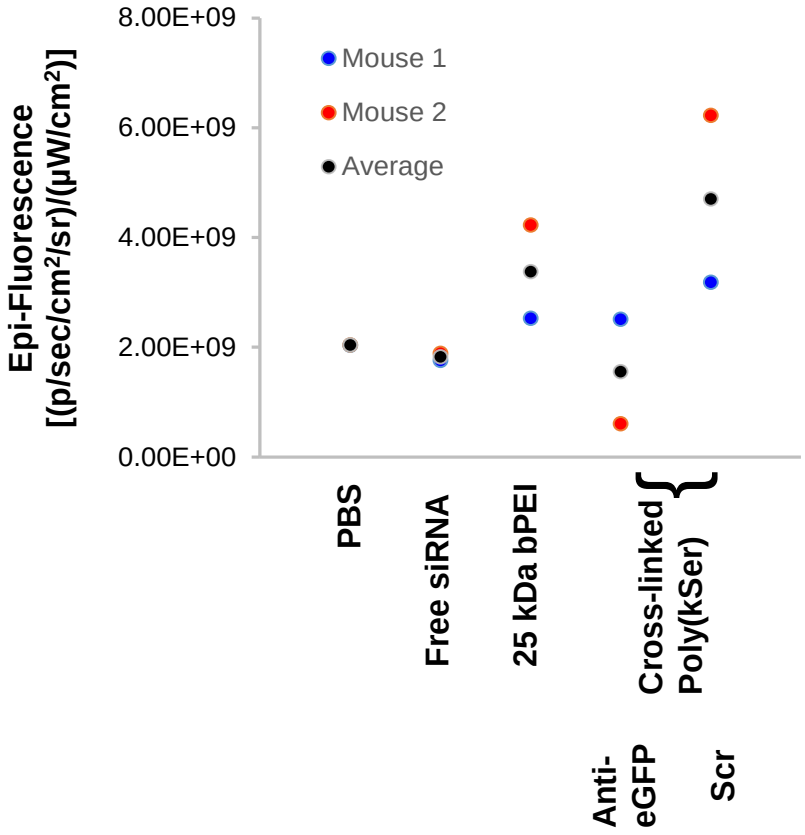

Figure 4.11. Epi-fluorescence imaging of harvested tumors after treatment with cross-linked poly(kSer)/anti-eGFP siRNA and controls.

linked in acetonitrile organic solvent. The method offers simplicity in formulation and ease in creating well-defined homogenous carriers that is essential for consistent clinical efficacy. The particles were able to efficiently encapsulate siRNA, mediate cellular uptake, and release siRNA from the endosome in a rapid manner under acidic conditions prompting fast accessibility and usage in cells. High cell viability was preserved due to low surface charge and high biocompatibility after acid-transformation into poly(serine). Higher dosages were required and the rationale for this may be due to incomplete disassembly of nucleic acids although future investigations are required. Prospects of in vivo usage was also demonstrated. Overall, cross-linked poly(kSer)/siRNA particles

formulated via solvent-driven self-assembly demonstrate a new and feasible strategy for tackling multiple hurdles in siRNA delivery for safe RNAi therapy.

4.5. References

[1] S. Deshayes, K. Konate, A. Rydström, L. Crombez, C. Godefroy, P.-E. Milhiet, A. Thomas, R. Brasseur, G. Aldrian, F. Heitz, M. A. Muñoz-Morris, J.-M. D. lle and G. Divita, *Small*, **2012**, 8, 2184.

[2] F. P. Manfredsson, A. S. Lewin, R. J. Mandel, *Gene Ther*., **2006**, 13, 517.

[3] J. M. Jacque, K. Triques, M. Stevenson, *Nature*, **2002**, 418, 435.

[4] P. K. Kaiser, R. C. A. Symons, S. M. Shah, E. J. Quinlan, H. Tabandeh, D. V. Do, G. Reisen, J. A. Lockridge, B. Short, R. Guerciolini, Q. D. Nguyen, *Am. J. Opthalmol.,* **2010**, 150, 33.

[5] C. E. Nelson, A. J. Kim, E. J. Adolph, M. K. Gupta, F. Yu, K. M. Hocking, J. M. Davidson, S. A. Guelcher, C. L. Duvall, *Adv. Mater*., **2014**, 26, 607.

[6] A. C. Mirsa, S. Bhaskar, N. Clay, J. Lahann, *Adv. Mater*., **2012**, 24, 3850.

[7] S.E. A. Gratton, P. A. Ropp, P. D. Pohlhaus, J. C. Luft, V. J. Madden, M. E. Napier, J. M. DeSimone, *Proc. Natl. Acad*. Sci. USA, **2008**, 105, 11613.

[8] H. Lee, A. K.R. Lytton-Jean, Y. Chen, K. T. Love, A. I. Park, E. D. Karagiannis, A. Sehgal, W. Querbes, C. S. Zurenko, M. Jayaraman, C. G. Peng, K. Charisse, A. Borodovsky, M. Manoharan, J. S. Donahoe, J. Truelove, M. Nahrendori, R. Langer, D. G. Anderson, *Nature Nanotechnol*., **2012**, 7, 389.

[9] A. E. Nel, L. Madler, D. Velegol, T. Xia, E. M. V. Hoek, P. F. Klaessig, V. Castranova, M. Thompson, *Nat. Mater*., **2009**, 8, 543.

[10] A. Albanese, P. S. Tang, W. C. W. Chan, *Annu. Rev. Biomed. Eng*., **2012**, 14, 1.

[11] I. Lynch, K. A. Dawson, *Nano Today*., **2008**, 104, 2050.

[12] J. Li, X. Yu, Y. Wang, Y. Yuan, H. Xiao, D. Cheng, X. Shuai, *Adv. Mater*., **2014**, 26, 8217.

[13] W. A. Petka, J. L. Harden, K. P. McGrath, D. Wirtz, D. A. Tirrell, *Science*, **1998**, 281, 389.

[14] S. Vauthey, S. Santoso, H. Gong, N. Watson, S. Zhang, *Proc. Natl. Acad. Sci. USA*, **2002**, 99, 5355.

[15] J. D. Hartgerink, E. Beniash, S. I. Stupp, *Science*, **2001**, 294, 1684.

[16] S. Szela, P. Avtges, R. Valluzzi, S. Wrinker, D. Wilson, D. Kirschner, D. L. Kaplan, *Biomacomolecules*, **2000**, 1, 534.

[17] H. Cui, M. J. Webber, S. I. Stupp, *Peptide Science*, **2010**, 94, 1.

[18] G. M. Whitesides, B. Grzybowski, *Science*, **2002**, 295, 2418.

[19] O. Ikkala, G. T. Brinke, *Science*, **2002**, 295, 2407.

[20] S. Wong, Y. J. Kwon, *J. Polym. Sci. Pol. Chem*., **2015**, 53, 280.

[21] H. Zeng, H. C. Little, T. N. Tiambeng, G. A. Williams, Z. Guan, *J. Am. Chem. Soc.,* **2013**, 135, 4962.

Chapter 5: Summary and future directions

5.1. Summary of dissertation

Chapter 1 served as an introduction to the dissertation. Peptides were introduced as versatile biomacromolecules that could be used in various biomedical applications including gene and drug delivery. Peptides are natural materials and confer high biocompatibility, high biodegradability, and low toxicity. Peptides also have protein-mimicking properties and can fold into various arrangements suitable for nanoparticle design and formulation. These versatile folding properties are a result of a combination of non-covalent forces from the backbone and the side chains. Moreover, stimuli-responsive peptides have attracted widespread attention as building blocks formulating safe, nontoxic, and smart vectors for gene and drug delivery. Particularly, those that respond to acidic cues have found great use, since most nanocarriers are taken up by the cells via endocytosis and utilize the increase in acidity in endosomal compartments to facilitate escape or disassembly of therapeutics from the carrier.

The previously synthesized acid-responsive PEGylated poly(ketalized serine) (PEG-poly[kSer]) was mentioned as a vector that demonstrated successful gene delivery.[1] Although gene delivery was accomplished, transfection rate could be improved upon. It was hypothesized that limited degrees of polymerization led to a short peptide which lacked flexibility and robustness. Therefore, the polymerization strategies needed to be revisited. Chapter 1 alluded to the discovery of a novel and successful polymerization strategy and an unexpected self-assembly phenomena. Chapter 1

presented the foundation for the dissertation which focuses on the synthesis and formulation of acid-responsive polypeptide vectors for gene therapy applications.

Chapter 2 explored various polymerization strategies to synthesize high molecular weight acid-labile poly(kSer), using carbodiimides, uronium salts, and phosgene-free synthesis of NCA for its polymerization. The shortcomings of each method were reported here and these flaws suggested that a more efficient coupling strategy was required. Both the carbodiimide and uronium salt coupling strategies were hampered by side reactions that caused termination. For instance, carbodiimide activation is started by a proton transfer followed by the formation of the O-acylisourea, a very reactive active ester. An amino component can attack and form the amide bond, but the O-acylisourea can also undergo an intramolecular rearrangement to form N-acylurea, which will terminate the polymerization. Similarly, carboxylates can react with the uronium salts to form an active ester, which can subsequently react with the amino component to form the amide bond. Tangentially, the uronium salts might instead react with the amino component and form a guanidine derivative to terminate the peptide chain. Therefore, a method that utilizes NCA ROP was performed by creating acid-labile NCA monomers using bisarylcarbonates. This method also had shortcomings as it was very sensitive to amine-containing contaminants. These contaminants disrupted the polymerization, terminated chain growth, and hindered a controlled polymerization process. Due to the insufficiencies of these polymerization strategies, a method that utilized urethane derivatives of amino acids as monomers was investigated in the next chapter.

Chapter 3 described the method of using urethane derivatives of amino acids as an alternative to NCA monomers for the synthesis of high molecular weight acid-labile

polypeptides. This method offers many advantages due to the stability of the urethane derivatives, its minimal sensitivity to moisture, and its efficiency as it undergoes NCA ROP as an intermediate in the reaction. Because the kSer(TFA)-urethane derivative was obtained as a carboxylate after purification from silica gel column chromatography, which utilized minimal amounts of base to preserve the ketal linkages, it conferred additional advantages towards the polymerization. For instance, temperature no longer needed to be elevated to promote intramolecular cyclization to form the NCA. Neither did the solvent have to be restricted to highly polar aprotic solvents. The carboxylate group resulted in very rapid completion of polymerization and now did not even necessitate the use of inert atmosphere like conventional NCA ROP. This facile method was reported to synthesize high molecular weight acid-labile peptides with low polydispersity under mild and easily achievable conditions.

Chapter 4 focused on a new formulation strategy constructing effective siRNA carriers from acid-responsive poly(Ser) and siRNA that self-assembled in organic solvent to yield monodisperse nanoparticles. Extensive characterization of the phenomena was conducted. A photo cross-linking strategy was able to stabilize the solvent-driven assembly so that it could be transferred into aqueous conditions. The particles showed the ability to encapsulate siRNA, release siRNA via acidic cues in a rapid manner, mediate cellular uptake, and also demonstrated moderate gene silencing while exhibiting limited toxicity. This formulation strategy offers a new and feasible way to create siRNA nanocarriers with the potential to tackle multiple hurdles in gene delivery.

Chapter 5 provides the summary of the dissertation and future directions of the study.

5.2. Future directions

Poly(kSer)-derived peptides offer the potential for numerous applications due to their versatility in formulation based on their molecular structures. For instance, the composition of their side chain can affect their self-assembly, as demonstrated earlier by the differences between attaching water soluble and water insoluble groups. This was also seen in the differences between hydrophobic and hydrophilic groups. This suggests that poly(kSer)-derived peptides can be conjugated with drugs of different properties, potentially hydrophobic , to formulate acid-responsive peptide delivering drugs. We also observed the phenomena of amine-deprotected poly(kSer) interacting with siRNA to formulate nucleic acid delivery vectors. Potentially, drugs resembling molecular properties of kSer can be attached onto the side chain while also interacting with siRNA to produce vectors that can synergistically deliver genes and drugs for combined therapy.

It has also been demonstrated that several cationic peptides can serve as cell penetrating peptides (CPPs), which have properties to interact with cell membranes and facilitate uptake through different mechanisms such as pore formation or membrane fusion. Therefore, similar molecular properties of these cationic peptides can be added as an appendage onto the kSer side chain to enhance cell uptake or endosomal escape. A library of peptides containing different side chains can be synthesized to screen for the most effective one.

Lastly, some preliminary studies focused on controlling morphology based on temperature, not yet discussed in this dissertation, will also be briefly mentioned here. Preliminary studies showed that applying elevated temperatures in a vacuum during the polymerization process yielded self-assembled particles of different morphologies, such

as rods instead of spheres. Therefore, another future application could be the development of vectors with different morphologies for improved uptake. These ideas will be explored in more detail in the following sections.

5.2.1. Nanomaterial shape modulation using poly(kSer)-derived peptides

Recently, many studies have correlated the properties of nanomaterials such as shape and size with various interactions on the biological system including cellular uptake, toxicity, and transportation. These findings have given scientists a foundation for engineering the next generation of nanoscale devices.[2-6] For instance, studies have demonstrated that rod-shaped nanoparticles have different uptake efficiencies than spherical ones.[3,6] In one study, a nanoparticle's shape was shown to directly influence its cellular uptake with rods showing highest uptake followed by spheres, cylinders, and cubes for nanoparticles larger than 100 nm in diameter.[3] It was demonstrated that particles with high aspect ratio with diameters of 150 nm and height of 450 nm got internalized by HeLa cells four times faster than symmetrical low aspect ratio particles with diameters of 200 nm and height of 200 nm).[3] In another study, rod-shaped DNA-*block*-poly(propylene) oxide (DNA-*b*-PPO) micelles showed twelve times more efficient internalization than spherical ones.[6] The authors allude to distinct uptake processes between rods and spheres in their system to be a result of differing surface chemistries interacting with the cell membrane. On the contrary, another study presented contradictory results with rod-shaped gold nanoparticles displaying lower uptake than spherical ones.[4] The phenomena may depend on the composition and surface chemistry

of the nanomaterials. Still, observations correlating nanoparticle geometries with uptake require further investigations for the advancement of nanoscale therapeutics.

During the polymerization step of poly(kSer)-derived peptides using urethane-derivative monomers, we unexpectedly observed through TEM analysis that polymerizing at different temperatures, notably 25 °C and 60 °C, yielded self-assembled particles of different geometries (**Figure 5.1**). Poly(kSer[TFA])' and poly(kSer[TFA]) (refer to Chapter 4 for their chemical structures) both were able to form rod-like shapes that were clustered together. Poly(kSer[TFA]) differed from its counterpart, poly(kSer[TFA])', by having a short repeated ethylene oxide chain which gives more water solubility to the peptide. Nonetheless, both peptides produced different self-assembled architectures when polymerized at 25 °C, revealing precisely spherical geometries. The explanation for temperature-dependent morphologies still requires further investigations.

This phenomena could be useful in developing drug delivery carriers but should be extensively studied before applying it to therapeutic use. First, intense characterization of this phenomena should be performed including analysis on any global molecular arrangement after polymerization in different temperatures, using circular dichroism to investigate if the peptide is folding in random coils, helices, or sheets. Next, the relationship between molecular structure of the peptide and molecular arrangements upon heating should be investigated. This requires changing basic properties on the side chain, such as hydrophobicity and hydrophilicity, to determine how structure affects geometries at elevated temperatures. Lastly, it would be interesting to study how temperature itself affects geometries. Therefore, different temperatures can be used for

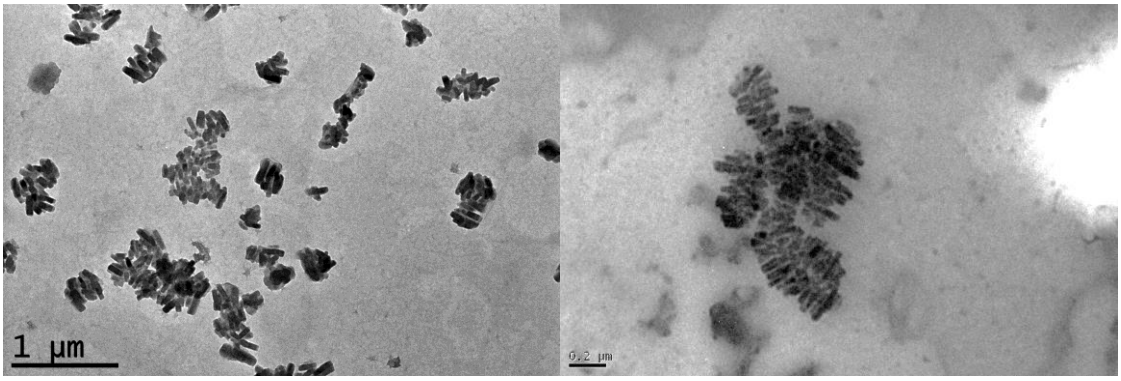

Figure 5.1. TEM images of crude samples of poly(kSer[TFA])' (left) and poly(kSer[TFA]) (right) after polymerization in acetonitrile at 60 °C. (Refer to Chapter 4 for chemical structures).

polymerization to see what threshold temperature is needed to make rod-like architectures. Polymerizing at other temperatures may even reveal fabrication of different interesting morphologies.

Just as the particles needed to be cross-linked in order to preserve morphology in aqueous media, as demonstrated in Chapter 4, the particles would again need to be cross-linked before any therapeutic applications can be tested. The SDAD cross-linker used previously in Chapter 4 may again serve as a feasible cross-linker.

One of the main advantages to fabricating nanomaterials of different geometries is different internalization efficiencies. As evidenced in previous studies, rod-like particles have shown enhanced uptake compared to spherical ones.[2] Rod-like particles produced using poly(kSer)-derived peptides may demonstrate utility when attaching drugs onto the side chain of the acid-responsive peptide, a property which will be further discussed in the next sections. Therefore, having drug-conjugated acid-labile peptides of rod-like morphology may be able to enhance cellular internalization of particles more efficiently than spherical counterparts. This incorporates another feature that overcomes hurdles in drug delivery.

5.2.2. Tailoring cell penetrating properties onto poly(kSer)-derived peptides

In addition to shape facilitating uptake, cell penetrating moieties can be conjugated into the side chain of poly(kSer)-derived peptides. It has been shown that permeability across the cell membrane remains a formidable challenge for nanoparticle-mediated drug/gene delivery to exert their efficacy. Therefore, CPPs, or cell penetrating peptides, have been widely conjugated into numerous systems and have shown in vitro and in vivo applications for various cargoes.[7-9] CPPs consist of 35 amino acids or less and are able to internalize cell membranes through various mechanisms such as pore formation, inverted micelles, membrane thinning, and endocytosis. These CPPs are divided into two classes: arginine-rich CPPs and amphipathic CPPs. It was found that out of all cationic amino acids, arginine possessed the greatest cell penetrating properties due to its more basic nature and its ability to form hydrogen bonds between the guanidine groups and anionic glycosaminoglycans on the cell membrane.[7] Nona-arginine, a peptide consisting of nine arginine residues is the most efficient oligo arginine for promoting cell entry. Guanidine-rich vectors have shown its ability to enhance uptake of multiple drug delivery systems including those for siRNA delivery.[8-10]

Amphipathic CPPs are different than arginine-rich CPPs in that they have fewer arginine residues and are amphipathic in nature, consisting of both hydrophobic and hydrophilic amino acid segments. Recently, it was also discovered that α-helical peptides balanced with appropriate hydrophilicity (for cationic DNA-binding motifs) and hydrophobicity were able to form efficient membrane disruptive capabilities.[11] These helical structures were able to resist charge repulsion and form a stable secondary structure due to sufficient distance between the charged groups of the side chains and

the backbone of the polypeptide (i.e., at least eleven sigma bonds between the peptide backbone and the charged species on the side chain). A library of amphipathic side chains was used to screen for efficient DNA condensation and cell penetrating properties.

A library of side chains with potentially cell membrane disruptive properties can also be tailored with poly(kSer) with the attachment formed via ketalization off the serine hydroxyl group. Feasible side chains include guanidine groups as well as amphipathic groups that have been investigated for CPP properties (**Figure 5.2**).[11] The newly synthesized peptides with membrane destabilization properties can be used in conjunction with poly(kSer) to encapsulate siRNA while adding membrane disruptive potential for improved uptake.

5.2.3. Chemotherapeutic drug conjugation

NP-mediated delivery of cancer drugs solves many limitations that conventional delivery of free drugs face.[12] Drugs can be loaded onto NPs either through physical entrapment or chemical conjugation and mediate enhanced delivery of drugs into cells. Drugs can be targeted to cancer microenvironments either through passive targeting or active targeting thereby limiting the dose to the minimal level that achieves sufficient cell death while avoiding excessive toxicities to noncancerous cells. Passive targeting involves taking advantage of the enhanced permeation and retention (EPR) effect, where NPs of appropriate size can easily enter the leaky vasculature of blood vessels near the tumor while being retained at the tumor site due to poor lymphatic drainage. Active targeting involves targeting ligands such as folic acid, transferrin, or antibodies that are overexpressed on selective cancer cells of interest. Moreover, for hydrophobic drugs,

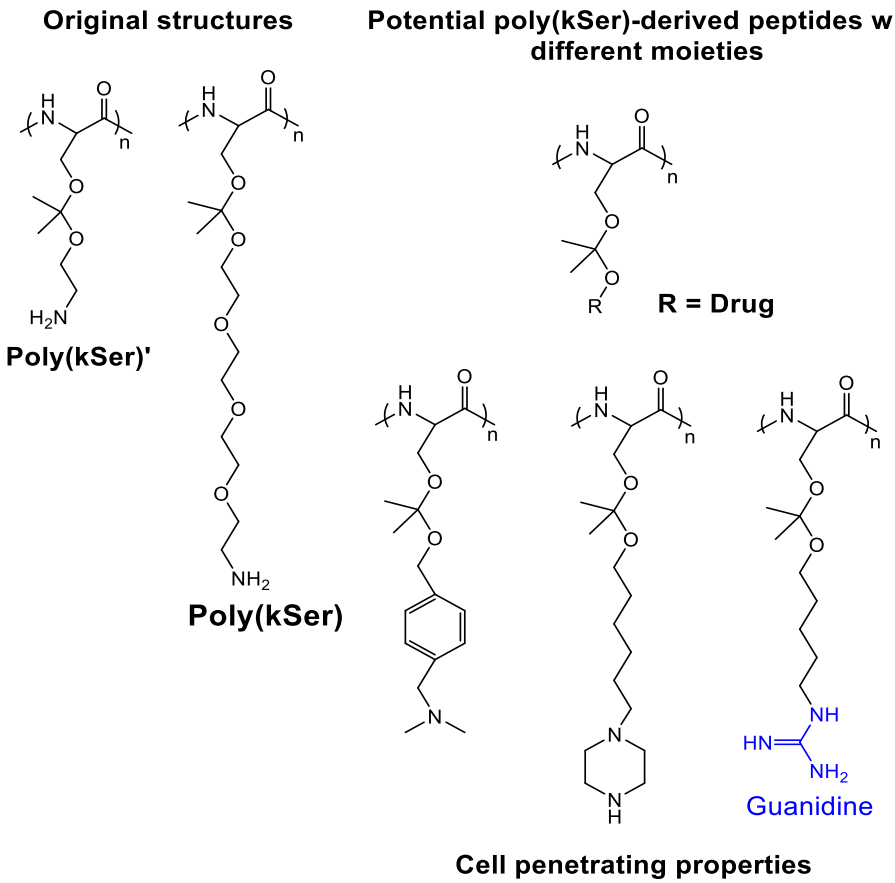

Figure 5.2. Chemical structures of potential conjugates with poly(kSer) via ketalization for additive cell penetrating properties and chemotherapeutic drug delivery.

improved water solubility can be attained by using hydrophilic carriers. Circulation time in the bloodstream can also be prolonged in order to improve biodistribution using Polyethylene glycol, or PEG-conjugated NPs. PEG plays an important role on steric repulsion, where it has shown to lower accumulation of PEGylated NPs in the liver after its coating.[13] PEG also minimizes adsorption onto plasma proteins by providing sterics via a hydrophilic shield. Controlled drug release mechanisms have also been incorporated by adding stimuli-responsive moieties that release drugs at a specific biochemical cue. Furthermore, NPs have the ability to bypass P-glycoprotein, one of the main mediators of chemo drug resistance. It has been suggested that NPs avoid

recognition of P-glycoprotein efflux pump by getting internalized via the endosome, leading to high intracellular concentrations of drugs.[12]

Model drugs that can be incorporated onto the side chain of poly(kSer) are hydrophobic ones containing some functional groups (hydroxyls and/or amines).[14-18] Due to the hydrophobicity of the drugs, attachment to poly(kSer) through ketal linkages would most likely yield self-assembled structures after polymerization in solvent. Removal of solvent and dispersing in water would probably also yield micelles which will consist of the hydrophobic tails in its interior core. Therefore, these micelles can be cross-linked via surface amines or other functional groups depending on the cross-linker used to form stable structures. After internalization into cells via endocytosis, these structures would be exposed to acidification which would hydrolyze ketal groups and cause endosomal escape as well as release of drugs into cytoplasm for therapeutic effects. Furthermore, as alluded earlier in this chapter, polymerization in elevated temperatures may result in different geometries which could have an impact on efficiencies in cellular uptake.

5.2.4 Formulation of multifunctional gene and drug nanocarriers

The technologies introduced in this chapter can all be combined into one vector serving as a multifunctional gene and drug delivery vehicle. The peptides consisting of different functionality can either be coupled through linking the peptides or though mixing at different ratios. Cell penetrating moieties such as guanidine groups will help facilitate efficient cellular uptake. Attaching cancer drugs can be used for combined gene and drug delivery. Lastly, the siRNA will be able to complement the drug depending on the specific type of cancer that is being targeted. The vector can be formulated in aqueous conditions

to see if efficient complexation is obtained. Otherwise, the vector can be formulated in acetonitrile to help self-assemble into precise architectures through solvent exclusion and then cross-linked for stabilization. The NP is hypothesized to get internalized efficiently using features from the CPPs. Acidification in endosomes will trigger endosomal escape and release of gene and drugs which will work synergistically to kill cancer cells. This platform allows flexibility and versatility incorporating different functional moieties and offers ease and simplicity in formulation to tackle multiple hurdles in drug delivery.

5.3. References

[1] M. S. Shim, Y. J. Kwon, *Biomaterials*, **2010**, 31, 3404-3413.

[2] A. Albanese, P. S. Tang, W. C. W. Chan, *Annu. Rev. Biomed. Eng*., **2012**, 14, 1.

[3] S. E. A. Gratton, P. A. Ropp, P. D. Pohlaus, J. C. Luft, V. J. Madden, M. E. Napier, J. M. DeSimone, P. *Natl. Acad. Sci. USA*, **2008**, 105, 11613.

[4] B. D. Chithrani, A. A. Ghazani, W. C. W. Chan, *Nano Letters*, **2006**, 6, 662.

[5] Arnida, A. Malugin, H. Ghandehari, *J. Appl. Toxicol*., **2010**, 30, 212.

[6] F. E. Alemadaroglu, N. C. Alemadaroglu, P. Langguth, A. Herrmann, *Macromol. Rapid Commun.*, **2008**, 29, 326.

[7] M. C.Shin, J. Zhang, K. A. Min, K. Lee, Y. Byun, A. E. David, H. He, V. C. Yang, *J. Biomed. Mater. Res. A*, **2014**, 102A, 575.

[8] P. A. Wender, M. A. Huttner, D. Staveness, J. R. Vargas, A. F. Xu, *Mol. Pharmaceutics*, **2015**, 12, 742.

[9] J. Beloor, C. S. Choi, H. Yeong, Nam, M. Park, S. h. Kim, A. Jackson, K. Y. Lee, S. W. Kim, P. Ku,ar, S.-K. Lee, *Biomaterials*, **2012**, 33, 1640.

[10] O. Weiseh, F. M. Kievit, H. Mok, J. Ayesh, C. Clark, C. Fang, M. Leung, H. Arami, J. O. Park, M. Zhang, *Biomaterials*, **2011**, 32, 5717.

[11] N. P. Gabrielson, H. Lu, L. Yin, D. Li, F. Wang, J. Cheng, *Angew. Chem. Int. Ed*., **2012**, 51, 1143.

[12] K. Cho, X. Wang, S. Nie, Z. Chen, D. M. Shin, *Clin. Cancer Res*., **2008**, 14, 1310.

[13] K. S. Soppimath, T. M. Aminabhavi, A. R. Kulkarni, W. E. Rudzinski, *J. Controlled Release*, **2001**, 70, 1.

[14] L. Zhang, H.-D. Wang, X.-J. Ji, Z.-X. Cong, J.-H. Zhu, Y. Zhou, *Oncol. Rep*., **2013**, 30, 2571.

[15] T. Ubai, H. Azuma, Y. Kotake, T. Inamoto, K. Takahara, Y. Ito, S. Kiyama, T. Sakamoto, S. Horie, S. Muto, S. Takahara, Y. Otsuki, Y. Katsuoka, *Anticancer Res*., **2007**, 27, 75.

[16] Q. Lin, X. Zhao, F. Frissora Y. Ma, R. Santhanam, D. Jarjoura, A. Lehman, D. Perrotti, C. S. Chen, J. T. Dalton, N. Muthusamy, J. C. Byrd, *Blood*, **2008**, 111, 275.

[17] B. Levine, G. Kroemer, *Cell*, **2008**, 132, 27.

[18] J. M. R. Lambert, P. Gorzov, D. B. Veprintsev, M. Soderqvist, D. Segerback, J. Bergman, A. R. Fersht, P. Hainaut, L. G. Wiman, V. J. N. Bykov, *Cancer Cell*, **2009**, 15, 376.

Appendix A: Supporting information for Chapter 3

This portion has been reproduced and slightly modified from:

Wong, S., Kwon, Y. J. (2015), Facile synthesis of high-molecular-weight acid-labile polypeptides using urethane derivatives. J. Polym. Sci. Pol. Chem., 53: 280-286.

with permission from Wiley Periodicals, Inc.

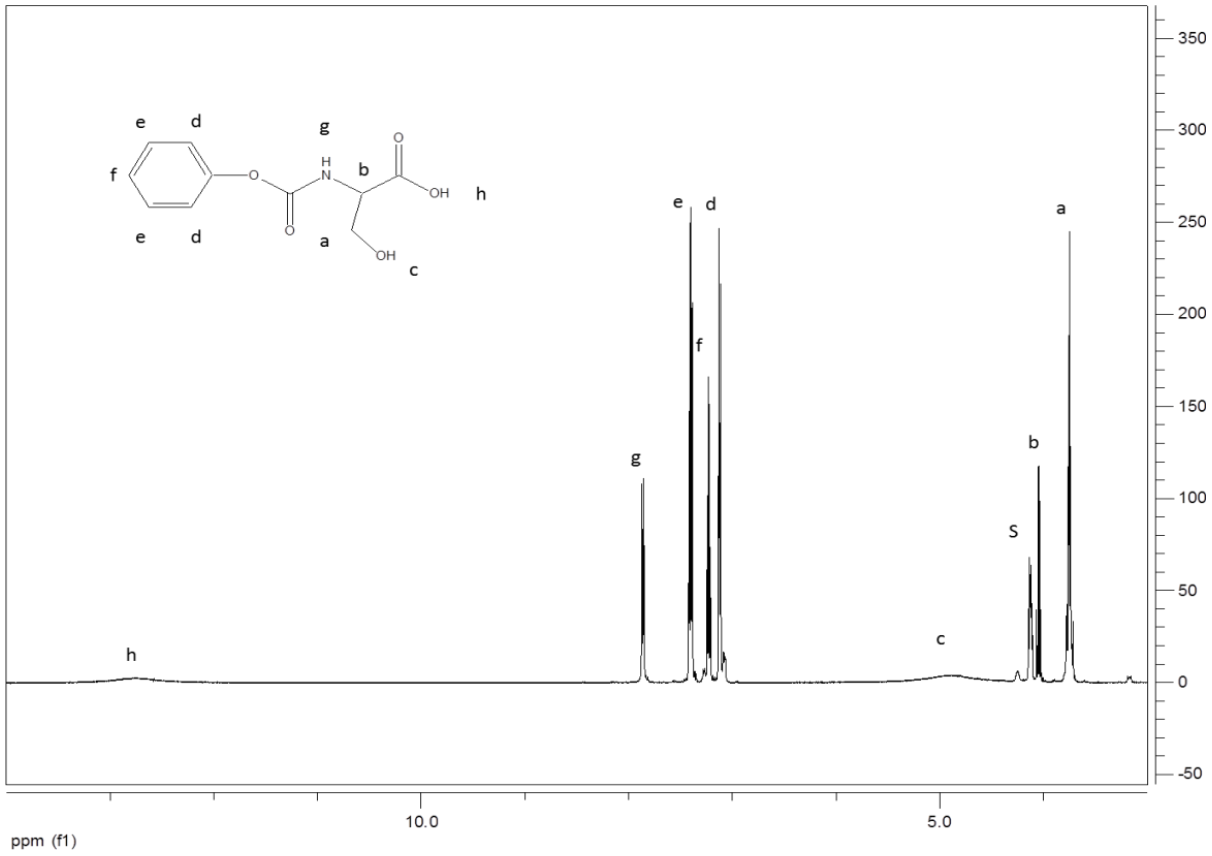

Figure A3.1. ^{1}H NMR spectra of Compound 1.

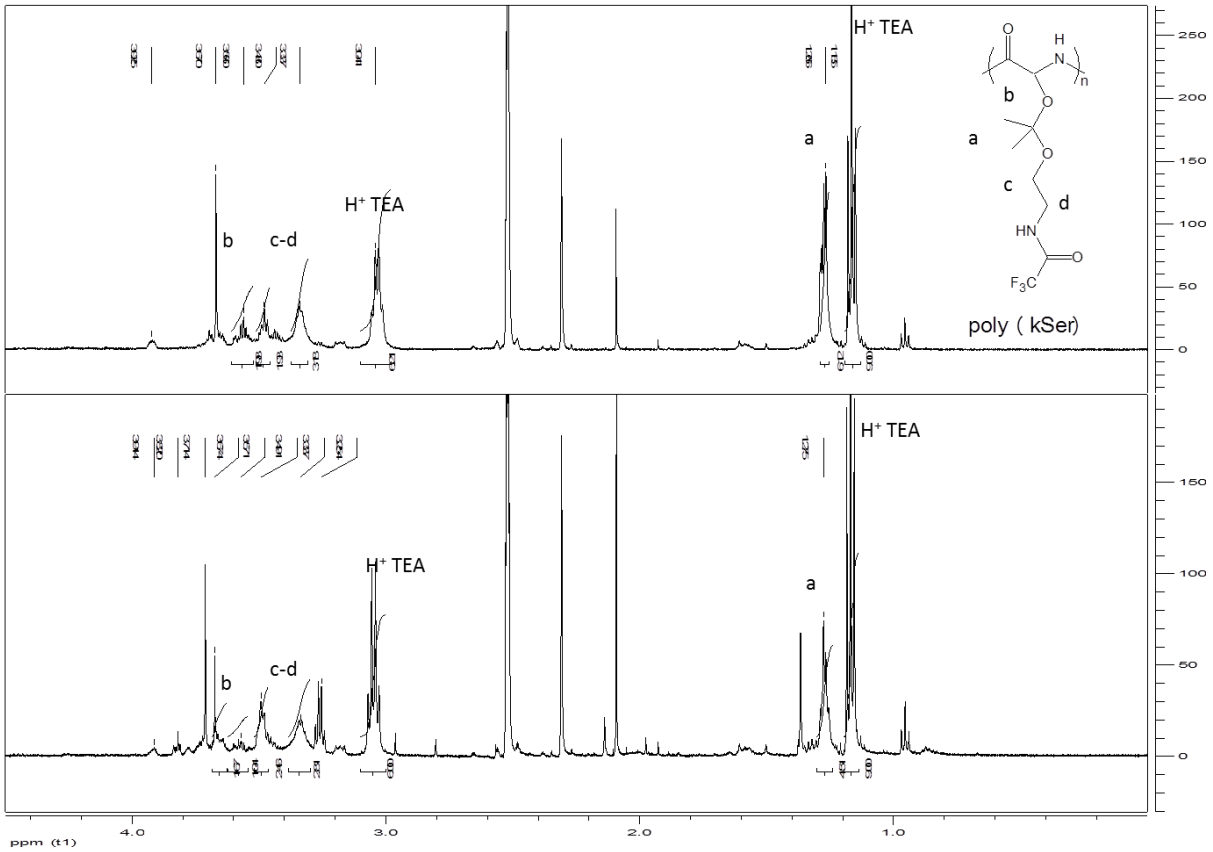

Figure A3.2. Comparison of ^{1}H NMR spectra of poly[kSer(TFA)] polymerized at 4 ˚C (top) and 60 ˚C (bottom). 25% loss of ketal peak (1.28 ppm) was observed at elevated temperatures (4.5H at 60˚C compared with 6.1H at 4˚C integrated based on TEA peaks at 1.14 ppm and 2.96 ppm).

Table A3.1. Kinetics of kSer(TFA) polymerization under different atmospheres

Atmosphere	Time (h)	M_n (Da)[a]	M_w (Da)[b]	PDI[c]	DP
Air	0.25	33,000	38,200	1.16	175
Air	0.5	30,800	35,600	1.15	163
Air	1	33,000	38,700	1.17	175
Air	6	32,200	37,200	1.15	171
Air	12	36,300	41,900	1.15	192
N_2	0.25	37,100	44,400	1.2	197
N_2	0.5	37,200	44,000	1.18	197
N_2	1	33,200	38,600	1.16	176
N_2	6	31,500	36,200	1.15	167
N_2	12	41,200	44,400	1.17	219
Vacuum	0.25	33,800	39,500	1.17	179
Vacuum	0.5	34,300	40,200	1.17	182
Vacuum	1	34,000	39,900	1.17	180
Vacuum	6	33,900	39,700	1.17	180
Vacuum	12	37,500	42,400	1.13	199

[a,b] Determined by MALDI-TOF after TFA de-protection. [c] Calculated by M_w/M_n.

The atmosphere was either left alone to air in a closed system, filled continuously with N_2 after purging three times, or subjected to a vacuumed closed system. 100 µL samples were obtained at 15 min, 30 min, 1 h, 6 h, and 12 h. Molecular weight was analyzed by MALDI-TOF after de-protection of trifluoroacetyl group to obtain final polymer.

Table A3.2. Acid-responsive properties of poly(kSer)

Sample	M_n (Da)[a]	M_w (Da)[b]	PDI[c]
Before hydrolysis	24,900	29,000	1.16
After hydrolysis	11,100	13,000	1.17

[a,b]Determined by MALDI-TOF after TFA de-protection. [c] Calculated by M_w/M_n.

Acid-responsive properties of poly(kSer) was evaluated by treating with 1M HCl for 4 h at 25˚C. Molecular weight before and after hydrolysis of ketal linkages were analyzed by MALDI-TOF.